

An investigation of changes in monocyte gene expression and CNS macrophage recruitment associated with the development of SIV encephalitis

Author: Brian Nowlin

Persistent link: <http://hdl.handle.net/2345/bc-ir:104084>

This work is posted on [eScholarship@BC](#),
Boston College University Libraries.

Boston College Electronic Thesis or Dissertation, 2014

Copyright is held by the author, with all rights reserved, unless otherwise noted.

Boston College
The Graduate School of Arts and Sciences
Department of Biology

An investigation of changes in
monocyte gene expression and CNS macrophage recruitment
associated with the development of SIV encephalitis

a dissertation

by

Brian Thomas Nowlin

Submitted in partial fulfillment of the requirements
for the degree of
Doctor of Philosophy

May 2014

© Copyright by Brian T. Nowlin

2014

ABSTRACT

Factors that impact the development of neuroAIDS include monocyte expansion and activation, viral neuroinvasion and replication, and accumulation of activated and infected macrophages in the CNS. To better understand changes in monocyte/macrophage biology associated with the development of SIV encephalitis (SIVE) and neuroAIDS, we: 1) performed gene expression analyses using high density microarrays to characterize the response of monocyte subsets to SIV infection, 2) serially labeled CNS macrophages with fluorescent dextrans by intracranial injection and labeled myeloid progenitors in the bone marrow with BrdU to determine the timing of SIV neuroinvasion and macrophage recruitment/turnover in the CNS, and 3) performed *in vitro* studies to determine the role of PCNA expression in macrophages with SIV infection. We found the majority of macrophages in SIVE lesions were present in the CNS early in infection and productively infected macrophages were recruited to the CNS terminally with AIDS. We observed differences in the timing of recruitment, rate of turnover, PCNA expression, and productive infection between CD163+ and MAC387+ macrophages in the CNS. SIV infection was associated with induction of interferon stimulated genes in all monocytes, maturation of the intermediate monocyte subset, and increased rate of monocyte/macrophage recruitment to the CNS. Greater ratios of CD163+ to MAC387+ macrophages in the CNS were associated with SIVE. We also found that PCNA expression decreased macrophage apoptosis with SIV infection. Together, these studies suggest that the development of SIVE is a dynamic process and that continuous recruitment of activated monocyte/macrophage and reintroduction of virus from the periphery is required to drive CNS disease.

Acknowledgements

I extend my sincere gratitude to my advisor, Dr. Kenneth Williams, for the amazing opportunities made available to me by working as part of his research team. His dedication to his work, scholarliness, and generosity have routinely impressed me. He has fostered a culture of high standards and pushed me to exceed my own expectations. I am thankful for his guidance and patience over the years.

I would also like to thank the current and past members of the Williams lab who have supported my education and growth. I thank Dr. Caroline Soulas for her willingness to help others learn and Dr. Patrick Autissier for his technical expertise. In particular, I would like to acknowledge Dr. Tricia Burdo whose day-to-day support and friendship have been invaluable over the years. I also thank Dr. Xavier Alvarez and Cecily Conerly Midkiff at TNRPC for their contributions to this work.

I thank the members of my thesis committee for their valuable time and insight, which have helped me complete this thesis. I thank Dr. Bradley Coleman, who is a role model for young researchers and educators. I thank the Higgins staff who have made it their job to make all of our lives a little easier. And I thank the biology graduate student community for their friendship and commiseration.

Finally, I would like to acknowledge my family and dear friends for the encouragement and love that has enabled me to come this far.

Table of Contents

Acknowledgements	i
Table of Contents	ii
List of Tables	vi
List of Figures	vii
List of Abbreviations	x
Chapter 1. Introduction.....	1
I. Thesis Overview	1
II. HIV, AIDS, and simian models of neuroAIDS	3
A. Clinical progression of HIV-1 infection	4
B. Simian models of neuroAIDS	6
III. Monocyte biology	8
A. Monocyte subsets	8
B. Monocytopoiesis	13
C. Monocytes and inflammation	14
IV. Biology of HIV and SIV	15
A. Viral genome and proteins	16
B. Viral life cycle	17
C. HIV and SIV tropism	19
D. Intra-host viral evolution	20
E. Viral reservoirs	21
V. Infection of monocytes and macrophages	23
A. Infection in the bone marrow	24

B. Infection of circulating monocytes	25
C. Infection of tissue macrophages	26
VI. Infection of the CNS	27
A. Populations of CNS macrophages	27
B. Viral neuroinvasion	29
C. AIDS neuropathogenesis and viral encephalitis	30
D. PCNA expression in CNS macrophages	34
VII. Summary	36
Chapter 2. Materials and Methods	38
Ethics Statement	38
Animals, viral infection, and CD8+ T-lymphocyte depletion	38
BrdU administration to SIV infected animals	39
Tissue collection at necropsy	39
Viral load determination	40
Isolation of monocyte subpopulations for microarray analysis	40
Microarray processing	41
Microarray data analysis	41
Quantitative real time PCR for microarray validation	42
Dextran uptake by uninfected monocytes	43
Intracisternal injection of dextran amines and detection in CNS tissues	43
Immunofluorescence microscopy	44
Detection and enumeration of dextran labeled macrophages	45
Single and double label immunohistochemistry	45

Isolation of primary monocytes for <i>in vitro</i> PCNA studies	46
Western blotting for PCNA studies	47
Quantitative real time PCR for PCNA studies	47
Cell culture for <i>in vitro</i> PCNA studies	48
Production of viral stocks	48
siRNA knockdown assays	49
TUNEL staining	50
sCD163 and SIVp27 ELISA	50
Chapter 3. Monocyte subsets exhibit transcriptional plasticity and a shared response to interferon in SIV-infected rhesus macaques.....	52
Results	53
Conclusions	66
Tables	70
Figures and figure legends	79
Chapter 4. SIVE lesions are comprised of CD163+ macrophages that are present in the CNS during early SIV infection and SIV+ macrophages recruited terminally with AIDS.....	89
Results	90
Conclusions	101
Tables	104
Figures and figure legends	107
Chapter 5. PCNA is expressed by CD163+ CNS macrophages in SIV-infected macaques and is associated with decreased macrophage	

apoptosis with SIV infection <i>in vitro</i>	127
Results	128
Conclusions	132
Tables	134
Figures and figure legends	135
Chapter 6. Discussion.....	145
I. Differences in gene expression between monocytes subsets and changes in gene expression with SIV infection	145
II. Recruitment and turnover of CNS macrophages, timing of viral neuroinvasion, and the development of SIVE	152
III. PCNA expression and macrophage retention in the CNS	161
IV. Summary and conclusions	164
References	168
Appendices	185
Publications	185
Conferences and Awards	186

List of Tables

Table 2.1 Sequence of oligonucleotides used for qRT-PCR	51
Table 3.1. Number and percentage of monocyte subsets and plasma viral load over time	70
Table 3.2. Microarray signal intensity correlates with MFI by FACS	71
Table 3.3. Top 50 genes expressed ≥ 2.0 -fold by classical monocytes in uninfected animals	72
Table 3.4. Genes expressed ≥ 2.0 -fold by intermediate monocytes in uninfected animals	73
Table 3.5. Top 50 genes expressed ≥ 2.0 -fold by nonclassical monocytes in uninfected animals	74
Table 3.6. Top 50 genes expressed ≥ 2.0 -fold by classical and intermediate monocytes in uninfected animals	75
Table 3.7. Genes expressed ≥ 2.0 -fold by intermediate and nonclassical monocytes in uninfected animals	76
Table 3.8. GO terms for biological process enriched in the set of genes differently expressed across monocyte subsets	77
Table 4.1: Experimental design for dextran labeling studies	104
Table 4.2: Macrophage traffic from the bone marrow to the CNS is greatest terminally with AIDS	105
Table 4.3: Distribution of dextran-labeled CD163+ macrophages in CNS tissues	106
Table 5.1: Phenotype of PCNA+ macrophages in SIVE lesions	134

List of Figures

Figure 1.1. Interplay of monocytes, macrophages, and SIV in the development of AIDS and SIV encephalitis	2
Figure 1.2. Clinical progression of HIV-1 infection	5
Figure 1.3. Schematic representation of lentiviral genomes	6
Figure 1.4. Phenotypic and transcriptional relationship of human monocytes	9
Figure 1.5. Development and function of monocyte subsets	10
Figure 1.6. BrdU is detected first in classical, then intermediate and nonclassical monocytes following BrdU administration in SIV-infected rhesus macaques	12
Figure 1.7. HIV-1 genome and virion structure	16
Figure 1.8. Life cycle of HIV-1	18
Figure 1.9. HIV-1 infection of monocytes and macrophages and systemic dissemination of virus	24
Figure 1.10. CD163+CD68+ perivascular macrophages, CD68+CD163- microglia, and MAC387+ inflammatory macrophages are distinct populations present in the CNS with HIV and SIV infection	28
Figure 1.11. CD163+CD68+ perivascular macrophages and CD68+CD163- microglia, but not MAC387+ macrophages are targets of SIV infection	30
Figure 1.12. Mechanisms of neurodegeneration and neuroprotection with AIDS	31
Figure 1.13. PCNA expression by macrophages in HIVE and SIVE lesions is associated with productive infection	35

Figure 3.1. Gating strategy, microarray validation, and identification of differently expressed genes	77
Figure 3.2. Expression profiles of subset-specific genes, prior to SIV infection	79
Figure 3.3. Identification of transcripts that differentiate the three monocyte subsets prior to and with SIV infection	81
Figure 3.4. <i>In silico</i> analysis of gene-associated biological processes reveals the functional nature of monocyte subsets	85
Figure 3.5. Changes in monocyte gene expression with SIV infection are present by 26 dpi and include induction of interferon stimulated and innate immune genes	87
Figure 4.1. CD163+ and MAC387+ macrophages accumulate in the perivascular space and SIVE lesions in SIV infected animals	107
Figure 4.2. Recruitment of MAC387+ and CD163+ macrophages from the bone marrow differs in timing and magnitude by CNS region	109
Figure 4.3. Experimental design for dextran labeling of CNS macrophages	111
Figure 4.4. Dextran dyes robustly label CD163+ and not MAC387+ macrophages	113
Figure 4.5. Dextran uptake varies between monocyte subsets <i>ex vivo</i>	115
Figure 4.6. Macrophages that enter the CNS late in animals with AIDS and SIVE are the primary cell type that is productively infected	117
Figure 4.7. The recruitment rate of CD163+ macrophages to the CNS is inversely proportional to time to death	119

Figure 4.8. The rate of CD163+ macrophage recruitment to the CNS is increased with SIV infection and is greater in animals with SIVE	121
Figure 4.9. Increased CD163+ macrophage recruitment in the perivascular space and SIVE lesions correlates with higher concentration of sCD163 in plasma in SIVE animals	123
Figure 4.10. CD163+ macrophage recruitment to the perivascular space and meninges is associated with lower numbers of CD14++CD16+ monocytes in the blood	125
Figure 5.1. PCNA is expressed by CD163+ CNS macrophages but is rarely present in MAC387+ or BrdU+ macrophages	135
Figure 5.2. PCNA is not expressed by CD14+ monocytes in uninfected or chronically SIV-infected animals	134
Figure 5.3. Monocyte-derived macrophages express PCNA <i>in vitro</i>	139
Figure 5.4. SIV infection increases PCNA expression in primary monocyte-derived macrophages (MDM)	141
Figure 5.5. PCNA knockdown in primary MDM increases SIVp27 production and increases the frequency of macrophage apoptosis	143

List of Abbreviations

AFC	Absolute fold change
AIDS	Acquired immunodeficiency syndrome
APC	Antigen presenting cell
ART	Antiretroviral therapy
BrdU	5-bromo-2'-deoxyuridine
CA	Capsid
CCL	Chemokine (C-C motif) ligand
CCR	Chemokine (C-C motif) receptor
CFU	Colony forming unit
CNS	Central nervous system
CSF	Cerebrospinal fluid
CX3CL	Chemokine (C-X3-C motif) ligand
CX3CR	Chemokine (C-X3-C motif) receptor
DAB	3,3'-diaminobenzidine tetrahydrochloride
DAPI	4',6-Diamidino-2-Phenylindole, Dihydrochloride
DC	Dendritic Cell
DDR	DNA damage repair
Dextran:AF647	Alexa Fluor 647 conjugated dextran
Dextran:Biotin	Biotinylated dextran
Dextran:FITC	Fluorescein conjugated dextran
dpi	Days post infection
EDTA	Ethylenediaminetetraacetic acid
ELISA	Enzyme-linked immunosorbent assay
ENV	Envelope polyprotein
FACS	Fluorescence activated cell sorting
FBS	Fetal bovine serum
GAG	Group-specific antigen polyprotein
GO	Gene Ontology
h	Hour
HAART	Highly active antiretroviral therapy
HAND	HIV associated neurological disorders
HIV	Human immunodeficiency virus
HIVE	Human immunodeficiency virus encephalitis
HSC	Hematopoietic stem cell
HRP	Horseradish peroxidase
icv	intracerebroventricular
ISG	Interferon stimulated gene
IF	immunofluorescence
IHC	immunohistochemistry
IN	Integrase
iv	intravenous
LTR	Long terminal repeat
MA	Matrix
MFI	Mean fluorescence intensity

MDM	Monocyte-derived macrophages
MNGC	Multinucleated giant cell
Mo	Monocyte
M ϕ	Macrophage
NC	Nucleocapsid
Nec	Necropsy
Nef	Negative factor
OCT	Optimal cutting temperature compound
ORF	Open reading frame
PBMC	Peripheral blood mononuclear cell
PCNA	Proliferating cell nuclear antigen
PCR	Polymerase chain reaction
PIC	Pre-integration complex
POL	Pol polyprotein
PR	Protease
RIPA	Radioimmunoprecipitation assay
RT	Reverse transcriptase
sCD163	Soluble CD163
SDS-PAGE	Sodium dodecyl sulfate polyacrylamide gel electrophoresis
SEM	Standard error of the mean
SIV	Simian immunodeficiency virus
SIVE	Simian immunodeficiency virus encephalitis
SU	Surface envelope glycoprotein
TAT	Trans-activator
TM	Transmembrane envelope glycoprotein
TMB	3,3',5,5'-Tetramethylbenzidine
TUNEL	Terminal deoxynucleotidyl transferase dUTP nick-end labeling
Vif	Viral infectivity factor
Vpr	Viral protein R
Vpu	Viral protein U
Vpx	Viral protein X
Rev	Regulator of expression of viral proteins

Chapter 1. Introduction

I. Thesis overview

This thesis investigates changes in the biology of monocytes and macrophages with simian immunodeficiency virus (SIV) infection and the role of monocytes/macrophages in the development of SIV encephalitis (SIVE). Human immunodeficiency virus (HIV) and SIV infection are characterized by monocyte dysregulation including an expansion of monocytes from the bone marrow and increased monocyte activation. Increased numbers of activated monocytes are associated with increased traffic of monocytes/macrophages to the CNS, some of which may be infected. Viral neuroinvasion and accumulation of activated macrophages in the CNS contribute to CNS inflammation and neuropathogenesis. In these studies we investigate: 1) differences in gene expression between monocyte subsets and changes in gene expression with SIV infection, 2) recruitment and turnover of CNS macrophages and the development of SIVE, and 3) proliferating cell nuclear antigen (PCNA) expression in CNS macrophages (Figure 1.1).

Monocytes are heterogeneous with regard to phenotype and three populations that differ in absolute number, biological function, and activation state are currently defined in rhesus macaques: classical, intermediate, and nonclassical monocytes. The specific role of each monocyte subset in SIV pathogenesis is not known at present. In the first set of studies (Chapter 3), we characterize the gene expression profile of classical, intermediate, and nonclassical monocytes in healthy animals and changes in gene expression that occur with SIV infection. These studies are unique in the specificity and

scope, as longitudinal studies of gene expression in monocytes with HIV or SIV infection that differentiate the monocyte subsets have not been done.

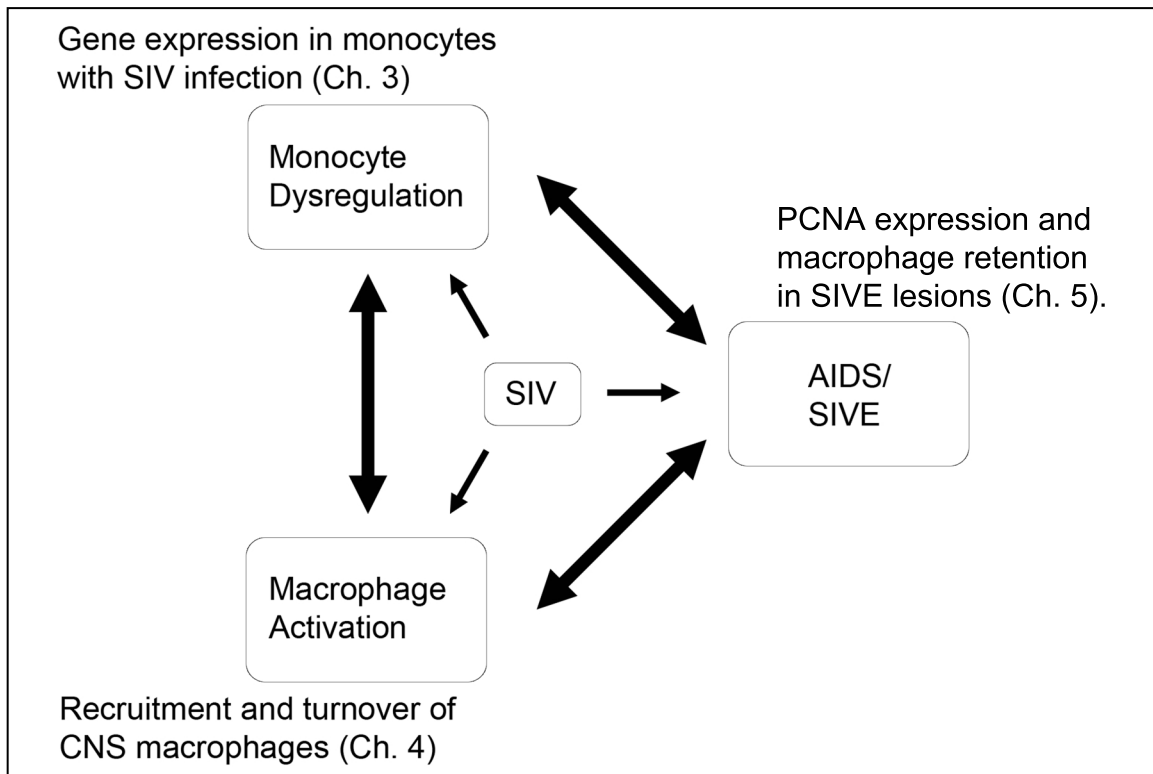


Figure 1.1. Interplay of monocytes, macrophages, and SIV in the development of AIDS and SIV encephalitis.

Due to the limitations of *in vivo* studies of CNS inflammation with HIV or SIV infection (e.g. unknown timing of HIV infection, inability to sample CNS tissue in live subjects), the dynamics of macrophage recruitment to the CNS, the timing of viral neuroinvasion, and the role of macrophage subpopulations in the development of HIV encephalitis (HIVE) and SIVE are understudied. In the second set of studies (Chapter 4), we use BrdU labeling and state of the art serial, intracisternal administration of fluorescent

dextrans *in vivo* to quantitate macrophage recruitment and turnover in the CNS with SIV infection. Additionally, we characterize the infection status of CNS macrophages with regard to time of CNS entry to investigate the timing of SIV neuroinvasion.

Proliferating cell nuclear antigen (PCNA) expression in CNS macrophages is associated with productive HIV and SIV infection in the absence of cell division. PCNA plays a role in multiple cell functions including DNA replication, apoptosis, and DNA damage repair. The specific function of PCNA in CNS macrophages with SIV infection is not known. In the third set of studies (Chapter 5), we characterize PCNA expression in monocytes and subpopulations of CNS macrophages in SIV-infected macaques. We also conduct *in vitro* studies to knockdown PCNA in macrophages to characterize the effect of PCNA expression on viral replication and apoptosis.

Together, these studies provide new insight regarding the role of specific monocyte/macrophage subsets in SIV pathogenesis, macrophage recruitment to the CNS and SIVE lesion formation, timing of SIV neuroinvasion, and the function of PCNA in CNS macrophages.

II. HIV, AIDS, and simian models of neuroAIDS

Presently more than 30 million people worldwide are infected with HIV (UNAIDS 2012), the etiological agent of acquired immune deficiency syndrome (AIDS). Although the advent of highly active antiretroviral therapy (HAART), which uses a combination of protease inhibitors and reverse transcriptase inhibitors, has mitigated the morbidity and

mortality of HIV infection, HIV-associated neurocognitive disorders (HAND) remain clinically relevant and are associated with a worse clinical prognosis¹⁻⁴. Though studies in humans are limited by ethical considerations, SIV infection of rhesus macaques results in a disease that is similar to HIV infection in humans pre-HAART. In this thesis we utilize an established model of SIV infection in rhesus macaques with CD8+ T-lymphocyte depletion that results in rapid AIDS with a high incidence of SIVE.

A. Clinical progression of HIV-1 infection

HIV type 1 (HIV-1) is transmitted by exposure of mucosal surfaces or intravenous/percutaneous exposure^{5,6}. In mucosal exposure DC's, CD4+ T lymphocytes, and macrophages have been implicated in mediating primary infection^{5,7-10}. Founder virus replicates in the mucosa and is subsequently disseminated systemically (Figure 1.2)^{6,7,10,11}. Within days to weeks of primary infection, HIV-1 replicates exponentially leading to acute viremia, which may present as acute retroviral syndrome (Figure 1.2)⁶. It is thought that during this stage latent viral reservoirs are established where virus is seeded in the brain and other tissues¹²⁻¹⁶. The initial host response to viral replication includes production of acute-phase proteins and inflammatory cytokines and induction of CD8+ cytotoxic T-lymphocyte (CTL) responses¹⁷⁻²⁰. Subsequently, humoral responses to HIV-1 are induced. HIV-specific antibodies are detectable several weeks after primary infection, and antibodies that are capable of neutralizing the virus are found approximately three months post infection^{21,22}. During the asymptomatic period, viral replication is controlled by the host immune responses. Ongoing viral replication leads to a progressive reduction in the number of CD4+ T-lymphocytes and sustained

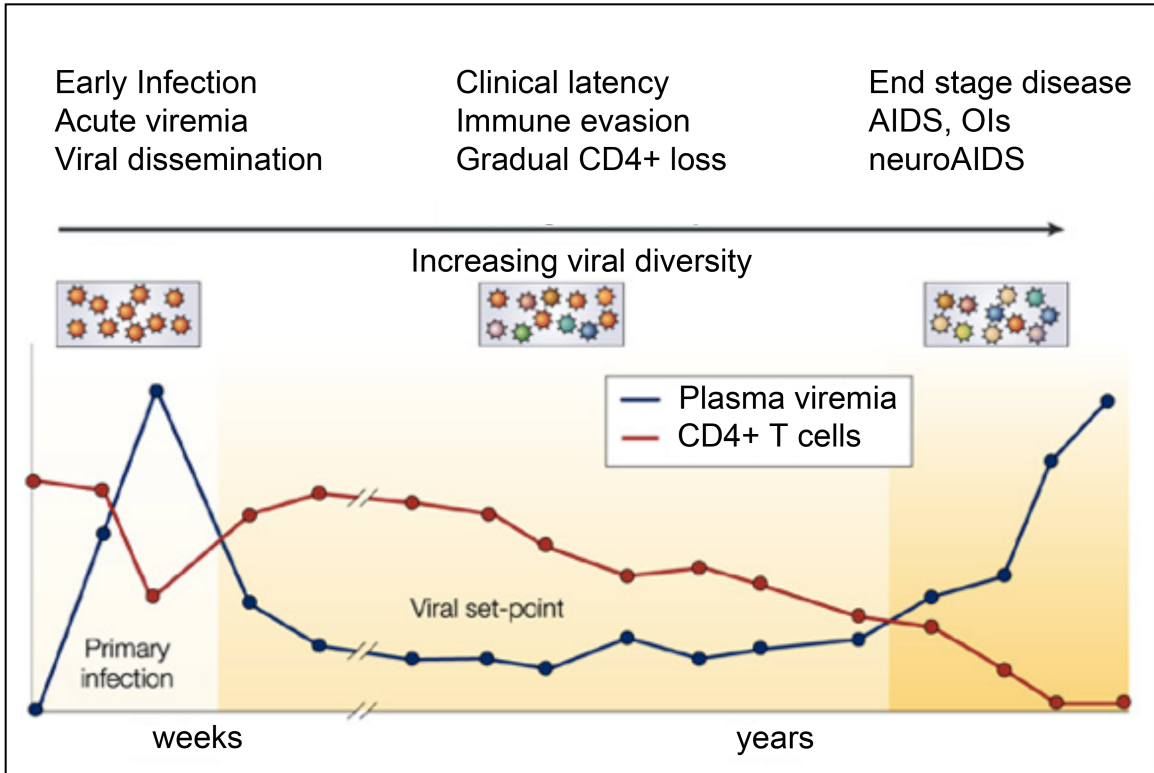


Figure 1.2. Clinical progression of HIV-1 infection

(adapted from Simon and Ho, Nat. Rev. Microbiol. 2003)

immune activation that culminates in the development of AIDS (Figure 1.2)²³. With AIDS, the host's ability to mediate normal immune responses is impaired leading to increased HIV-1 in plasma (viremia), opportunistic infections (OIs), increased incidence of cancer, organ failure, and possibly death (Figure 1.2)²⁴. End stage disease without HAART is frequently associated with organ specific pathologies such as HIV-associated respiratory diseases and HAND^{3,24-26}.

B. Simian models of neuroAIDS

Shortly after the identification of HIV and AIDS in humans, Desrosiers and colleagues identified a virus from immune compromised rhesus macaques (now known as SIV) with antigenic similarity to HIV that induced a disease in macaques similar to AIDS, including: wasting syndrome, primary viral encephalitis (SIVE), opportunistic infections, and destruction of CD4+ T lymphocytes²⁷⁻²⁹. SIV in rhesus macaques (SIVmac) was

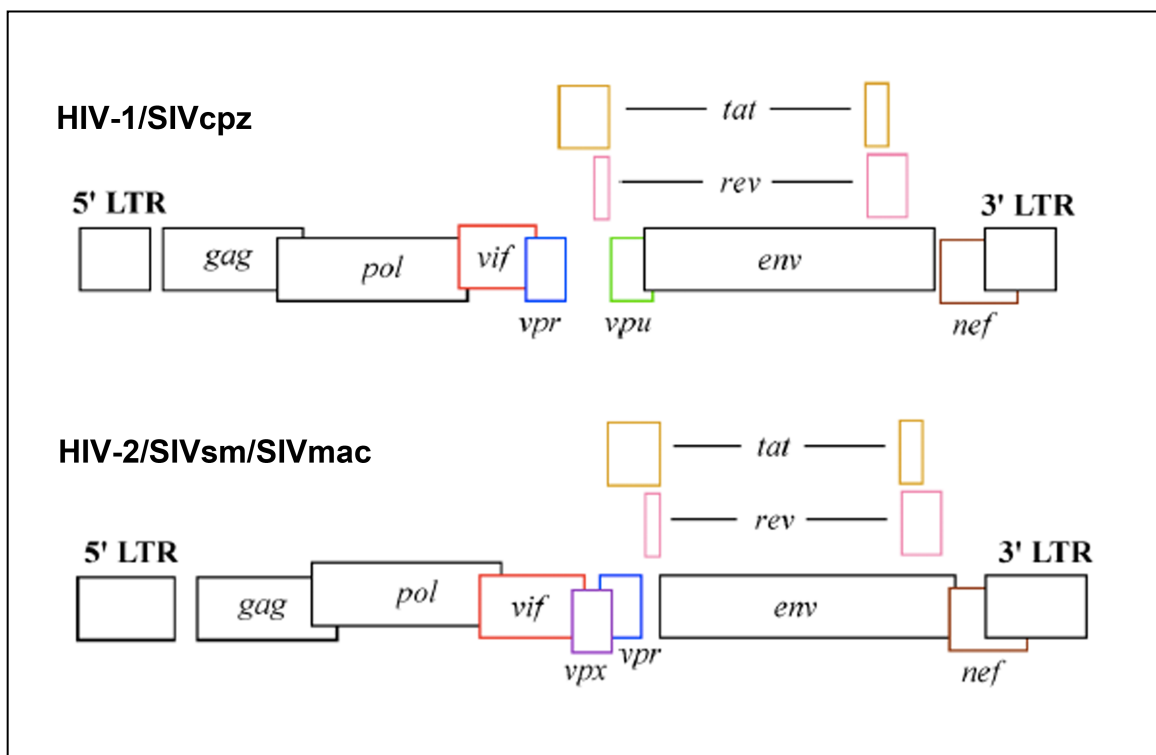


Figure 1.3. Schematic representation of lentiviral genomes

(adapted from Peeters and Courgnaud 2002)

found to be the result of exposure to SIV from infected sooty mangabees (SIVsm) in regional primate centers in the United States (Figure 1.3)³⁰. In humans, HIV-1 is derived from chimpanzee SIV (SIVcpz) and represents the primary HIV burden in the world

(Figure 1.3)³¹. HIV-2 is derived from SIVsm and is restricted primarily to individuals in West Africa (Figure 1.3)³¹. Interestingly, SIVs are generally only found to be pathogenic in a non-native host primate, as a result of zoonotic infection³². This idea is recapitulated in pathogenic HIV infection in humans, who are a non-native host to lentivirus from chimpanzee or sooty mangabees.

A simian model of rapid AIDS using SIVmac251 infection and CD8+ T-lymphocyte depletion

Studies of SIV neuropathogenesis in rhesus macaques frequently use the molecular clone SIVmac239 or the viral swarm SIVmac251 that are R5 tropic (see below) and neurovirulent³³⁻³⁷. SIVmac251 infection in macaques recapitulates the major features of HIV infection in humans (dynamic viremia, CD4+ T cell depletion, biphasic monocyte expansion, AIDS) and results in similar neuropathology (early neuroinvasion, meningitis, perivascular cuffing, infected perivascular macrophages and microglia, decreased neuronal integrity, MNGCs, SIVE lesions)^{7,11,38,39}. Faster disease progression and increased incidence of SIVE can be achieved by the administration of a chimeric humanized mouse anti-CD8 antibody, which results in depletion of CD8 expressing lymphocytes and NK cells^{18,39-43}. CD8+ lymphocyte depletion results in loss of viremic control through impaired ability to mount cellular and humoral immune responses and increased destruction of CD4+ T cells^{17,18,40,44-46}. SIVmac251 infected macaques develop AIDS within 1-3 years of infection with a 25% incidence of SIVE. In contrast, CD8+ T-lymphocyte depleted animals develop AIDS in 3-4 months with SIVE in more

than 75% of animals³⁹. The SIVmac251, CD8+ depletion rapid AIDS model is well established, reproducible, and results in uniform pathogenesis^{18,39-43}.

III. Monocyte Biology

In HIV and SIV infection, the progression to AIDS is associated with changes in monocyte biology including increased egress from the bone marrow, accelerated turnover in the blood, and increased activation^{42,47-52}. Importantly, monocytes are phenotypically and functionally heterogeneous, and subpopulations likely differ with regard to putative immune functions, activation status, migratory properties, and susceptibility to HIV or SIV infection^{49,53-56}. Due to functional differences between the classical, intermediate, and nonclassical monocyte subsets, perturbations to normal monocyte homeostasis and the relative proportion of each subset may influence disease progression. The gene expression profiles of classical, intermediate and nonclassical monocytes and the specific immune response of each subset to SIV infection are characterized in Chapter 3.

A. Monocyte Subsets

Monocytes are mononuclear phagocytes that comprise 5-10% of circulating leukocytes in humans⁵⁷. Antigens commonly used as pan-monocyte markers include CD14 (LPS coreceptor) and CD11b (macrophage receptor 1, integrin $\alpha M\beta 2$) in humans and CD11b, CSFR1 (macrophage colony-stimulating factor 1 receptor, CD115), and F4/80 (EMR1 hormone receptor) in mice^{58,59}. Monocytes are heterogeneous, and multiple subpopulations can be defined by differences in surface antigens, morphology (size,

granularity), and function (antigen presentation, phagocytosis, cytokine secretion)^{49,56,57,60,61}. Human monocytes have been historically defined as CD14+ (LPS coreceptor) mononuclear phagocytes. In 1989, Zeigler-Heitbrock and colleagues defined a second population of monocytes that expressed CD16 (Fc γ RIII) and were morphologically and functionally distinct from classical monocytes⁶⁰. For two decades monocytes were phenotypically defined as CD14+CD16- or CD14+CD16+ monocytes (often referred to as CD16- and CD16+ monocytes respectively)⁵⁴. Recent research

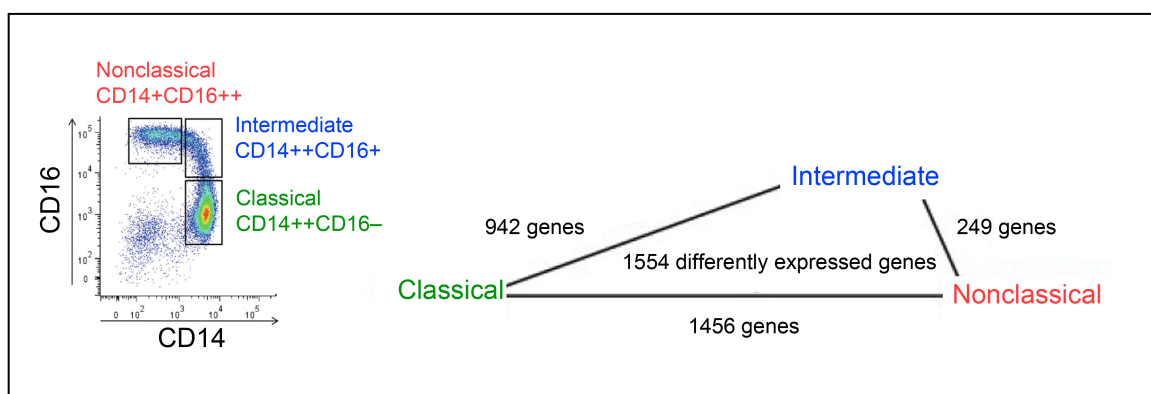


Figure 1.4. Phenotypic and transcriptional relationship of human monocytes

(adapted from Wong et al. Blood 2011)

has revealed heterogeneity within CD16+ monocytes that lead to a new nomenclature for three monocyte subsets defined by expression of CD14 and CD16: CD14++CD16- classical monocytes, CD14++CD16+ intermediate monocytes, and CD14+CD16++ nonclassical monocytes (Figure 1.4)^{61,62}. It is not known whether these subpopulations are unique monocyte subsets or whether they represent progressive stages of activation/maturation of a single monocyte lineage.

Current understanding of the biology of monocyte subpopulations comes from studies in human and macaques as well as homologous monocyte populations in mice. Mouse Ly6C⁺, Ly6C^{int}, and Ly6C⁻ monocytes correspond to classical, intermediate, and nonclassical monocytes respectively^{57-59,63,64}. In humans, circulating monocytes are comprised of approximately 80% classical monocytes, 5% intermediate monocytes, and 10% nonclassical monocytes (Figure 1.4)^{49,61,65}. Classical monocytes exhibit high phagocytic ability and produce reactive oxygen species and interleukin (IL)-10 in response to LPS^{54,60,65}. Additionally, classical monocytes express CCR2 and CD62L, migrate in response to inflammation, and may differentiate into classically activated, M1 polarized macrophages or dendritic cells (DC) in inflamed tissue (Figure 1.5)^{58,59,61,63,64,66}. Intermediate monocytes express proteins associated with MHC class II

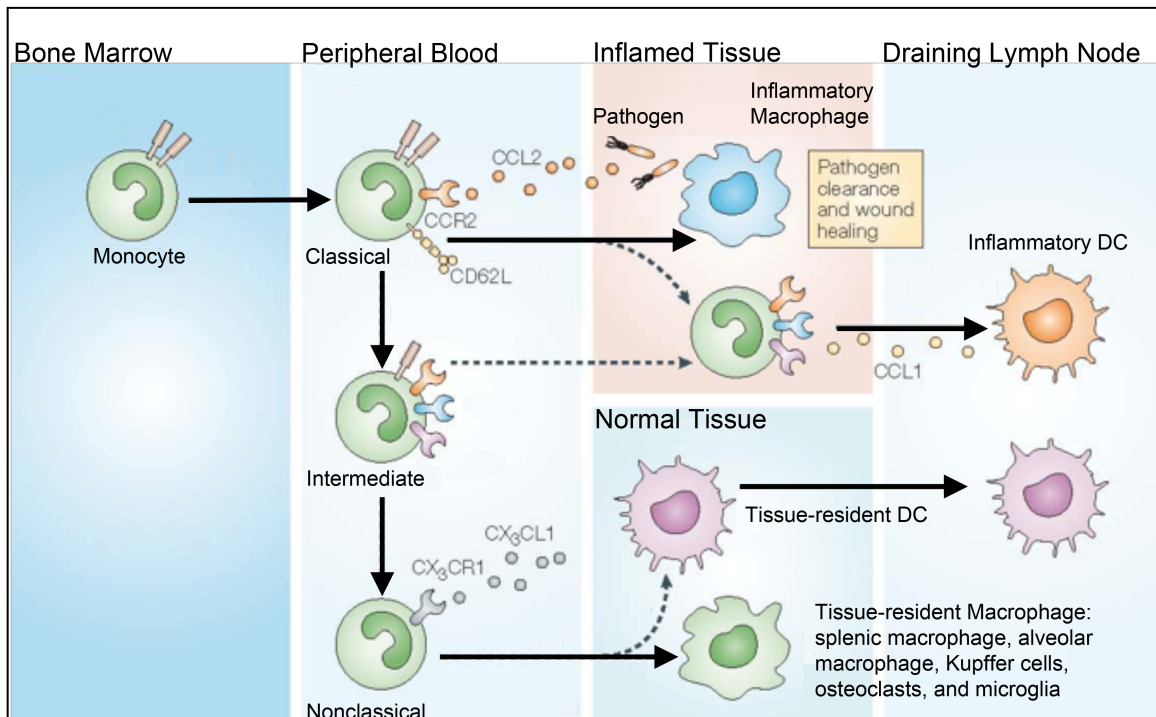


Figure 1.5. Development and function of monocyte subsets

(adapted from Gordon and Taylor, Nat. Rev. Immunol. 2005)

presentation, are capable of T-cell activation, and may be a transitional population between classical and nonclassical monocytes (Figure 1.5)^{49,61}. In response to LPS, intermediate monocytes produce $\text{TNF}\alpha$ and $\text{IL-1}\beta$ ⁶⁵. Nonclassical monocytes migrate along the luminal face of the vasculature, express CX3CR1 (fractalkine receptor), and may extravasate into tissue to replenish resident macrophage populations (Figure 1.5)^{49,58,59,61,62,65}. In response to TLR7/TLR8 agonists (viruses, nucleic acids) nonclassical monocytes produce proinflammatory cytokines $\text{TNF}\alpha$, $\text{IL-1}\beta$, and $\text{CCL3/MIP-1}\alpha$ ⁶⁵. Thus monocyte subsets differ in abundance, phenotype, migratory ability, and response to immune stimuli.

The developmental relationship of monocyte subsets.

If classical monocytes mature into intermediate then nonclassical monocytes, expansion of CD16+ monocyte populations with SIV infection may represent increased activation/maturation of classical monocytes. A developmental relationship between classical, intermediate, and nonclassical monocytes is suggested by several lines of evidence. In mice, classical monocytes exit the bone marrow and mature into nonclassical monocytes (Figure 1.5). In humans treated with a two-week regimen of macrophage colony-stimulating factor (M-CSF) there was an increase in the number of intermediate monocytes at day 8 followed by an increase in the number of nonclassical monocytes at day 15⁶⁷. Similarly, studies in SIV infected rhesus macaques found that after labeling promonocytes with BrdU (5-bromo-2'-deoxyuridine), BrdU+ monocytes were present in the classical subset at 24-48 hours post treatment, followed by the intermediate subset at 72-96 hours post treatment, and the nonclassical subset at 96-

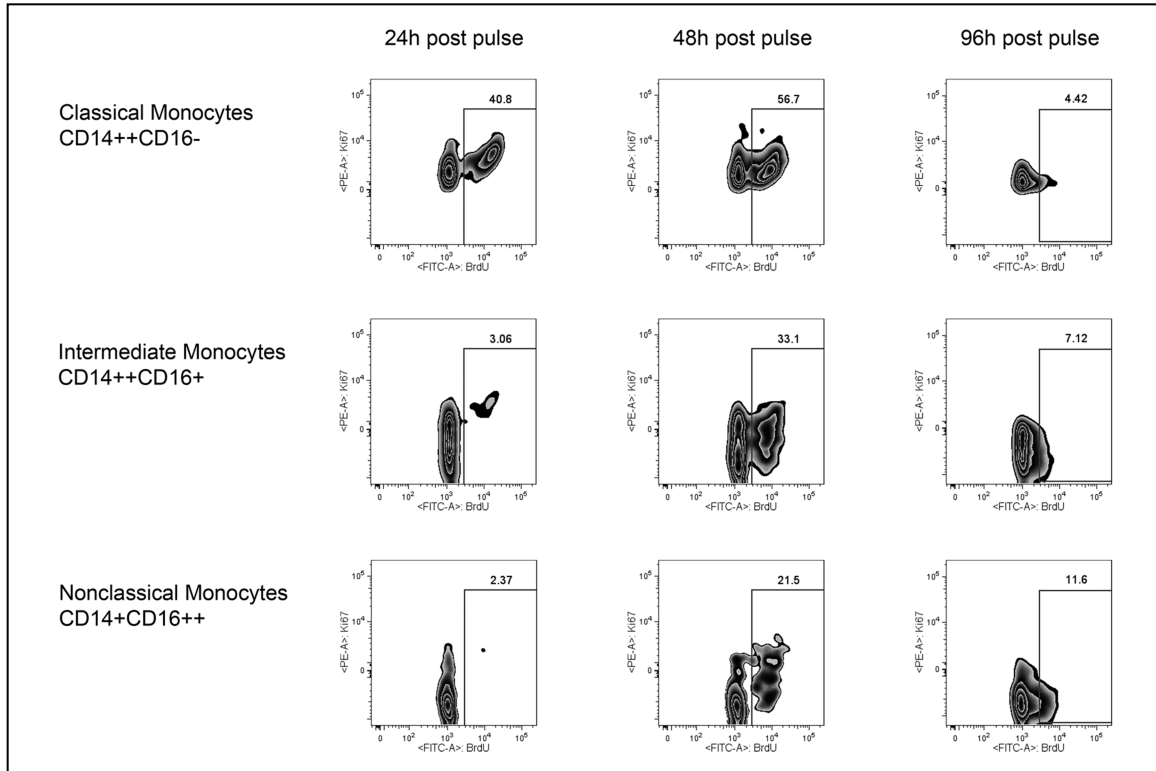


Figure 1.6. BrdU is detected first in classical then intermediate and nonclassical monocytes following BrdU administration in SIV-infected rhesus macaques
(T.H. Burdo, unpublished data)

144 hours post treatment (Figure 1.6)^{42,52}. These dynamics mirror kinetic studies in human monocytes that indicate monocytes leave the bone marrow 13- 26 hours after the promonocyte division and circulate in the blood with a half life of 71 hours^{68,69}. When cultured *in vitro*, classical monocytes acquire expression of CD16 suggesting a transition to the intermediate phenotype⁷⁰. Consistent with the notion that intermediate monocytes are a transitional population, analysis of cell surface markers and gene expression profiles of the three monocyte subsets indicates that intermediate monocytes express a majority of transcripts and surface proteins at levels between

classical and nonclassical monocytes in humans and rhesus macaques^{49,61}. In humans, transcripts associated with withdrawal from cell cycle, maturation, and macrophage phenotype are associated with nonclassical or both intermediate and nonclassical monocytes suggesting these cells are more terminally differentiated compared to classical monocytes^{56,61}. Together such evidence suggests that there is a progression from classical to intermediate to nonclassical monocytes. An alternative hypothesis is that the three monocyte subsets are independent monocyte lineages with unique turnover characteristics.

B. Monocytopoiesis

Increased egress of monocytes from the bone marrow suggests that monocytopoiesis is altered with HIV and SIV infection. Also, anemia is a comorbidity of HIV infection and increased bone marrow diffusivity is shown to correlate with HAD⁷¹. The mononuclear phagocyte system is composed of monocytes and macrophages as well as their developmental precursors. During early development monocytes and macrophages are produced from primitive precursors in the yolk sac and later by hematopoiesis in the fetal liver^{57,72,73}. In the adult, monocytes are produced from hematopoietic stem cells (HSC) in the bone marrow^{57,58}. Monocytes are derived from a common myeloid progenitor that commits to a granulocyte/macrophage lineage (granulocyte/macrophage colony forming unit, GM-CFU) then a macrophage lineage (macrophage colony forming unit, M-CFU)⁵⁷. In subsequent divisions, the M-CFU becomes a monoblast then a promonocyte, which is the immediate precursor of monocytes^{57,58,74}. Human monocytes

and macrophages are not thought to divide after the promonocyte stage, although macrophage proliferation has been reported in mice^{57,74,75}.

Newly formed monocytes exit the bone marrow and enter the circulation. In mice traffic of classical Ly6C⁺ monocytes out of the bone marrow is dependent on CCR2 and its ligands CCL2 (Macrophage Chemoattractant Protein 1, MCP-1) and CCL7 (Macrophage Chemoattractant Protein 3, MCP-3)⁷⁶⁻⁷⁸. Additionally, a reduced number of nonclassical Ly6C⁻ monocytes was reported in CX3CR1^{-/-} knockout mice⁷⁸. This suggests that the specific receptor-ligand interactions controlling bone marrow egress vary between monocyte subsets. It is not known if a retention mechanism exists to keep monocytes in the bone marrow.

C. Monocytes and inflammation

Monocyte emigration from the bone marrow is increased with inflammation^{42,52,76,77,79}. In inflammatory states, there is an increased production of monocyte mobilization ligands that may contribute to monocyte expansion and recruitment^{50,80,81}. Recent research has identified a splenic reservoir of monocytes in mice that is also mobilized in response to inflammation^{66,82-84}. In mice, both classical Ly6C⁺ and nonclassical Ly6C⁻ monocytes are deployed from the spleen in response to atherosclerosis and myocardial infarction. Splenic Ly6C⁺ monocytes are recruited to the site of inflammation in a CCR2 dependent manner and differentiate into classically activated, M1-polarized macrophages^{83,84}.

The progression of CNS disease is directly influenced by monocyte dysregulation in HIV and SIV infection^{39,51,68,85}. Importantly, traffic of infected monocytes/macrophages is a potential mechanism of dissemination of virus across the blood brain barrier (BBB)⁸⁶⁻⁹⁰. With HIV and SIV infection, increased numbers of circulating monocytes and increased monocyte activation correlate with the development of encephalitis and dementia^{41,42,91,92}. Given the low rate of monocyte infection *in vivo*, the changes observed in monocyte biology are most likely the result of systemic immune activation, altered cytokine signaling, and other indirect mechanisms resulting from chronic infection. Historically in HIV research, particular attention has been paid to activated CD16+CD69+ monocytes (intermediate monocytes), which expand with inflammation, are precursors of tissue macrophages, and targets of HIV infection^{42,50,52,88,91-93}. Classical and nonclassical monocytes in contrast have received little attention. In Chapter 3 of this thesis, we perform microarray analyses to investigate the shared and unique biology of the three monocyte subsets and the response of each to SIV infection.

IV. Biology of HIV and SIV

HIV and SIV are related lentiviruses with similar biology and disease progression in their respective hosts. Primary infection is mediated by a small population of founder viruses that expands and evolves over the course of infection. Evolution of viral quasispecies results in changes in tropism that allow virus to infect different cell types and anatomical compartments and establish viral reservoirs. In particular, the ability of virus to replicate in macrophages in the CNS is an important factor in the development of HIV dementia and SIVE. The studies in this thesis were conducted in SIV-infected rhesus macaques,

but we will take advantage of the abundance of information regarding HIV in addressing the general biology of lentiviruses by discussing both HIV and SIV and noting relevant differences where applicable.

A. Viral genome and proteins

HIV and SIV are enveloped retroviruses composed of 15 unique proteins and two copies of an RNA genome (Figure 1.7)^{31,94,95}. The viral genome consists of 9 open reading frames (ORF's) (Figure 1.7). Three of these encode the Gag, Pol, and Env polyproteins found in all retroviruses (Figure 1.7). Polyproteins are proteolytically cleaved

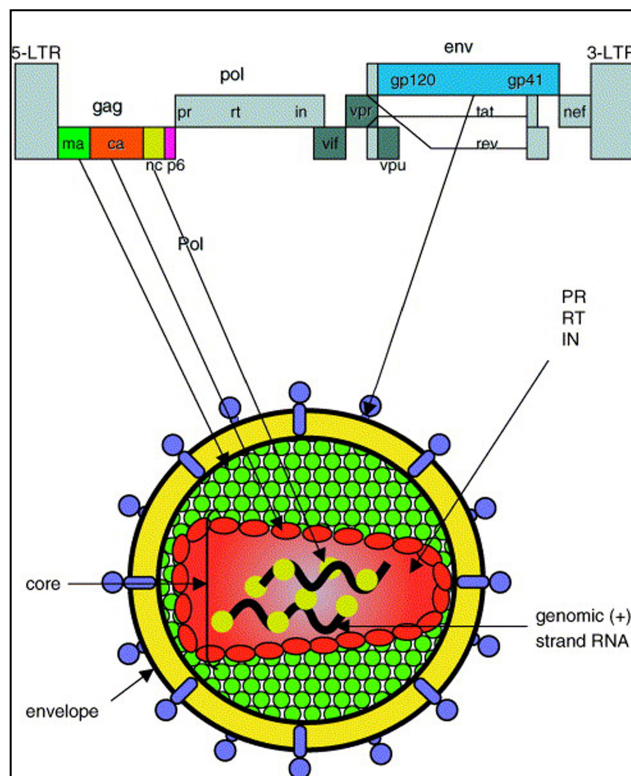


Figure 1.7. HIV-1 genome and virion structure

(Scarлата and Carter Biochim. et Biophys. Acta 2003)

into individual proteins by viral protease. Gag is processed into the structural proteins matrix (MA), capsid (CA), nucleocapsid (NC) and p6 (Figure 1.7). Pol encodes the viral enzymes protease (PR), reverse transcriptase (RT), and integrase (IN) (Figure 1.7). Env is processed into the two envelope proteins gp120/surface (SU) and gp41/transmembrane (TM) (Figure 1.7). The remaining ORFs encode regulatory (Rev, Tat, Nef) and accessory proteins (Vif, Vpr, and Vpu in HIV-1 or Vpx in SIV/HIV-2) that function in regulating viral infectivity, transcription of the viral genome, and production of progeny virions^{31,95,96}. Noncoding, long terminal repeats (LTRs) are present at the 5' and 3' ends of the viral genome that regulate transcription of viral genes (Figure 1.7)⁹⁷.

B. Viral life cycle

The individual steps that comprise the life cycle of HIV have been described extensively and will be briefly summarized here^{23,86,94,95,97,98}. Beginning with a mature virion, gp120/SU binds CD4, the primary HIV and SIV receptor, and relevant coreceptors (discussed below) on the target cell which leads to conformational changes in gp41/TM that promote fusion of the viral envelope with the cell membrane (Figure 1.8)^{99,100}. Once in the cell, the viral core particle is uncapisdated, and RT transcribes the RNA genome into dsDNA (Figure 1.8). A preintegration complex (PIC) consisting of the HIV genome and viral and host derived factors is translocated to the nucleus (Figure 1.8). Viral integrase catalyzes the insertion of the HIV provirus into the host genome, and the DNA is repaired by the host DNA damage repair machinery (Figure 1.8). Once the cell is infected, viral transcripts and full-length genomic RNA are transcribed and exported to the cell cytoplasm (Figure 1.8). The *env* transcripts are translated at the endoplasmic

reticulum while the other viral mRNAs are translated in the cytoplasm. Envelope proteins, now in the lipid bilayer, traffic to the cell membrane where the viral

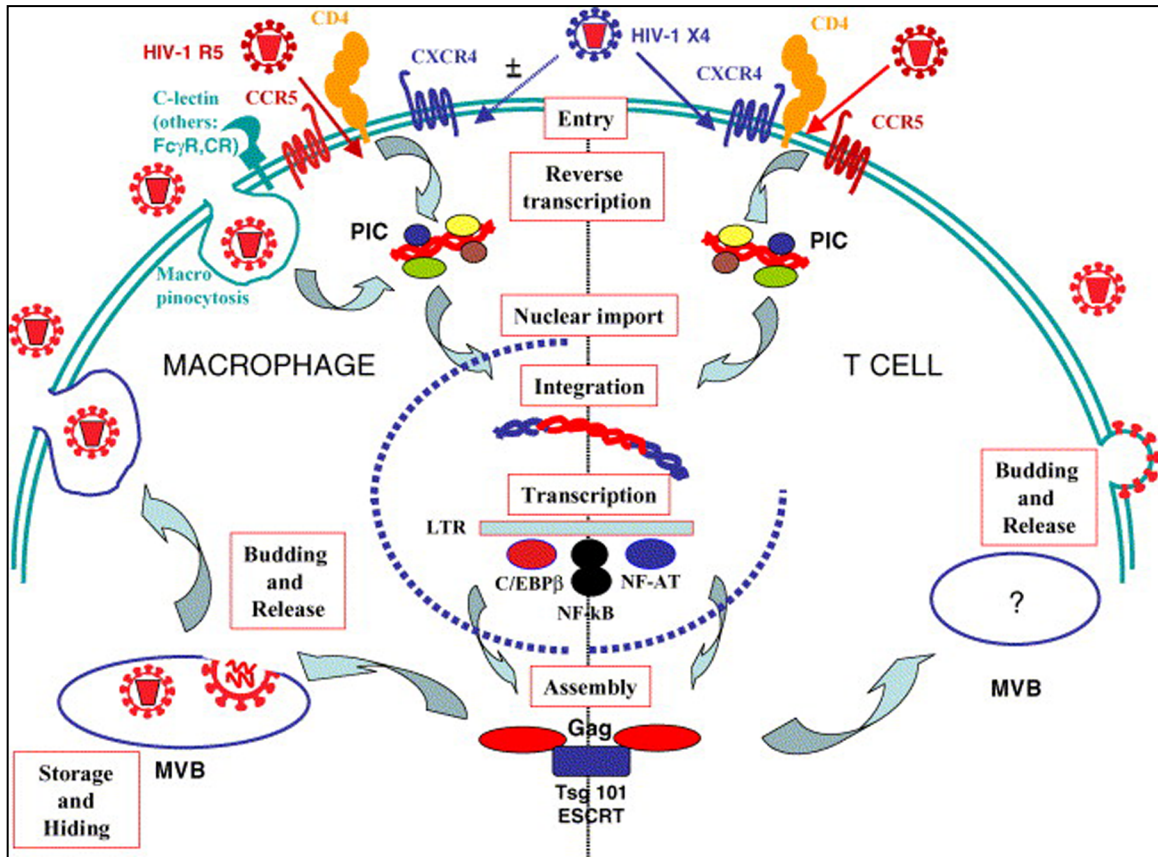


Figure 1.8. Life cycle of HIV-1

(Verani et al. Molec. Immunol. 2005)

core particle is assembled from the Gag polyprotein (Figure 1.8). The immature virion buds from the cell membrane and is released into the extracellular space (Figure 1.8). In macrophages, HIV may also bud into late endosomes/multi-vesicular bodies (LE/MVB) that release virus into the extracellular space through exocytosis (Figure 1.8)⁹⁸. Proteolytic cleavage of Gag into the individual structural proteins leads to

rearrangement of the immature virion into an infectious virus particle⁹⁴. Although the life cycle of SIV differs from HIV with regard to coreceptor usage, the interaction between viral accessory proteins and host restriction factors, and transcriptional regulation of viral genes, the general features of HIV and SIV replication are the same.

C. HIV and SIV Tropism

Viral tropism can be described in terms of viral entry by coreceptor usage, the preferred target cell for viral replication, and tissue specificity. The identification of chemokine receptors CCR5 and CXCR4 as the primary coreceptors for HIV lead to classification of the virus as R5, X4, or R5X4 based on the ability of HIV to use one or both coreceptors^{86,101-107}. CD4+ cells, monocytes/macrophages and CD4+ T lymphocytes, express varying levels of both CCR5 and CXCR4^{86,95}. Although CCR5 usage is associated with macrophage tropism and CXCR4 usage is associated with T cell tropism *in vitro*, HIV target cell preference *in vivo* cannot be explained solely by differences in coreceptor usage. The majority of SIVs use CCR5 as the primary coreceptor and additional coreceptors include GPR15 and STRL33¹⁰⁸⁻¹¹¹. Both macrophage and T-cell tropic SIV use CCR5 and not CXCR4¹⁰⁹. Coreceptor usage, target cell preference, and tissue specificity influence the progression of HIV and SIV infection. HIV infection in humans is associated with a switch from R5 tropic strains during primary/early infection to R5X4 or X4 tropic strains during end stage disease^{25,102,105,112-114}. Changes in receptor tropism are also associated with infection of specific tissues, which is likely dependent on the major cell type infected in each tissue. Distinct subtypes of HIV and different strains of SIV show different patterns of tissue

distribution and neuropathogenesis suggesting that differences in the viral genome are associated with altered tissue tropism and pathogenesis^{9,38,80,90,115}. Analyses of HIV and SIV envelope sequences indicate that infection of the CNS is associated with expansion of sequence variants with neurotropic/macrophage-tropic motifs in the plasma as well as in the lung and the bone marrow^{37,116,117}. This may indicate that during end stage disease novel sequence variants that are able to replicate in CNS macrophages are introduced into the CNS and contribute to the development of HIV/SIV and neuroAIDS. That the development of CNS disease is associated with the ability of virus to replicate in macrophages in the CNS is particularly relevant to this thesis.

D. Intra-host viral evolution

Primary infection at the mucosa is mediated by transmission of a small number (1 to 5) of R5 tropic virions^{6,10,118}. In chronically HIV-infected individuals or SIV-infected macaques, numerous sequence variants can be isolated indicating an evolution and expansion of the transmitted/founder sequence^{37,118-120}. This diversity contributes to the ability of HIV to evade immune responses and generate resistance to antiretroviral therapy. Multiple mechanisms contribute to increased genetic diversity¹²¹. Viral reverse transcriptase is error prone and may generate *de novo* mutations^{122,123}. Additionally, two copies of the RNA genome are packaged into each virion with both being used to generate a single provirus in a process facilitated by recombination¹²⁴. Moreover, superinfection of a target cell may result in recombination of two genetically distinct viral variants^{121,125}. Host factors also contribute to viral diversity. For example, members of

the APOBEC family of cytidine deaminases are packaged into newly synthesized virions and lead to G to A hypermutation of the viral genome¹²⁶⁻¹²⁸.

Innate, cellular, and humoral immunity each apply a selective pressure that promotes survival of viral variants that are able to evade the host immune response. Beginning in early infection CTL responses select for escape mutants^{6,10,20,129,130}. Humoral immune responses result in production of HIV specific antibodies that drives variation in the viral envelope proteins. In particular, changes to the hypervariable regions of Env allow the virus access to additional target cell types or anatomical compartments. An important factor in HIV pathogenesis is the evolution of virus that is able to infect long-lived cell types (e.g. macrophages, resting memory CD4+ T cells) or anatomical locations (e.g. CNS, bone marrow) that promote the establishment of viral reservoirs.

E. Viral reservoirs

At present, combination antiretroviral therapy (cART) is able to suppress plasma viral loads below the current limit of clinical detection (<50 copies/mL). However, ultrasensitive assays indicate persistent low-level viremia that is not sensitive to drug intensification and is able to rebound to pre-treatment levels when ART is interrupted¹³¹⁻¹³³. These observations indicate the presence of viral reservoirs capable of supporting productive infection in spite of host immune responses and effective ART.

Macrophages and latently infected resting memory CD4+ T-lymphocytes are the two major cellular reservoirs of HIV-1^{68,86,89,131,134-136}. These cellular reservoirs are thought to

be established during acute viremia and prior to the initiation of ART. Analysis of decay kinetics of the latent CD4+ reservoir in HIV+ patients on ART determined the half-life to be 44 months and the latently infected population to be more than a million cells¹³⁷. In rhesus macaques infected with a highly pathogenic chimeric SIV/HIV (SHIV), macrophages comprised the major cellular reservoir of virus after depletion of the CD4+ T cell population¹³⁵. Macrophages are resistant to the cytopathic effects of HIV infection and have low turnover rates that may contribute to persistent viremia particularly during end stage disease^{89,134,135,138}. Antiretroviral drugs that target reverse transcription or integration have no effect on macrophages that are already infected¹³⁹. In addition, protease inhibitors, the only class of drug that acts on post-integration stages of the viral life cycle, are only effective in macrophages at high concentrations that are at the upper limit of what is physiologically achievable⁸⁹. The ability of macrophages to support viral replication without cytopathic effects, increased macrophage longevity with HIV infection, and the decreased sensitivity to ART make macrophages an important mediator of persistent viremia in chronic HIV infection.

Tissue reservoirs of virus may be formed in anatomical sites where drug penetrance is low or immune responses are lacking, such as the CNS, genital tract, or bone marrow, which may lead to compartmentalized replication of virus¹³¹. In this thesis, we address the CNS as a site of ongoing inflammation and a viral reservoir. Several factors make the CNS a particularly well-suited anatomical reservoir of HIV: 1) low drug penetrance into the CNS termed CNS penetration-effectiveness (CPE), 2) the absence or restriction of normal immune responses, and 3) the presence of multiple target cells (perivascular

macrophages and microglia) that support productive infection. With ART, HIV decay is slower in the cerebrospinal fluid than in plasma in agreement with compartmentalized virus replicating in a long-lived cell type^{25,140}. This is pathologically important as increased compartmentalization of virus in the CNS has been associated with HIV-associated dementia (HAD)¹⁴¹. HIV is also able to infect bone marrow macrophages and multipotent hematopoietic precursor cells (HPC) and establish latent reservoirs in the bone marrow^{136,142}. HPC are able to differentiate into multiple hematopoietic lineages, and differentiation results in increased susceptibility to infection and increased viral replication^{136,142}. HIV-infected HPC may give rise to infected daughter cells, including monocytes/macrophages, that subsequently traffic through the periphery and infect tissues including the CNS^{39,42,48,51,52,56,88,142}. Sequestration of virus in anatomical reservoirs and dissemination of virus from these sites into the periphery is a potential mechanism of sustained viremia and a barrier to treatment in HIV infection.

V. Infection of monocytes and macrophages

In addition to CD4+ T-cells, monocytes and macrophages are targets of HIV and SIV infection and may be infected in the bone marrow, in the periphery, or in tissues (Figure 1.9)¹⁴³. Infection of the bone marrow, may contribute to changes in monocyte homeostasis including increased activation and accelerated turnover, which results in increased traffic of monocytes/macrophages to the CNS. In addition infection of monocytes or their progenitors may lead to dissemination of virus into the CNS (Figure 1.9)¹⁴³. Viral replication and accumulation of activated macrophages in the CNS contribute to the development of CNS disease.

A. Infection of the bone marrow

The primary targets of HIV and SIV infection in the bone marrow are macrophages and multipotent hematopoietic progenitor cells^{136,144,145}. Bone marrow macrophages are susceptible to infection by a broader range of HIV strains, including T cell tropic virus, than blood macrophages¹⁴⁵. Reports of infection of HPCs indicate that susceptibility to HIV is dependent on the level of maturation or lineage commitment of the HPCs¹⁴². Importantly, primitive hematopoietic stem cells are refractory to HIV-1 infection via a p21 dependent block prior to integration and inhibition of coreceptor binding by production of

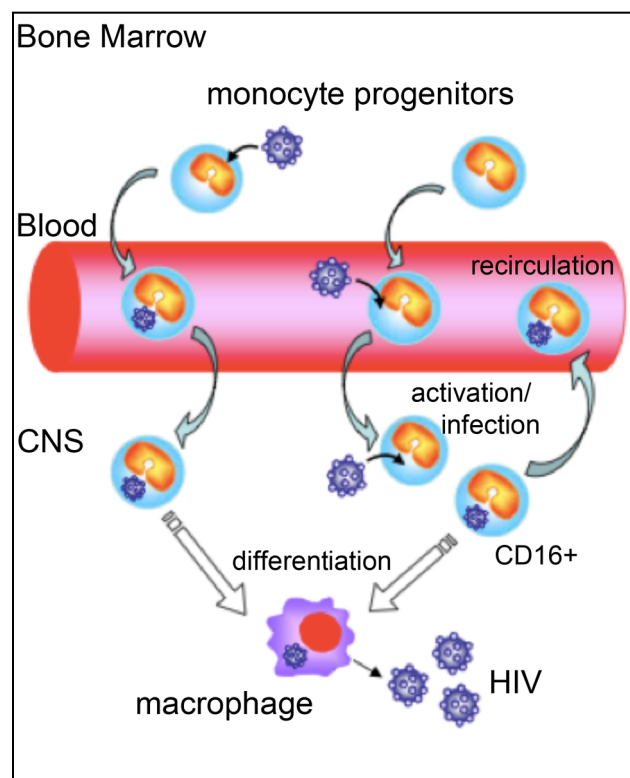


Figure 1.9. HIV-1 infection of monocytes and macrophages and systemic dissemination of virus

(adapted from Bergamaschi and Pancino *Retrovirol.* 2010)

CCR5 ligands^{136,146-148}. The clinical significance of HPC infection has been contested because HIV-infected CD34+ cells in the bone marrow are not universally observed *in vivo*¹⁴⁹⁻¹⁵¹. However, HIV infection of the bone marrow is associated with hematological abnormalities such as leukopenias, dysplasia, and anemia^{71,142}. These effects are thought to be directly mediated by both infectious virus and viral proteins interacting with hematopoietic progenitors and stromal cells in the bone marrow¹⁵²⁻¹⁵⁵. Changes to bone marrow homeostasis are also implicated in neuropathogenesis. Decreased bone marrow diffusivity and increased monocyte egress from the bone marrow are associated with the development of HIV dementia and SIV encephalitis^{42,71}. Also, sequence similarity between HIV isolated from the CNS and from bone marrow in a patient with HIV dementia suggests traffic of infected monocytes/macrophages from bone marrow may influence CNS disease¹⁵⁶. HIV infection of the bone marrow leads to altered hematopoiesis and potential dissemination of virus by infected daughter cells, which may negatively impact immune regulation of monocytes/macrophages and CNS pathology (Figure 1.9).

B. Infection of circulating monocytes

HIV can replicate in monocytes although the frequency of productively infected monocytes *in vivo* is low^{55,143,157,158}. HIV-1 replication in monocytes is restricted at or prior to reverse transcription; however, the block to infection is not absolute^{68,143,158}. Monocytes are refractory to HIV and SIV infection compared to macrophages, and susceptibility to infection has been shown to increase with maturation/differentiation¹⁵⁸⁻¹⁶⁰. Compared to macrophages, monocytes express higher levels of the restriction

factors APOBEC3A and 3G and lower levels of HIV coreceptor CCR5^{159,161}. CD16+ monocytes are more permissive to HIV and SIV infection compared to CD16- monocytes and are preferentially infected *in vivo*^{49,55}. This is due, in part, to higher expression of CCR5 and lower levels of the active form of the restriction factor APOBEC3G in CD16+ monocytes⁵⁵. In patients on ART, the mean half-life of HIV-1 DNA in monocytes was found to be greater than 40 months indicating persistent monocyte infection in spite of effective therapy¹⁶².

C. Infection of tissue macrophages

Macrophages from different donors are highly variable in the ability to replicate virus indicating that intrinsic genetic differences affect susceptibility to HIV-1 infection¹⁴³. Lentiviral infection of monocytes and macrophages occurs independently of cell division and requires the ability of the viral preintegration complex to cross the nuclear envelope, which is achieved through utilization of host factors such as transportin-SR2 and the nuclear envelope protein emerin^{86,163,164}. Infected macrophages appear to be resistant to both the cytopathic effects of lentiviral infection and immune detection and consequently may be long lived *in vivo*. Proposed mechanisms of the ability of infected monocytes and macrophages to avoid the immune response and cytopathic effects of viral replication include inhibition of apoptotic signaling, limited viral replication, and viral assembly at sites other than the cell surface^{86,98,165,166}. Infected macrophages contribute to HIV pathogenesis through production of toxic viral proteins and elaboration of inflammatory cytokines that increase local inflammation, recruit additional target cells, and increase viral replication^{39,87,97,98,167}. Infected macrophages are also able to transfer

virus directly to T cells¹⁶⁸⁻¹⁷⁰. Because HIV-infected macrophages are long lived they also contribute to the formation of a viral reservoir in the CNS. In Chapter 4 of this thesis, we characterize productive SIV infection in resident CNS macrophages present in the CNS prior to infection and in macrophages recruited to the CNS from the blood terminally with AIDS in animals with SIVE.

VI. Infection of the CNS

HIV and SIV are thought to enter the CNS through traffic of infected monocytes/macrophages. In the CNS perivascular macrophages and parenchymal microglia are the primary cell types that are productively infected. CNS inflammation is mediated in part by activated macrophages that replicate virus and produce proinflammatory and neurotoxic substances. Multiple populations of macrophages exist in the CNS and the ratio of macrophage subsets may influence disease progression. Importantly, multiple rounds of neuroinvasion and continued traffic of activated macrophages to the CNS terminally with AIDS may be required for the development of HIVE and SIVE. CNS macrophage recruitment, SIV neuroinvasion, and the role of macrophage subsets in the development of SIVE are investigated in Chapter 4.

A. Populations of CNS macrophages

CNS macrophages are comprised of parenchymal microglia and macrophages of the perivascular space, meninges, and choroid plexus^{57,88,171-173}. Microglia are embryonically derived and have negligible turnover in humans and nonhuman primates^{174,175}. Perivascular, meningeal, and choroid plexus macrophages are derived

from the bone marrow and turnover on the order of months to years^{88,171,176-180}. In the healthy CNS, both microglia and perivascular macrophages are immune reactive to the pan-macrophage marker CD68 (Figure 1.10). Recruited macrophages (CD163+CD68+) can be differentiated from microglia (CD68+CD163-) by expression of CD163, a type B scavenger receptor that is only expressed by perivascular macrophages (Figure 1.10)^{88,181,182}. CD14+CD16+CD163+ monocytes are thought to be the immediate precursors of CD163+ perivascular macrophages in the CNS^{88,183}. Importantly, hematogenous macrophages recruited to the CNS remain distinct from parenchymal

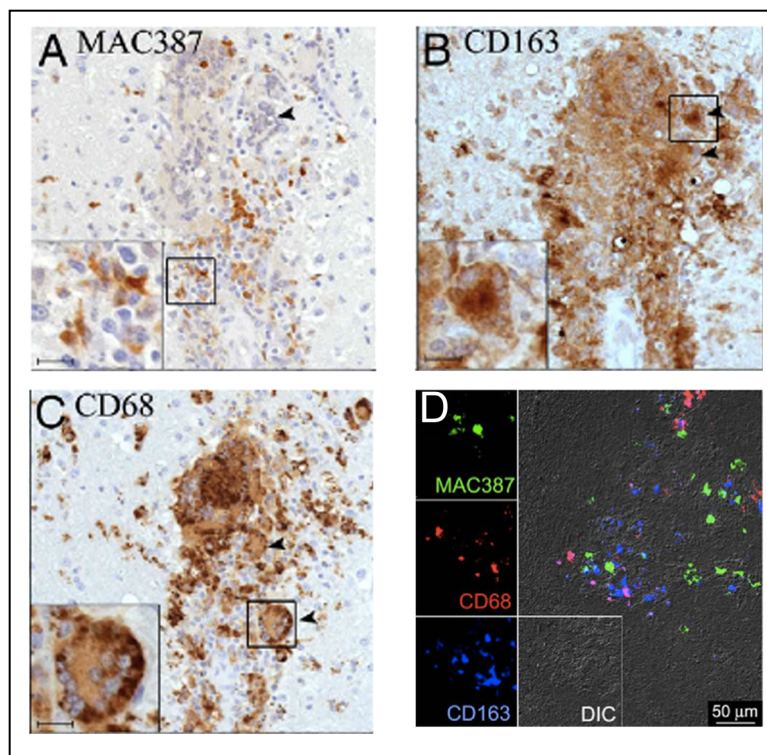


Figure 1.10. CD163+CD68+ perivascular macrophages, CD68+CD163- microglia and MAC387+ inflammatory macrophages are distinct populations present in the CNS with HIV and SIV infection

(adapted from Soulas et al. Am. J Pathol. 2011)

microglia in phenotype and CNS location^{88,173,181}. Microglia help maintain homeostasis in the CNS parenchyma and are necessary for normal glial function^{174,175}. Perivascular macrophages function in immune surveillance at the blood brain barrier and express proteins that suggest the ability to function as antigen presenting cells^{88,177,178}. A third population of inflammatory macrophages (MAC387+CD163-CD68-) that is immune reactive to the antibody MAC387, which recognizes MRP14 or the MRP8/MRP14 heterodimer, is not present in the healthy CNS but is recruited to the CNS with inflammation (Figure 1.10)^{181,184}. CD163+ perivascular macrophages and microglia are targets of HIV and SIV infection, but MAC387+ inflammatory macrophages are not (Figure 1.11)^{88,181,183,185}.

B. Viral neuroinvasion

HIV and SIV can be detected in the CNS within days to weeks of primary infection¹²⁻¹⁶. Seeding of the CNS with virus is thought to be mediated by the traffic of infected monocytes/macrophages into the CNS; although, the contribution of cell free virus to CNS infection cannot be excluded. CD163+ perivascular macrophages represent the primary cell type infected in the CNS^{88,183,185,186}. Also, parenchymal microglia extend foot processes that comprise part of the glia limitans and are therefore in direct contact with infected cells or virus in the perivascular space. Infected microglia are primarily observed only during end stage disease^{186,187}. During acute infection HIV DNA, RNA, and proteins are present in the CNS indicating productive infection. Inflammation of the choroid plexus and meninges can present with acute viremia, but is not thought to contribute to long-term viral pathogenesis in the CNS^{12,15,188-191}. Productive infection is

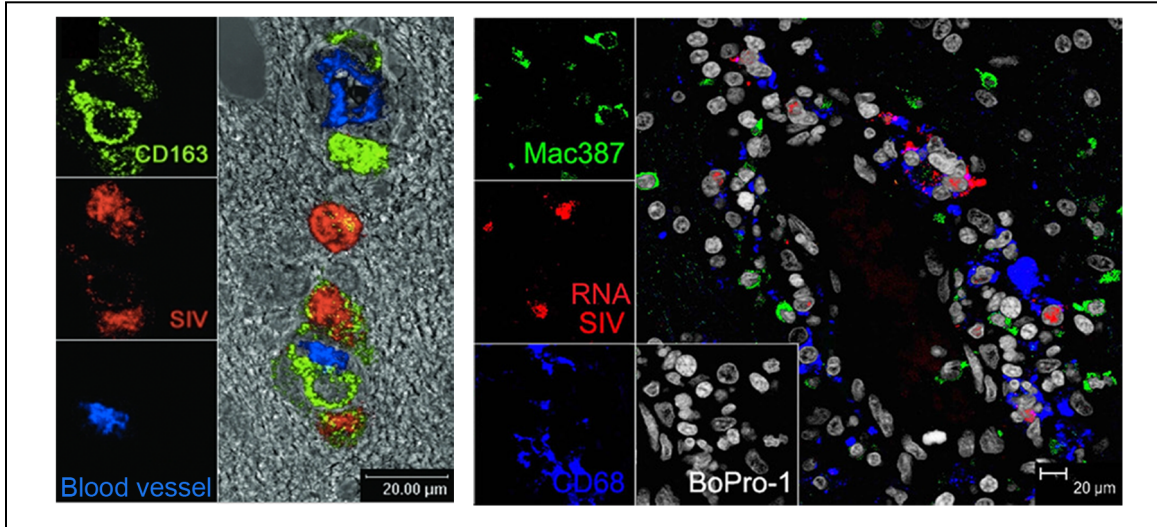


Figure 1.11. CD163+CD68+ perivascular macrophages and CD68+CD163- microglia, but not MAC387+ macrophages are targets of SIV infection

(adapted from Kim et al. Am J Pathol. 2006 and Soulas et al. Am. J Pathol. 2011)

not observed in the CNS during clinical latency. HIV-1 DNA has been detected in the CNS macrophages during the asymptomatic period, though it is not known if such provirus is replication competent or pathologically important^{186,189,192,193}. Extensive productive infection of the CNS is observed terminally with AIDS in ART naïve patients. It is not known whether productive CNS infection with AIDS is due to reemergence of virus seeded in the CNS during acute infection or reintroduction of virus via traffic of activated and infected monocytes/macrophages to the CNS during end stage disease.

C. AIDS neuropathogenesis and viral encephalitis

Mechanisms of neuropathogenesis

Infection of the CNS compromises normal function leading to a range of neurological disorders categorized as HIV-associated neurocognitive disorders (HAND):

asymptomatic neurocognitive impairment (ANI), mild neurocognitive disorder (MND, formerly MCMD), and HIV-associated dementia (HAD)¹⁹⁴. Anti-retroviral therapy initially decreased the apparent incidence of the most severe neurological complications^{2,195}. However, with increased longevity of HIV infected individuals on durable ART, the continued presence of HAD and the less fulminant MND indicate that CNS disorders are still clinically relevant^{2,195}. Neuroinflammation with AIDS is characterized by microglial activation, increased macrophage infiltration, focal accumulation of macrophages and multinucleated giant cells (MNGCs), atrophy of the cerebral cortex, myelin pallor, and loss of BBB integrity^{87,196-198}. The observation that neurological complications are associated with aging of the HIV-infected population suggests that neurodegeneration may be progressive.

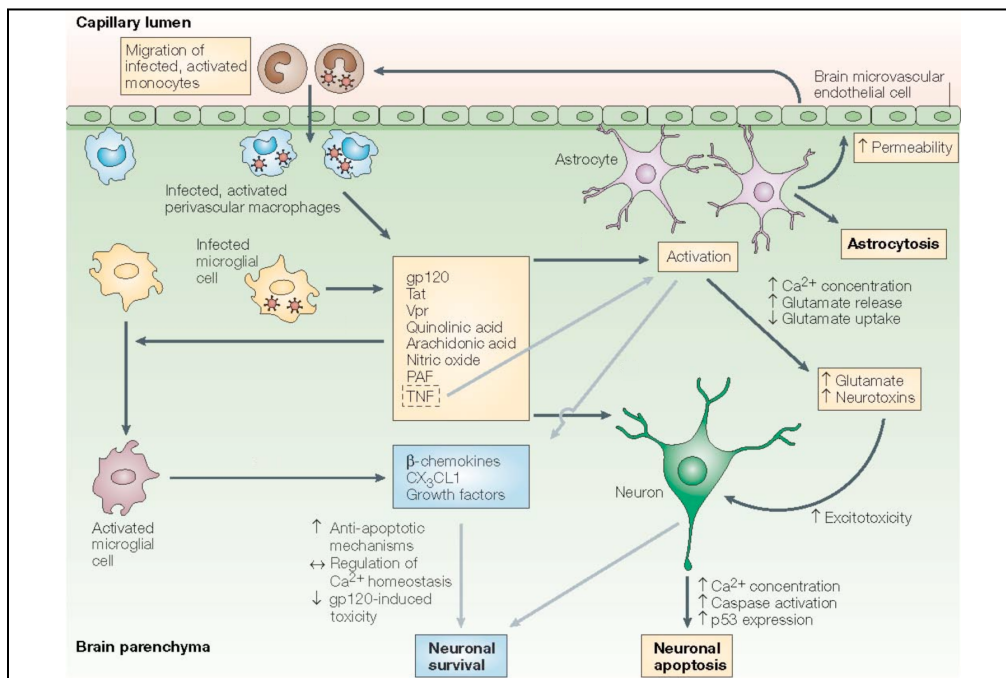


Figure 1.12. Mechanisms of neurodegeneration and neuroprotection in AIDS

(Gonzalez-Scarano and Martin-Garcia Nat. Rev. Immunol. 2005)

Neuronal damage in HIV infection of the CNS is not likely due to direct cytopathic effects of HIV infection as neurons are not productively infected *in vivo*. Traffic of activated monocytes from the periphery and infection of CNS macrophages result in the production of inflammatory cytokines, infectious virus, and viral proteins in the CNS (Figure 1.12)⁸⁷. Inflammatory mediators and viral proteins may exert direct effects on astrocytes, neurons, the vascular endothelium, and microglia (Figure 1.12)¹⁹⁹. Neuronal apoptosis can be induced by exposure to tumor necrosis factor (TNF) and the viral proteins gp120, Tat, and Vpr (Figure 1.12)^{87,200-203}. Additionally, activation of astrocytes alters calcium and glutamate homeostasis potentially leading to increased neuronal excitotoxicity and apoptosis (Figure 1.12). Macrophage-mediated inflammation in the CNS can be elaborated through bystander macrophages (Figure 1.12). Additionally, loss of BBB integrity, endothelial activation, and production of chemoattractant cytokines provide a mechanism of continued recruitment and accumulation of activated monocytes and macrophages. Microglia are also targets of HIV infection and may contribute to neuropathogenesis, but also maintain homeostasis in the normal CNS. As such, microglia (and recruited macrophages?) may also be able to produce chemokines and growth factors that inhibit cellular activation and apoptosis and contribute to neuronal survival (Figure 1.12)^{204,205}.

HIV and SIV encephalitis

HIV encephalitis is the histopathological correlate of HIV-associated dementia (HAD), the most severe form of HAND^{194,206}. Necropsy tissues from HIVE cases have evidence of viral replication in the CNS, focal accumulation of activated macrophages (HIVE

lesions), and multinucleated giant cells^{12,195-198,206,207}. In macaques SIV encephalitis (SIVE) is associated with rapid disease progression and death⁸⁰. The number of activated macrophages in the CNS is a better correlate of HAD than the number of productively infected macrophages¹⁹⁸. This suggests that chronic immune activation in the CNS may contribute to the development of HIVE and SIVE. HIV-1 neuroinvasion during acute viremia coincides with intrathecal immune activation that persists throughout HIV-1 infection^{12,15}. Ongoing inflammation may be the result of low-level viral replication and persistent immune activation in the CNS, although productive infection of the CNS is not detected during clinical latency or in virally suppressed individuals. In the blood, greater numbers of circulating monocytes, increased monocyte activation, and expansion of monocytes from the bone marrow correlate with the development of HIVE (pre-ART) or SIVE^{42,71,93,198,206,208}. Thus, increased traffic of activated macrophages to the CNS, some of which may be infected, is likely another mechanism by which ongoing inflammation is maintained in the CNS. Additionally, increased compartmentalization of virus in the CNS during end stage disease is also associated with the development of HAD¹⁴¹. Thus, reintroduction of virus into the CNS terminally with AIDS may be necessary to drive HIVE.

We have previously shown animals with severe SIVE had higher ratios of CD68+ to MAC387+ macrophages in SIVE lesions and more extensive viral replication compared to animals with mild SIVE¹⁸¹. MAC387+ macrophages may be considered to be classically activated, M1-polarized macrophages that mediate proinflammatory responses favoring an anti-microbial microenvironment. In contrast, CD68+

macrophages may be considered to be alternatively activated, M2-polarized macrophages that favor resolution of inflammation and are able to support viral replication^{181-183,209}. The existence of multiple macrophage subsets with contrasting function have been widely reported in sterile inflammation, infection, and wound repair^{83,181,184,210-214}. Importantly, proper coordination of M1 and M2 responses may be necessary to remove the inflammatory insult and remediate injured tissue^{213,215}. Thus SIV inflammation in the CNS may share general features with the normal immune response to infection or injury. The development of HIVE may reflect a lack of proper resolution of the inflammatory response in the CNS, likely due to chronic infection and increased macrophage activation as the immune system compensates for the loss of CD4+ T-lymphocyte mediated immunity.

D. PCNA expression in CNS macrophages

Studies investigating local macrophage proliferation as a source of macrophage accumulation with HIV and SIV infection found that CNS macrophages lack standard markers of proliferation (Ki67, Topoisomerase IIa, BrdU uptake) but do express proliferating cell nuclear antigen (PCNA)²¹⁶⁻²¹⁸. PCNA expression is detected in CD68+ macrophages in the perivascular space and in HIVE and SIVE lesions (Figure 1.13)^{216,217}. PCNA expression is also associated with productive HIV and SIV infection in the same cell (Figure 1.13)^{216,217}. PCNA is a processivity factor for DNA polymerase delta during cellular division, but is also involved in DNA damage repair (DDR) and p53 dependent cell survival pathways in non-dividing cells²¹⁹⁻²²². It is not known whether PCNA is expressed by CNS macrophages prior to or as a result of HIV and SIV

infection. Studies investigating the specific role of PCNA in HIV and SIV infection of macrophages have not been done.

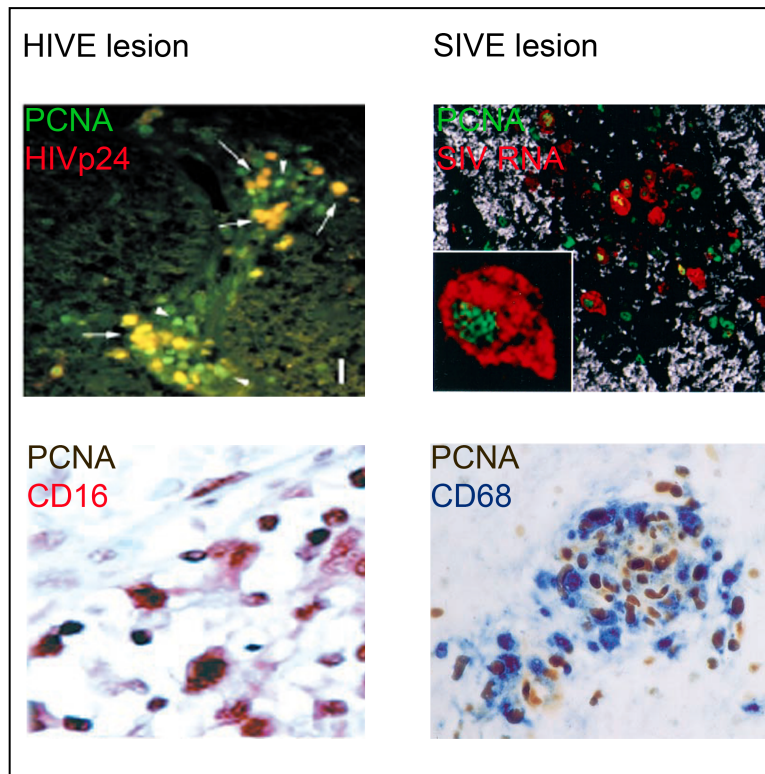


Figure 1.13. PCNA expression by macrophages in HIVE and SIVE lesions is associated with productive infection

(adapted from Williams et al. Am. J Pathol. 2002 and

Fisher-Smith et al. Am. J Pathol. 2004)

PCNA expression in productively infected macrophages may indicate a mechanism of preferential infection of CD68+ macrophages in the CNS. During proviral integration, viral integrase trims the 3' ends of the viral DNA and creates double strand breaks in the host DNA where the provirus is inserted²²³⁻²²⁵. The resulting DNA lesion is repaired by

the host DDR machinery^{224,226}. Induction of DDR in response to double-strand breaks has been shown to increase lentiviral transduction^{227,228}. Thus, PCNA expression may be associated with induction of DDR pathways that facilitate viral integration into the host genome. Alternatively, DDR pathways may recognize the incoming provirus as a DNA lesion and inhibit integration^{224,229}. Evidence for this includes previous reports that PCNA-associated proteins p21, Rad18, and Rad52 attenuate HIV infection^{147,230-232}.

It has also been proposed that induction of cell survival pathways may explain retention of HIV+PCNA+ macrophages in the CNS²¹⁷. PCNA is induced downstream of p21 and p53 in response to genotoxic stress and is associated with inhibition of apoptosis^{233,234}. HIV infection increases macrophage longevity *in vitro* and reduces the frequency of apoptotic CD68+ macrophages in the CNS^{165,235}. Accumulation of macrophages in HIVE and SIVE lesions may therefore be mediated in part by inhibition of apoptosis in subpopulations of CNS macrophages. PCNA expression in monocytes and CNS macrophages and the role of PCNA induction in macrophage infection are investigated in Chapter 5.

VII. Summary

As innate immune cells and targets of HIV infection, monocytes and macrophages are important in HIV pathogenesis. Monocytes and macrophages are heterogeneous and are comprised of phenotypically distinct subpopulations that differ in immune function and susceptibility to infection. Increased monocyte egress from the bone marrow and expansion of activated monocyte subsets in the blood correlate with increased

monocyte traffic to the CNS and the development of HIVE and SIVE. Infection of the CNS is associated with persistent macrophage activation and inflammation that contribute to the development of CNS disease. In the CNS, CD163+ perivascular macrophages and CD68+ parenchymal microglia are productively infected, whereas MAC387+ inflammatory macrophages are not. Productive infection of CNS macrophages correlates with PCNA expression in the same cell. In end stage disease, HIVE (pre-ART) and SIVE are characterized by viral replication, increased numbers of activated macrophages, and focal accumulation of macrophages in HIVE lesions. Thus, HIV infection is associated with changes in the biology of monocytes and macrophages that contribute to the development of CNS disease and HIVE.

This thesis investigates the biology of monocytes and macrophages in rhesus macaques using a rapid model of neuroAIDS. In these studies we characterize the gene expression profiles of classical, intermediate and nonclassical monocytes and investigate changes in gene expression that occur in each subset with SIV infection (Chapter 3). Additionally, we investigate the relationship between SIV infection, monocyte activation, CNS macrophage recruitment, viral neuroinvasion, and the development of SIVE (Chapter 4). Finally, we characterize PCNA expression within monocyte and macrophage subsets *in vivo* and investigate the role of PCNA in macrophages with regard to viability and the ability to promote or inhibit SIV infection (Chapter 5).

Chapter 2. Materials and methods

Ethics Statement

All animals were handled in accordance with good animal practice as defined by the Tulane National Primate Research Center's Institutional Animal Care and Use Committee (IACUC). All animal work was approved by this committee and the IACUC of Boston College.

Animals, viral infection, and CD8+ T-lymphocyte depletion

Twelve adult male rhesus macaques were infected intravenously with 1ng of SIVp27 of SIVmac251, a generous gift from Dr. Ronald Desrosiers (New England Regional Primate Research Center). CD8+ lymphocytes were depleted in order to achieve rapid AIDS (3-4 months) with greater than 75% incidence of SIV encephalitis (SIVE)^{42,43,52,181}. While there is an increase in the number of monocytes/macrophages and virus in the CNS of CD8+ Lymphocyte depleted animals compared to non-depleted animals, with AIDS and SIVE, the pathology is the same. The chimeric anti-CD8 antibody cM-T807 (NIH Non-human Primate Reagent Resource) was administered s.c. (10mg/kg) at 6 days post infection (dpi) and *i.v.* (5mg/kg) on 8 dpi and 12 dpi^{42,91}. Complete blood counts and flow cytometry to monitor leukocyte populations and CD8+ lymphocyte depletion were performed prior to infection and weekly thereafter. Blood and cerebrospinal fluid were sampled weekly, and CNS and other tissues were collected at necropsy. Choroid plexus tissue was available from 7 of the 12 animals.

SIV-infected animals were sacrificed with any of the following criteria, indicative of AIDS when present: >15% decrease of body weight in 2 weeks or >30% decrease of body weight in 2 months; documented opportunistic infection; persistent anorexia >3 days without explicable cause; severe, intractable diarrhea; progressive neurological symptoms; significant cardiac or pulmonary symptoms. Prior to sacrifice, animals were anesthetized with ketamine-HCl and euthanized by an intravenous pentobarbital overdose and exsanguinated. A post mortem diagnosis of AIDS was confirmed by the presence of AIDS defining lesions including: Pneumocystis pneumonia, Mycobacterium avium infection, and intestinal adenovirus infection. SIVE was defined by the presence of multinucleated giant cells (MNGCs), accumulation of macrophages in the CNS, and productive viral infection^{42,80,207,236}.

BrdU administration to SIV infected animals

A stock solution of 5-bromo-2'-deoxyuridine (BrdU, 30 mg/mL, Sigma-Aldrich) was prepared in calcium and magnesium free PBS (U.S.P. grade) as previously described^{52,237}. BrdU was administered as an *i.v.* injection at a dose of 60 mg BrdU/kg body weight. BrdU was administered either at: 1) 6 dpi and 20 dpi (termed "Early") or 2) 49 dpi and 48 hours prior to necropsy (termed "Late"). The percentage of BrdU+ monocytes was determined by flow cytometry 24h post-administration.

Tissue collection at necropsy

Necropsy tissues were either: 1) collected in 10% neutral buffered formalin and embedded in paraffin, 2) fixed with 2% paraformaldehyde for 4h and embedded in

optimum cutting temperature compound (OCT, Miles Scientific), or 3) embedded in OCT without fixation and snap-frozen. Formalin-fixed, paraffin-embedded tissues were cut into 5 μ m thick sections and frozen tissues were sectioned at 10 μ m. CNS tissues from three uninfected control animals which received autologous CD34+ bone marrow stem cells transduced with an EGFP-expressing lentiviral construct were used to determine basal turnover of CNS macrophages¹⁷⁹.

Viral load determination

SIV RNA in the plasma was quantitated by real-time PCR as previously described.²³⁸ SIV virions were pelleted from 0.5ml EDTA plasma by centrifugation at 20,000 g for 1 hour. The fluorescently labeled, real-time PCR probe employed contained a non-fluorescent quencher, BHQ-1, at its 3' end. The threshold of sensitivity was 100 copy equivalents/mL, with an average interassay coefficient of variation of less than 25%.

Isolation of monocyte subpopulations for microarray analysis

Prior to infection, at 26 dpi, and at necropsy, mononuclear cells were isolated from 10mL EDTA treated whole blood (n = 4 animals: CM07, DB79, FD05, FB92) by density gradient centrifugation over Ficoll-Hypaque (GE Healthcare). Buffy coats were collected and washed in calcium and magnesium free PBS and stained for 15 minutes with anti-CD14-PacificBlue, anti-CD16-PE, anti-HLA-DR-PerCP-Cy-5.5, anti-CD3-FITC, and anti-CD20-APC (BD Biosciences) in PBS containing 2% FBS. Monocytes were isolated by forward and side scatter characteristics and CD14 antigen expression. HLA-DR+CD3-CD20- cells were selected to exclude B-cells and T-cells. Non-overlapping

populations of classical, intermediate, and nonclassical monocytes were isolated based on expression of CD14 and CD16 on a BD FACS ARIA (BD Biosciences). FACS isolated monocytes were washed in PBS to remove residual FACS buffer and vacuum pelleted to preserve RNA integrity.

Microarray processing

RNA extraction, labeling, and hybridization were performed by the Beth Israel Deaconess Medical Center Genomics Core Laboratory as previously described^{239,240}. Briefly, total RNA was extracted with TRIzol (Life Technologies) according to the manufacturer's instructions. RNA quality at all steps was assayed on an Agilent 2100 Bioanalyzer (Agilent Technologies). RNA (>500pg) was amplified using the Ovation pico WTA system (NuGEN Technologies Inc.). 20 µg cRNA was fragmented as described and hybridized with a preequilibrated Affymetrix GeneChip Rhesus Macaque Genome Array (Affymetrix) at 45°C for 16 hours. After the hybridization cocktails were removed, the chips were washed, stained, and scanned according to the manufacturer's protocols as previously described²³⁹.

Microarray data analysis

The gene expression data generated (>47,000 rhesus transcripts interrogated per array) were analyzed with Partek Express Genomics Suite software (Partek Inc.). The data were normalized by using a robust multi-chip average (RMA) algorithm^{241,242}. Due to the low abundance of the nonclassical monocyte subset, insufficient RNA was isolated from this population at preinfection from animals FD05 and FB92, and at necropsy from

animal CM07. These samples did not meet quality control parameters and were excluded from further analysis.

Probe sets with a significant p-value corrected with a 5% false discovery rate between monocyte subset or SIV infection timepoint were filtered based on a fold change $\geq |2|$. Probe sets were annotated with the human official gene symbol based on information provided by the manufacturer and supplementary annotation data from the Norgren lab, which collaborated in the development of the Affymetrix rhesus macaque genome array (<http://www.unmc.edu/rhesusgenechip/#RhesusGeneChip>). Heatmaps were generated using dChip software²⁴³. Gene lists were subjected to functional annotation clustering with DAVID bioinformatics tools to identify enrichment clusters associated with specific biological processes according to gene ontology annotations^{244,245}.

Quantitative real time PCR for microarray validation

RNA from each sample was extracted with TRIzol as indicated above. First strand cDNA was generated from >40ng total RNA with Superscript III first strand synthesis kit (Invitrogen). Quantitative real-time PCR was performed on 3ng of cDNA with the Platinum qPCR SuperMix-UDG kit (Invitrogen) using a Step One Plus system (Life Technologies). Samples were analyzed in duplicate and normalized to the GAPDH housekeeping gene. Relative gene expression was determined using the $\Delta\Delta CT$ method and converted to arbitrary units relative to a reference RNA sample from pooled CD14+ monocytes. qPCR expression data were correlated with normalized log₂ expression

data from the microarray also normalized to GAPDH. Oligonucleotides (IDT Inc.) used are listed in Table 2.1.

Dextran uptake by uninfected monocytes

EDTA anti-coagulated whole blood from uninfected rhesus macaques (n = 6 animals) was incubated with fluorescein-conjugated dextran (1mg/mL) (Molecular Probes) for 15 minutes at 37°C. Erythrocytes were lysed using the ImmunoPrep Reagent System (Beckman Coulter), washed twice with PBS containing 2% FBS and incubated for 15 minutes at room temperature with fluorochrome-conjugated surface antibodies: anti-HLA-DR-ECD (Immu-357, Beckman Coulter), anti-CD16-PE-Cy7 (3G8, Biolegend), anti-CD3-APC (SP34-2, BD Biosciences), anti-CD8-APC (RPA-T8, BD Biosciences), anti-CD20-APC (2H7, BD Biosciences) and anti-CD14-Pacific blue (M5E2, BD Biosciences). Data were acquired on a BD FACS Aria (BD Biosciences) and analyzed with Flow Jo version 8.7 (Tree Star Software).

Intracisternal injection of dextran amines and detection in CNS tissues

Animals were tranquilized with ketamine or telazol and anesthetized with sodium pentobarbital. One milliliter of dextran amines (25mg/mL) dissolved in 0.9% saline was injected into the cerebellomedullary cistern using a stereotaxic apparatus. Following intracranial injection, the hydrophilic fluorescent dextran dyes diffuse along the perivascular space and are taken up by essentially all perivascular macrophages (>98%) via nonspecific micropinocytosis^{88,176,177}. To establish a baseline for subsequent turnover, all animals (n=12) received fluorescein-conjugated dextran (abbreviated

“Dextran:FITC”, Molecular Probes) at 20 dpi (Table 4.1). Five animals received a second injection of Alexa Fluor647-conjugated dextran (abbreviated “Dextran:AF647”, Molecular Probes) 48h prior to necropsy to determine macrophage recruitment from 20 dpi to necropsy. Four additional animals received a second injection of Alexa Fluor 647-conjugated dextran at 49 dpi and a third injection of biotinylated dextran (Molecular Probes) 48h prior to necropsy to determine macrophage recruitment from 20 dpi to 49 dpi and 49 dpi to necropsy, respectively (Table 4.1).

Immunofluorescence microscopy

Fixed tissue samples on slides were washed and permeabilized with PBS containing 0.2% fish skin gelatin (Sigma-Aldrich), and 0.1% Triton X-100 (Sigma-Aldrich).

Nonspecific binding was blocked with 10% normal goat serum (Invitrogen) and 2% normal human serum (Valley Biomedical Inc.) in wash buffer. Alexa Fluor 568- or Alexa Fluor 350-conjugated secondary antibodies were used to detect primary antibodies according to standard protocols⁸⁸. Background endogenous autofluorescence was reduced by incubating sections with 50 mM CuSO₄ as previously described prior to mounting in Prolong Gold Antifade reagent (Invitrogen) with DAPI (4',6-Diamidino-2-Phenylindole, Dihydrochloride)²⁴⁶. Slides were viewed on a 4-color Zeiss Axio Imager M1 microscope (Carl Zeiss MicroImaging, Inc.).

For the dextran dye studies, antibodies against macrophage markers anti-CD163 (EDHu-1, AbD Serotec) and anti-myeloid histiocyte antigen (MAC387, DAKO), or

against viral capsid anti-SIVp28 (3F7, Fitzgerald Industries) were used. For PCNA *in vitro* studies anti-PCNA (PC10, DAKO) was used.

Detection and enumeration of dextran labeled macrophages

The fluorescent dextran conjugates are directly visualized by fluorescence microscopy in sections of paraformaldehyde-fixed, OCT-embedded frozen tissue after washing and mounting as above. Biotinylated dextran was detected with streptavidin conjugated to Alexa Fluor 568 or Alexa Fluor 647 (Invitrogen). Dextran dye labeled macrophages in CNS tissues were counted by sampling 3000-4000 cells from frontal, temporal, and parietal cortices; 1000 cells from meninges; and 2 sections of choroid plexus per animal. Additionally, 10 or more SIVE lesions were evaluated for animals with AIDS and SIVE (n=5). For one of the SIVE animals, only three SIVE lesions were found in the frozen tissue available; this animal was excluded from the analysis of macrophage turnover in SIVE lesions.

Single and double label immunohistochemistry

Immunohistochemistry was performed in formalin-fixed paraffin embedded tissues. For BrdU staining, tissue sections were treated with antigen unmasking solution (Vector Labs). A dual endogenous enzyme block (DAKO) and serum-free protein block (DAKO) was applied prior to immunostaining followed by visualization with EnVision+ horseradish peroxidase (HRP) system (DAKO) using DAB (3,3'-diaminobenzidine tetrahydrochloride) as the chromogen. For detection of two epitopes, the EnVision G2 doublestain system (DAKO) was used with DAB as the HRP substrate and Vector Blue

(Vector Labs) or permanent red (DAKO) as the alkaline phosphatase substrate. Isotype-matched immunoglobulin (DAKO) served as controls. Tissue sections were visualized using a Zeiss Axio Imager M1 microscope using Plan-Apochromat 620/0.8 and 640/0.95 Korr objectives.

For the dextran dye studies, anti-CD163 (EDHu-1, AbD Serotec), anti-myeloid histiocyte antigen (MAC387, DAKO), and anti-BrdU (Bu20a, DAKO) were used to determine macrophage accumulation and the phenotype of BrdU-labeled macrophages. More than twenty, 20x fields were examined from each of three cortical sections with associated meninges, and one section of choroid plexus per animal for each stain. For PCNA studies, CNS tissues were stained with anti-PCNA (PC10, DAKO) and either anti-BrdU (Bu20, DAKO), anti-myeloid histiocyte antigen (MAC387, DAKO), or anti-CD163 (EDHu-1, AbD Serotec). For each of 4 SIVE animals, SIVE lesions from 3-5 cortical sections were counted for each stain.

Isolation of primary monocytes for *in vitro* PCNA studies

Blood from uninfected and SIV-infected animals was obtained by venipuncture, collected in EDTA, and processed within six hours. Whole blood was diluted with Ca/Mg-free PBS (Thermo Scientific) and PBMCs were obtained by centrifugation over Ficoll-Hypaque (GE Healthcare). CD14⁺ monocytes were isolated from total PBMCs with anti-CD14 immunomagnetic beads according to the manufacturer's instructions (Miltenyi Biotech). CD14⁺ purity was determined by labeling with anti-CD14-Pacific Blue antibody (M5E2, BD Biosciences). Samples were acquired on a BD FACS Aria (BD

Biosciences) and analyzed with Flow Jo version 8.7 (TreeStar Software). Samples with less than 90% purity were not used. Mean CD14+ purity was $94 \pm 0.8\%$ (Mean \pm SEM).

Western Blotting for PCNA studies

All steps prior to SDS-PAGE were performed at 4°C. Cells were lysed in RIPA buffer (50mM Tris HCl, 150mM NaCl, 1% Triton X-100, 0.5% sodium deoxycholate, 0.1% SDS) containing complete protease inhibitor cocktail (Roche). Lysates were sonicated to free nuclear proteins and incubated at 4°C for 30 minutes. Insoluble material was removed by centrifugation and total protein was quantified by Bradford assay.

Approximately 20µg of total lysate was resolved on a 4-15% polyacrylamide gel (BioRad). Protein was transferred to Hybond-ECL membrane (GE Healthcare) blocked with 5% nonfat milk and probed for PCNA (PC10, Chemicon). HRP conjugated goat anti-mouse antibody (Jackson Labs) was used to detect the primary antibody, and the chemiluminescence reaction was performed with Supersignal West Pico kit (Thermo Scientific). Hybond autoradiography film (Denville Scientific) was exposed to the labeled blots and developed with an X-OMAT 2000A processor (KODAK). Blots were stripped in 0.2M NaOH in PBS for 30 minutes, washed extensively, and re-blocked with 5% nonfat milk. Anti-actin (Thermo Scientific) was used as the loading control. Bands were quantitated using Image J software (NIH).

Quantitative real time PCR for PCNA

RNA was extracted with RNeasy micro kit (Qiagen) according to the manufacturer's instructions. First strand cDNA was generated from approximately 100ng total RNA with

Superscript III first strand synthesis kit (Invitrogen). Quantitative real-time PCR was performed on approximately 25ng cDNA with the Platinum qPCR SuperMix-UDG kit (Invitrogen) using a Step One Plus system (Applied Biosciences). Samples were analyzed in duplicate and normalized to the GAPDH housekeeping gene. Relative gene expression was determined using the $\Delta\Delta CT$ method. Oligonucleotides (IDT Inc.) used are listed in Table 2.1.

Cell culture for *in vitro* PCNA studies

Cells were cultured in treated polystyrene plates or flasks (Costar) or in chamber slides (Lab-Tek). CD14⁺ monocytes were cultured in RPMI 1640 (Thermo Scientific) with 10% fetal bovine serum (Atlas Biologicals) and 10ng/mL recombinant, human macrophage colony stimulating factor (M-CSF, Peprotech). 293T cells were maintained in DMEM (Cellgro) with 10%FBS.

Production of SIVmac316-E767* viral stocks for *in vitro* PCNA studies

High titre viral stocks were produced by transfecting 5ug of proviral plasmid into 2×10^6 293T cells in a T75 flask using a calcium phosphate transfection kit (Profection, Promega) according to the manufacturer's instructions. The medium was changed daily and virus containing medium was harvested at 72h post transfection. The amount of virus was quantitated by SIVp27 ELISA (ABL).

siRNA knockdown assays

Two siRNA constructs specific for human PCNA were used in this study (Qiagen). One construct, designated siRNA-5, had the same sequence as the *Macaca mulatta* PCNA reference sequence: sense 5'-(GGA UCU UAG GCA UUC UUA ATT)-3'; antisense 5'-(UUA AGA AUG CCU AAG AUC CTT)-3'. The second construct, designated siRNA-6, had a single basepair mismatch (in bold) relative to the *Macaca mulatta* PCNA reference sequence: sense 5'-(GGA UUU **AGA** UGU UGA ACA ATT)-3', antisense 5'-(UUG UUC AAC AUC **UAA** AUC CAT)-3'. A proprietary nonsilencing control, designated siRNA-NS, was used as a control (Allstars Negative siRNA, Qiagen).

CD14⁺ monocytes were cultured with M-CSF for 5 days to yield monocyte-derived macrophages (MDM) and replated at 3×10^5 cells/well in a 12 well plate. Oligofectamine (Invitrogen) was used to transfect 100 pmol PCNA-specific or control siRNA per well according to the manufacturer's instructions. The procedure was repeated the next day to increase the transfection efficiency. The following day macrophages were infected (20ng SIVp27/well) with SIVmac316-E767*, a macrophage tropic variant with a high replicative capacity (hereafter called SIV316*)²⁴⁷. At 1 dpi, the medium was changed and the cells were washed to remove the inoculum. Protein RNA and culture supernatants were harvested at 3 dpi. Viral replication was quantitated by SIVp27 ELISA. Three experiments were performed in triplicate

TUNEL staining

TUNEL (Terminal deoxynucleotidyl transferase dUTP nick-end labeling) staining to detect apoptotic cells was performed using the ApopTag Fluorescein kit (Millipore) according to the manufacturer's instructions. Incorporation of fluorescein-conjugated nucleotides allows for direct detection of apoptotic nuclei by immunofluorescence. Nuclei were counterstained with DAPI.

sCD163 and SIVp27 ELISA

ELISA kits for soluble CD163 (Trillium Diagnostics) and SIVp27 (Advanced Bioscience Laboratories) were used according to the manufacturers' protocols as previously described^{42,248,249}. Briefly, plasma (sCD163) or culture supernatant (SIVp27) were added to the ELISA plate for 1h. Bound antigen was detected using HRP conjugated detection antibodies. TMB was used as the chromogenic substrate. Protein concentration was determined by measuring the 450nm absorbance versus a reference standard.

Table 2.1 Sequence of oligonucleotides used for qRT-PCR

Target	Sequence (5' – 3')
CD14	
Forward	CCGAGATGTATGTGGTCCAG
Reverse	GATCGAGCACTCTGAGCTTG
Probe ^a	AGCGCCCTAAACTCCCTCAATCTGT
CD16	
Forward	GCTCCGGATATCTTTGGTGA
Reverse	AGCACCTGTACCATTGAGG
Probe ^a	TTTCAGCTGGCATGCGGACTGAAGAT
S100A9	
Forward	GGACACAAATGCAGACAAGC
Reverse	AGACCTGGCTTATGGTGGTG
Probe ^a	AGTTCATCATGCTGATGGCGAGGCTA
CCR2	
Forward	CTTCTTCATCATCCTCCTGA
Reverse	GAATCTTCTTCCTGGCATT
Probe ^a	TGGTTGGTGGCTGTGTTTGCTTCTGT
PCNA	
Forward	GCGGAGCAGAGTGGTAGTTC
Reverse	GCCTCCAACACCTTCTTCAG
Probe ^a	ACCGGCTACACTTTCCTCCT
GAPDH	
Forward	GCACCACCAACTGCTTAGCAC
Reverse	TCTTCTGGGTGGCAGTGATG
Probe ^a	TCGTGGAAGGACTCATGACCACAGTCC

a. Probes were modified with 5'– (6-carboxyfluorescein) and 3'– (tetramethylrhodamine) as the fluorophore and quencher respectively.

Chapter 3. Monocyte subsets exhibit transcriptional plasticity and a shared response to interferon in SIV-infected rhesus macaques

Chapter Overview

The progression to AIDS is associated with phenotypic and functional alterations to monocyte biology and is influenced by the relative proportion of heterogeneous monocyte subsets. Classical (CD14⁺⁺CD16⁻), intermediate (CD14⁺⁺CD16⁺), and nonclassical (CD14⁺CD16⁺⁺) monocytes are distinct populations that may represent progressive stages of monocyte maturation or disparate myeloid lineages with different turnover rates and function. To investigate the relationship between monocyte subsets and differences in the response to SIV infection, we conducted a microarray analysis of the monocyte subsets in rhesus macaques at three timepoints: 1) prior to SIV infection, 2) at 26 days post infection, and 3) necropsy terminally with AIDS. Transcripts that identify classical and nonclassical monocytes in humans and mice were conserved in rhesus macaques. We found that the majority of markers that differentiate monocyte subsets in uninfected animals are not differently expressed between monocyte subsets in SIV-infected animals. We found that classical monocytes expressed transcripts associated with cell proliferation, wound repair, and responses to immune stimuli, while nonclassical monocytes expressed transcripts associated with macrophage phenotype, withdrawal from cell cycle, and immune effector functions. Intermediate monocytes were more similar to classical monocytes than nonclassical monocytes overall, but showed increased transcriptional similarity to nonclassical monocytes terminally with AIDS. Changes to monocyte gene expression occurred within weeks of primary infection and

were sustained throughout the course of infection. Transcripts associated with innate immune responses, particularly interferon stimulated genes, were induced in all monocyte subsets in SIV infected animals. These studies indicate that the set of genes expressed by each monocyte subset is altered with SIV infection, but each subset retains its putative functional characteristics. Additionally, the innate immune response to SIV infection, including induction of interferon stimulated genes, is conserved across monocyte subsets.

Monocyte populations expand with SIV infection

The absolute number and relative percentage of each monocyte subset were determined for each animal (n = 4): 1) prior to infection, 2) at 26 dpi when increased monocyte egress from the bone marrow is initially observed, and 3) at necropsy, terminally with AIDS (Table 3.1). At the same time points, monocytes were isolated from each of the four animals for gene expression analysis. Prior to infection, classical monocytes accounted for 196 ± 56 cells/ μ L ($87.7 \pm 4.3\%$ of total monocytes), intermediate monocytes were 18 ± 4 cells/ μ L ($7.8 \pm 1.2\%$ of total monocytes), and nonclassical monocytes were 11 ± 5 cells/ μ L ($4.4 \pm 1.5\%$ of total monocytes) (Table 3.1). With SIV infection, the absolute number of each of the three monocyte subpopulations increased as well as the percentage of both intermediate and nonclassical monocytes. At 26 dpi, classical, intermediate and nonclassical monocytes expanded to 332 ± 40 cells/ μ L ($73.9 \pm 3.4\%$), 87 ± 16 cells/ μ L ($19.3 \pm 3.1\%$, $p = 0.03$ 26 dpi vs. preinfection), and 34 ± 15 cells/ μ L ($6.8 \pm 2\%$) respectively (Table 3.1). An increased absolute number of monocytes was also observed at necropsy terminally with AIDS: classical monocytes

329 ± 75 cells/μL (74.1 ± 10.7%), 103 ± 60 cells/μL (16.9±6.1%), and 79 ± 70 cells/μL (9.0 ± 6.1%) (Table 3.1). These data indicate that the absolute number of total monocytes increases with SIV infection and that intermediate and nonclassical monocytes account for a greater percentage of total monocytes in SIV-infected animals compared to uninfected animals.

Isolation of monocyte populations and microarray analysis

To collect samples for microarray analysis, peripheral blood mononuclear cells were isolated from EDTA anti-coagulated whole blood, and the three monocyte subsets were collected by fluorescence activated cell sorting (FACS) (Table 3.1, Figure 3.1A).

Monocytes were selected based on high forward scatter and low side scatter and HLA-DR expression. CD3 and CD20 were used to exclude T-cells and B-cells, respectively (Figure 3.1A). Classical, intermediate, and nonclassical monocyte populations were sorted based on expression of CD14 and CD16 from each animal at each timepoint (Table 3.1, Figure 3.1A). A minimum of 1000 cells were collected for each sample (Range: 24 x 10³ – 1 x 10⁶ classical monocytes, 4 x 10³ – 110 x 10³ intermediate monocytes, 1 x 10³ – 100 x 10³ nonclassical monocytes) (Table 3.1). RNA from each sample (n = 33 samples, Table 3.1) was hybridized to Affymetrix rhesus macaque genome arrays. Each array interrogates approximately 47,000 transcripts per sample using probes designed from the Baylor School of Medicine rhesus macaque whole-genome shotgun assembly and from the Affymetrix Human Genome U133 Plus 2.0 Array. Partek Express Genomic Suite software was used to normalize the raw microarray signal intensities and analyze the gene expression data.

The total variation in gene expression across all samples can be measured by the effect size (F ratio) of the three variables that define each sample: animal (F = 3.01), monocyte subset (F = 2.98), and infection status (F = 1.83). The differences in effect size indicate that, across all samples, inherent differences between individual animals and differences between monocyte subsets account for a greater proportion of the total variation in gene expression compared to differences in gene expression due to SIV infection.

Identification of transcripts that differentiate monocyte subsets or infection timepoints.

To identify differently expressed transcripts, gene expression data from each of the four animals were grouped and compared based on the variables of interest: monocyte subset and infection timepoint. 3418 probe sets were identified as significantly, differently expressed. This list was then filtered based on an absolute fold change (AFC) ≥ 2.0 between monocyte subsets or infection timepoints and a p-value < 0.05 . Probe sets were annotated with the corresponding human official gene symbol and redundant probe sets representing the same gene and probe sets representing hypothetical genes were removed. In agreement with the observed effect sizes, we found 2023 genes that were significantly, differently expressed between monocyte subsets at one or more timepoint and 424 genes that were significantly differently expressed between infection timepoints in at least one monocyte subset.

Validation of microarray data by qRTPCR and FACS

To validate the microarray expression data, we generated cDNA from available RNA and performed quantitative real time PCR (qRTPCR). Gene expression as determined by qRTPCR correlated with gene expression as determined by microarray ($r = 0.56$, $p = 0.0003$) (Figure 3.1B). Additionally, we compared gene expression as determined by microarray to protein expression as determined by flow cytometry for a panel of monocyte related proteins (CD14, CD16, CD68, CD163, S100A8, HLA-DR, CD44v6, CX3CR1, CCR2). Protein expression (MFI by FACS) correlated with gene expression determined by microarray for 8 of the 9 target genes investigated (Table 3.2).

Intermediate monocytes are more similar to classical monocytes than nonclassical monocytes overall, and the number of genes differently expressed between intermediate and nonclassical monocytes decreases with AIDS.

To investigate the relationship between the three monocyte subsets in uninfected and SIV-infected animals we compared the number of genes differently expressed in at least one comparison between monocyte subsets (classical vs. intermediate, classical vs. nonclassical, or intermediate vs. nonclassical), at each infection timepoint (Figure 3.1C). Of the 2023 genes identified as differently expressed between monocyte subsets, 1295 genes were differently expressed preinfection, 1178 genes were differently expressed at 26 dpi, and 1272 genes were different expressed at necropsy (Figure 3.1C). Intermediate monocytes expressed 69% (890 genes, preinfection), 68% (914 genes, 26 dpi), and 75% (960 genes, necropsy) of differently expressed genes at levels between

classical and nonclassical monocytes. Based on the number of differently expressed genes, intermediate monocytes were more similar to classical monocytes than nonclassical monocytes, and classical monocytes and nonclassical monocytes were most dissimilar at all timepoints (Figure 3.1C). We observed that the number of genes differently expressed between intermediate and nonclassical monocytes decreased terminally with AIDS. Intermediate and nonclassical monocytes were differentiated by 847 genes preinfection, 869 genes at 26 dpi, and 624 genes at necropsy (Figure 3.1C). Conversely, the number of genes differentiating intermediate and classical monocytes increased from 237 genes in uninfected animals and 201 genes at 26 dpi to 286 genes at necropsy (Figure 3.1C). The number of genes differently expressed between classical and nonclassical monocytes did not significantly change with SIV infection: 1139 genes preinfection, 1179 genes at 26 dpi, and 1105 genes at necropsy (Figure 3.1C). Increased similarity between the intermediate and nonclassical monocyte subsets with SIV infection may reflect increased activation or maturation of the intermediate subset in chronic SIV infection and suggests that the set of genes that differentiate monocyte subsets may exhibit plasticity in response to SIV infection and inflammation. Despite changes in gene expression with SIV infection, Intermediate monocytes were more similar to classical monocytes than nonclassical monocytes at all timepoints investigated.

Gene signature of monocyte subsets in uninfected animals

In order to characterize genes specific to each monocyte subset in uninfected animals, we selected genes that were differently expressed (≥ 2.0 AFC) in each subset

compared to the other two subsets (Figure 3.2, Tables 3.3-3.7). Prior to infection, we identified 99 genes expressed ≥ 2.0 -fold by classical monocytes relative to intermediate monocytes (range: 2.0- 5.3 fold, median: 2.6) or nonclassical monocytes (range: 2.0- 80 fold, Median: 4.2) (Table 3.3, Figure 3.2). Only 17 genes were expressed ≥ 2.0 -fold by intermediate monocytes relative to classical (range: 2.1- 3.8 fold, median: 2.5) or nonclassical monocytes (range: 2.2- 20 fold, median: 3.4) (Table 3.4, Figure 3.2). Nonclassical monocytes expressed 242 genes ≥ 2.0 -fold relative to classical (range: 2.0- 82 fold; median: 4.0) or intermediate monocytes (range: 2.0- 27 fold; median: 3.1) (Table 3.5, Figure 3.2). The low number of genes expressed ≥ 2.0 -fold uniquely by CD14⁺⁺CD16⁺ intermediate monocytes is the result of an overlap in shared gene expression with both classical and nonclassical monocytes. There were 426 genes expressed ≥ 2.0 -fold in both classical (range: 2.0- 148.2 fold; median: 3.6) and intermediate monocytes (range: 2.0- 86.7 fold; median: 3.2) compared to nonclassical monocytes (Table 3.6, Figure 3.2). Relative to classical monocytes, 29 genes were expressed ≥ 2.0 -fold in intermediate monocytes (range: 2.0- 22.6 fold; median: 2.9) and nonclassical monocytes (range: 2.1- 46.5 fold; median: 4.4) (Table 3.7, Figure 3.2). Because intermediate monocytes shared a greater number of expressed genes with classical monocytes than nonclassical monocytes, and because nonclassical monocytes had the greatest number of uniquely expressed genes, we conclude that classical and intermediate monocytes are more similar to one another than the nonclassical monocytes that more transcriptionally dissimilar.

With regard to maturation, nonclassical monocytes expressed transcripts associated with macrophage or DC phenotypes (*e.g.* CD16, CD83, SPN, ITGAL, BTLA), and classical and intermediate monocytes expressed transcripts associated with myeloid and granulocyte phenotype (*e.g.* CD14, TREM1, CD93, CD114, CD116). This may indicate that classical monocytes have a more “immature” granulocyte/monocyte phenotype while nonclassical monocytes have a more “mature” macrophage-like phenotype. Additionally, expression of genes associated with proliferation (JUN, FOSL2, RUNX1, RUNX2) in classical monocytes and genes associated with inhibition of cell cycle (CDKN1C) in nonclassical monocytes may indicate that nonclassical monocytes are more differentiated than classical monocytes.

The set of genes specific to each subset is altered with SIV infection

We found that of the 813 genes expressed in a subset-specific manner preinfection, only 172 genes were also subset-specific at 26 dpi and terminally with AIDS (Figure 3.3). Ten genes were consistently expressed ≥ 2.0 -fold by classical monocytes including S100A8, S100A9, and SELL (L-selectin, CD62L) (Figure 3.3). These genes are expressed by classical monocytes in humans and mice. Only the complement receptor C3AR1 (C3a receptor 1) and MERTK tyrosine kinase were consistently expressed ≥ 2.0 -fold by intermediate monocytes at all timepoints (data not shown). Nonclassical monocytes had consistently higher expression of 22 genes involved with inflammatory response (CX3CR1, CCL5, TNF, BTLA, GZMB) and inhibition of cell cycle (CDKN1C) (Figure 3.3). Both intermediate and nonclassical monocytes were consistently differentiated by expression of 22 genes relative to classical monocytes including CD16

and integrins ITGAL, ITGAD, and ITGAX (Figure 3.3). We identified 116 genes expressed ≥ 2.0 -fold by classical and intermediate monocytes relative to nonclassical monocytes, including many immune receptors (CD14, CD163, FCGR1B, FCGR2B, FCAR, CCR1, CCR2, C5AR1). In particular, we have identified C3AR1 and MERTK as potential surface markers of intermediate monocytes. These data also indicate that SELL/CD62L is expressed by classical monocytes and CX3CR1 is expressed by nonclassical monocytes in rhesus macaques, as has previously been demonstrated in humans and mice.

***In silico* analysis of gene-associated functions suggests classical monocytes are immune sensors and nonclassical monocytes are immune effectors.**

In order to investigate whether the genes that were differently expressed between the monocyte subsets were associated with specific biological processes, we performed an *in silico* analysis using DAVID bioinformatics tools^{244,245}. Human official gene symbols were used in order to take advantage of the relative abundance of gene annotation data for humans relative to macaques. With DAVID tools, gene lists were annotated with the gene ontology (GO) terms for biological process - a controlled vocabulary for describing the biological function of gene products - and statistically overrepresented GO terms were identified. The analysis was performed for each of the infection timepoints (Table 3.8). Interestingly, we found that the GO terms that were enriched for each subset were generally the same in uninfected and SIV-infected animals suggesting that the functional role of each subset is maintained with SIV infection and inflammation (Table 3.8).

We found that genes expressed ≥ 2.0 -fold by classical monocytes or both classical and intermediate monocytes were enriched for biological processes including defense response, positive regulation of cell proliferation, regulation of protein kinase cascade, endocytosis, and wound healing in uninfected and SIV-infected animals (Figure 3.4, Table 3.8). Defense response genes expressed in classical monocytes include inflammatory mediators (e.g. IL-8, S100A8, and S100A9). Interestingly, S100A9 and the S100A8/S100A9 heterodimer comprise the epitope recognized by the antibody MAC387, which defines a subset of macrophages that is recruited in response to inflammation^{181,250}. Both classical and intermediate monocytes express receptors associated with detection of immune ligands including TLR4 and CD14 (LPS receptor), FCGR1A, CCR1, CCR2, and IL-6R. Genes associated with regulation of protein kinase cascade include genes involved in MAPK and NF κ B signaling, which are important pathways in mitogenic signaling, cell survival, and cytokine secretion. Enrichment of MAPK-associated genes and transcription factors involved in proliferation may indicate that the classical subset may be or has recently been progressing through the cell cycle. Thus, biological processes associated with genes enriched in classical monocytes include proliferation, detection of innate immune stimuli, and response to inflammation.

We found that genes expressed ≥ 2.0 -fold by nonclassical monocytes or by intermediate and nonclassical monocytes were enriched for biological processes including defense response, negative regulation of cell proliferation, regulation of T-cell activation, and cellular activation in uninfected and SIV-infected animals (Figure 3.4,

Table 3.8). Defense response genes in nonclassical monocytes are associated with a range of effector functions including initiation of complement cascades (C1QA, C1QB, C1QC), cell-mediated cytotoxicity (GZMA, GZMB, GZMH, LTB, GNLY), and T-cell activation (CD4, CD47, CD83, SPN). Nonclassical monocytes may also be able to contribute to proinflammatory responses and recruit monocytes and T-cells to sites of inflammation through production of TNF α and CCL5. We found nonclassical monocytes express the fractalkine receptor (CX3CR1) and integrins (ITGAD, ITGAL, ITGAX, ITGB2). Additionally, nonclassical monocytes express transcripts associated with negative regulation of cell cycle. Thus, biological processes associated with genes enriched in nonclassical monocytes are consistent with this subset having exited the cell cycle, mediating immune effector functions, producing chemoattractant ligands, and being able to extravasate vessels to become tissue macrophages.

Changes in monocyte gene expression occur early in SIV infection

To investigate subset-specific changes in gene expression with SIV infection, we identified genes that were differently expressed (≥ 2.0 AFC) between infection timepoints for each monocyte subset (Figure 3.5A). Between preinfection and necropsy, more genes were differently expressed in the nonclassical subset (265 genes) than in the classical (227 genes) or intermediate subsets (202 genes) (Figure 3.5A). In all subsets, the majority of changes in gene expression had occurred by 26 dpi, indicating that changes in gene expression due to SIV infection are established early (Figure 3.5A). The majority of genes differently expressed at 26 dpi were upregulated relative to preinfection in the classical and intermediate subsets. In the nonclassical subset,

upregulated and downregulated genes were present in approximately equal numbers (Figure 3.5A). Between 26 dpi and necropsy, the majority of differently expressed genes were downregulated relative to 26 dpi (Figure 3.5A). Many of these downregulated genes were transcription factors. These data suggest that changes to monocyte gene expression occur early in SIV infection prior to AIDS onset. Additionally, we observed that the pattern of changes in gene expression with SIV infection is more similar between classical and intermediate monocytes compared to nonclassical monocytes.

Characterization of the monocyte immune response to SIV infection

We next sought to characterize the immune response of each monocyte subset to SIV infection. Genes with GO annotation for innate immune response (62 genes, GO: 0045087), interferon stimulated genes (44 genes, GO: 0034340, 0034341, or previous description in the literature), and adaptive immune response (24 genes, GO:0002250) were selected from the set of genes differently expressed with SIV infection (Figure 3.5B-D). Almost all immune associated genes were upregulated relative to the preinfection timepoint. Additionally, genes modulated with SIV infection had a similar pattern of expression in classical, intermediate, and nonclassical monocytes (Figure 3.5B-D).

Hierarchical clustering was used to identify patterns of expression of innate immune response genes across monocyte subsets (Figure 3.5B). The largest cluster (Group II) was comprised of genes that were upregulated in all monocyte subsets with SIV infection. Interferon stimulated genes (ISG) as well as cytosolic sensors of nucleic acids

(DDX58, DDX60, RARRES3, AIM2), restriction factors (APOBEC3A, TRIM5, SAMHD1), and ubiquitin associated genes (HERC6, TRIM14, UBE2L6) are representative of this group. The second largest cluster (Group II) consisted of genes that were upregulated primarily in classical and intermediate monocytes. These include genes associated with defense response to bacteria or viruses (CD163, APOBEC3F, S100A9, HLA-B, LY96, SP100). Two minor clusters consisting of genes downregulated in all monocyte subsets (Group I), and genes upregulated primarily in intermediate and nonclassical monocytes (Group IV) contained transcription factors (PIAS1, IRF4, IRF8, AKIRIN2) and genes associated with chemotaxis (PTAFR, CXCL16), respectively. Upregulation of defense response genes, restriction factors, and cytosolic sensors of nucleic acids may suggest a mechanism of limiting SIV infection in monocytes. Immune associated genes were upregulated at 26 dpi and terminally with AIDS, which indicates these changes in gene expression in monocytes occur early and are sustained throughout infection. Additionally, the pattern of gene expression was similar across the three subsets, which suggests that the innate response to virus is conserved in spite of subset heterogeneity.

Induction of interferon-stimulated genes are part of the innate immune response to HIV and SIV infection and have been implicated in viral pathogenesis²⁵¹. We identified 44 ISG that were changed expression in response to SIV infection (Figure 3.5C). Most ISGs (38/44 genes) were upregulated in all three subsets and were associated with an antiviral function (OAS1-3, GBP1-2, MX1-2, ISG15, ISG20). ISGs were also associated with myeloid cell differentiation (IRF4, IRF8, IFI16), JAK-STAT signaling (JAK2, PIAS1, STAT2), and response to cytokine stimulus (SP100, CXCL16, PML, SOCS3). Sustained

induction of interferon signaling in monocytes may be a mechanism of monocyte dysregulation and chronic immune activation, which contribute to SIV pathogenesis.

We identified 24 adaptive immune response genes that changed expression with SIV infection (Figure 3.5D). 16 of these were upregulated in all subsets or intermediate and nonclassical subsets. These genes were associated with Th1 polarization (GIMAP1, GIMAP4) and T-cell binding or regulation (IDO1, SIGLEC1, ADAMDEC1). Additional genes associated with modulation of T-cell function were upregulated in intermediate and nonclassical monocytes terminally with AIDS (CD3E, CD28, CD5, CTLA4).

Downregulated genes include the MHC class II invariant chain (CD74) and cytokine associated genes (IRF4, IL-1 β , ADORA2B). Induction of genes associated with a Th1 type adaptive response and costimulatory molecules, particularly in intermediate and nonclassical monocytes, implies that SIV infection affects the ability of monocytes to regulate T-cell function.

Conclusions

Identification of unique biological functions associated with genes expressed by each monocyte subset recapitulates the fact that functional differences exist between monocyte subsets. We found that classical monocytes express genes associated with detection of innate immune ligands, angiogenesis, and wound repair. Nonclassical monocytes expressed genes associated with cellular activation and immune effector functions including T-cell activation, initiation of complement cascade, and cell-mediated cytotoxicity. Interestingly, the biological processes associated with each subset were the same in uninfected and SIV-infected animals.

We also observed an increase in the number of total monocytes and in the relative percentage of intermediate and nonclassical monocytes in SIV-infected macaques. Because monocytes are functionally heterogeneous, increased number and relative percentage of intermediate and nonclassical monocytes, which are activated and promote immune effector functions, may contribute to sustained immune activation and mediate injurious processes that contribute to SIV pathogenesis including disseminating of virus into tissues, producing proinflammatory cytokines, and initiating T-cell responses. Additionally intermediate and nonclassical monocytes are more susceptible to HIV and SIV infection, compared to classical monocytes, and are putative precursors of tissue macrophages. Expansion of activated monocyte populations is thought to contribute to increased traffic of activated/infected monocytes to the CNS and the development of HIV and SIV encephalitis.

Similarities in gene expression between classical and intermediate monocytes and between intermediate and nonclassical monocytes may suggest that classical monocytes mature into nonclassical monocytes via the intermediate subset. We observed that classical monocytes expressed phenotypic markers of granulocytes and monocytes and genes associated with proliferation while nonclassical monocytes expressed macrophage-like transcripts and genes associated with cell cycle inhibition. This observation may indicate that classical monocytes are at an earlier stage of maturation compared to nonclassical monocytes. Intermediate monocytes were more similar to classical monocytes in uninfected and SIV-infected animals. The similarity in gene expression profiles may indicate that classical and intermediate monocytes are developmentally related, with classical monocytes progressing to intermediate monocytes in response to activating stimuli or as part of normal monocyte maturation. With SIV infection and AIDS, transcriptional similarity between intermediate and nonclassical monocytes increased, which may suggest a developmental relationship between intermediate and nonclassical monocytes and increased maturation of the intermediate subset with AIDS. Overlap in gene expression and phenotypic plasticity of monocyte subsets support the hypothesis that the three subsets are developmentally related.

We found that each subset maintained a gene expression profile that allowed differentiation of the three populations at each of the timepoints investigated, despite changes in gene expression with SIV infection. In macaques SELL/CD62L was expressed by classical monocytes and CX3CR1 was expressed by nonclassical

monocytes, as has previously been described in humans and mice. Importantly, we also identified C3AR1 and MERTK as potential markers of intermediate monocytes.

We found the majority of changes in gene expression occurred within weeks of primary infection and were then sustained through end-stage disease. Importantly, this indicates that monocyte dysregulation begins early in the course of SIV infection. Genes associated with innate and adaptive immunity had a similar pattern of expression in each of the three monocyte subsets with SIV infection. All three subsets upregulated defense response genes, cytosolic sensors of nucleic acids, and restriction factors. Induction of genes associated with detection and restriction of viral infection may contribute to the low prevalence of SIV infection in monocytes. Additionally all three subsets upregulated a number of interferon stimulated genes. This suggests that interferon signaling and response to interferon is also conserved across the three monocyte subsets. The majority of ISG were upregulated at both 26 dpi and terminally with AIDS. Sustained induction of interferon signaling in monocytes may also contribute to monocyte dysregulation and chronic immune activation, which drive SIV pathogenesis. Adaptive immune response genes also showed a similar pattern of expression in all three subsets. Nonclassical and intermediate monocytes upregulated a greater number of genes associated with adaptive immunity compared to classical monocytes in agreement with the observed enrichment of genes associated with T-cell activation in these subsets. Interestingly, these observations indicate that the immune response to SIV infection is largely conserved in monocytes despite functional heterogeneity between subpopulations. Additionally monocyte activation, as indicated

by upregulation of ISG and innate immune response genes, is observed early in infection and is sustained throughout disease progression.

These studies identify classical, intermediate, and nonclassical monocytes as distinct subpopulations with unique transcriptional signatures. Despite plasticity in gene expression with SIV infection, the functional phenotype associated with genes expressed by each subset does not change. Overlap in gene expression and a conserved immune response to SIV infection indicate shared biology between monocyte subsets. Importantly, we observe that changes in monocyte gene expression occur prior to AIDS onset and are sustained through end-stage disease. These studies also provide evidence of chronic immune activation of all monocyte subsets with SIV pathogenesis.

Table 3.1. Number and percentage of monocyte subsets and plasma viral load over time.

Animal ID	CM07			DB79			FD05			FB92		
CNS pathology^a	SIVE			SIVE			SIVE			SIVnoE		
Timepoint (dpi)^b	0	26	75	0	26	91	0	26	95	0	26	118
Viral Load (x10⁶, Copy Eq./mL)	U ^c	24.0	7.4	U ^c	23.0	11.0	U ^c	48.0	58.0	U ^c	21.0	NA ^d
Monocyte Count (Cells/μL)												
CD14++CD16-	204	265	188	246	443	508	116	334	222	217	285	400
CD14++CD16+	28	93	13	21	91	271	9	119	99	14	44	28
CD14+CD16++	13	26	6	24	76	289	2	22	17	6	11	4
Percent of Total Monocytes (%)												
CD14++CD16-	83.5	69.0	90.5	84.5	72.6	47.5	91.3	70.3	65.7	91.6	83.8	92.6
CD14++CD16+	11.2	24.3	6.4	7.1	14.9	25.4	7.1	25.1	29.3	5.9	12.9	6.5
CD14+CD16++	5.2	6.7	3.1	8.4	12.5	27.1	1.6	4.6	5.0	2.5	3.2	0.9
Cells per sample (x10³)^e												
CD14++CD16-	130	1000	24	100	65	190	62	46	NA ^d	50	38	57
CD14++CD16+	36	110	18	10	54	100	14	100	NA ^d	4	60	24
CD14+CD16++	11	15	10 ^f	13	35	100	1 ^f	10	NA ^d	1.8 ^f	15	16

a. SIVE: SIV encephalitis, SIVnoE: SIV no encephalitis.

b. dpi: days post infection.

c. U: undetectable (< 100 copy equivalents/mL).

d. NA: sample not available.

e. Total number of FACS-sorted monocytes collected from each subset.

f. Sample failed quality control and was excluded from analysis.

Table 3.2. Microarray signal intensity correlates with mean fluorescence intensity (MFI) by FACS

Gene/Protein	Spearman's R^a	p-value
CD14	0.75	< 0.0001
FCGR3A/CD16^b	0.80	< 0.0001
FCGR3B/CD16^b	0.48	< 0.0001
CD68	0.68	< 0.0001
CD163	0.67	0.003
S100A8	0.46	0.04
HLA-DR	0.64	0.001
CD44/CD44v6^b	0.48	0.03
CX3CR1	0.48	< 0.0001
CCR2	0.48	NS ^c

- a. The normalized log₂ microarray signal intensity was plotted vs. the median fluorescence intensity (MFI) as determined by FACS for each target.
- b. For these gene/protein target pairs, the microarray probe or antibody recognize a specific isoform of the gene or protein, as indicated
- c. Not significant

Table 3.3. Top 50 genes expressed ≥ 2.0 -fold by classical monocytes in uninfected animals

Gene	Gene name	Fold change classical versus	
		Intermediate	Nonclassical
THBS1	thrombospondin 1	2.6	80.0
TREM1	triggering receptor expressed on myeloid cells 1	3.0	63.1
SERPINB10	serpin peptidase inhibitor, clade B member 10	2.6	61.8
CRISPLD2	cysteine-rich secretory protein LCCL domain containing 2	2.2	41.2
S100A8	S100 calcium binding protein A8	4.5	40.5
SLC7A11	solute carrier family 7 member 11	3.6	40.5
S100A9	S100 calcium binding protein A9	4.7	26.2
SLC2A3	solute carrier family 2 member 3	2.2	21.4
GAF1	FGF2-associated protein GAF1	2.3	16.6
IL8	interleukin 8	2.4	14.5
OSM	oncostatin M precursor	2.4	12.6
QPCT	glutaminyl-peptide cyclotransferase	3.6	10.5
KCNAB1	Potassium voltage-gated channel subunit beta 1	2.7	9.4
AAK1	AP2 Associated Kinase 1	3.5	9.1
BCL9L	B-cell CLL/lymphoma 9-like	2.5	8.4
ACSL1	acyl-CoA synthetase long-chain family member 1	2.2	7.0
SELL	selectin L	4.2	7.0
RAB3D	RAB3D, member Ras oncogene family	2.7	6.9
NRG1	neuregulin 1	2.6	6.6
ELL3	elongation factor RNA polymerase II-like 3	3.4	6.3
NCAM1	neural cell adhesion molecule 1	2.9	5.9
ZCCHC11	zinc finger, CCHC domain containing 11	2.8	5.6
FOSL2	FOS-like antigen 2	3.5	5.6
C6orf192	chromosome 6 open reading frame 192	2.2	5.6
NP	nucleoside phosphorylase	2.1	5.5
MGST1	microsomal glutathione S-transferase 1	3.6	5.5
CARS	cysteinyl-tRNA synthetase	2.6	5.4
KIN	KIN, antigenic determinant of recA protein homolog (mouse)	2.2	5.3
ATP13A3	ATPase type 13A3	2.5	5.1
JUN	jun oncogene	2.3	5.1
DCUN1D3	DCN1, defective in cullin neddylation 1, domain containing 3	3.6	5.1
PARD3	Par-3 Partitioning Defective 3 Homolog (C. elegans)	3.9	5.0
NUP188	nucleoporin 188kDa	3.3	5.0
SLC16A6	solute carrier family 16, member 6	2.7	5.0
TREML4	triggering receptor expressed on myeloid cells-like 4	3.9	4.9
TTC19	tetratricopeptide repeat domain 19	2.6	4.8
ERCC8	excision repair cross-complementing rodent repair deficiency, 8	3.5	4.7
RABEPK	Rab9 effector p40	3.5	4.7
BAG2	BCL2-associated athanogene 2	2.1	4.7
RAB23	RAB23, member Ras oncogene family	2.9	4.5
EEPD1	endonuclease/exonuclease/phosphatase family domain containing 1	2.3	4.5
TGFBR1	transforming growth factor, beta receptor 1	2.5	4.5
TSPAN3	tetraspanin 3	2.3	4.4
EML1	echinoderm microtubule associated protein like 1 isoform b	2.5	4.4
PRKCI	protein kinase C, iota	2.3	4.3
CDC42EP3	CDC42 effector protein (Rho GTPase binding) 3	2.2	4.2
SVIL	supervillin	2.6	4.2
LILRBC	leukocyte immunoglobulin-like receptor, subfamily B, member c	2.0	4.2
MALT1	mucosa associated lymphoid tissue lymphoma translocation gene 1	2.1	4.2
GCA	granulocyte, EF-hand calcium binding protein	4.8	4.2

Table 3.4. Genes expressed ≥ 2.0 -fold by intermediate monocytes in uninfected animals

Gene	Gene name	Fold change intermediate versus	
		Classical	Nonclassical
CD1B	CD1b molecule	2.2	20.0
GCNT1	glucosaminyl (N-acetyl) transferase 1, core 2	2.1	8.0
CD1C	CD1c molecule	2.2	7.3
LIPA	lipase A precursor	2.1	4.8
VSIG4	V-set and immunoglobulin domain containing 4	2.5	4.2
A2M	alpha-2-macroglobulin	2.8	4.1
ASPHD2	aspartate beta-hydroxylase domain containing 2	3.1	3.9
MERTK	c-mer proto-oncogene tyrosine kinase	2.7	3.6
ST3GAL5	ST3 beta-galactoside alpha-2,3-sialyltransferase 5	2.4	3.4
MPZL2	myelin protein zero-like 2	2.5	3.3
CDC42BPA	CDC42-binding protein kinase alpha isoform B	2.5	3.0
FABP5	fatty acid binding protein 5 (psoriasis-associated)	2.9	2.9
C3AR1	complement component 3a receptor 1	3.8	2.8
ABI3	ABI family, member 3	2.1	2.6
CLEC7A	C-type lectin domain family 7, member A	2.1	2.4
RAB11FIP4	RAB11 family interacting protein 4 (class II)	2.1	2.4
MGLL	monoglyceride lipase	2.8	2.2

Table 3.5. Top 50 genes expressed ≥ 2.0 -fold by nonclassical monocytes in uninfected animals

Gene	Gene Title	Fold change nonclassical versus	
		Classical	Intermediate
GNLY	granulysin	82.2	27.0
MS4A7	membrane-spanning 4-domains, subfamily A, member 7	47.2	5.5
AHNAK2	AHNAK nucleoprotein 2	36.2	15.1
FCGR3A	Fc gamma receptor IIIa	35.6	4.1
GZMB	granzyme B	31.5	13.3
GZMH	Granzyme H precursor	30.1	14.8
CDKN1C	cyclin dependent kinase inhibitor 1C	25.2	10.8
C1QA	complement component 1, q subcomponent, A chain	23.3	3.4
SEPP1	selenoprotein P	22.9	2.5
LPL	lipoprotein lipase	19.4	3.9
DUSP5	dual specificity phosphatase 5	18.0	9.1
MTSS1L	metastasis suppressor 1-like	17.4	7.6
RAMP2	receptor (G protein-coupled) activity modifying protein 2	16.4	3.7
MT1E	metallothionein 1E	16.2	7.4
HTR7A	5-hydroxytryptamine receptor 7 isoform a	16.1	4.6
CD300E	CD300E molecule	15.8	2.7
TCF7L2	similar to Transcription factor 7-like 2	14.9	4.1
ADA	adenosine deaminase	14.0	4.1
GZMA	granzyme A	13.4	10.3
TOB1	transducer of Erbb2 1	12.8	5.2
C11orf95	chromosome 11 open reading frame 95	12.3	5.5
PSMC2	Similar to proteasome (prosome, macropain) 26S subunit, ATPase 2	12.2	4.6
NEU1	Sialidase 1 (lysosomal sialidase)	11.5	6.7
PAG1	phosphoprotein associated with glycosphingolipid microdomains 1	11.4	5.8
IFT81	intraflagellarTransport81	11.2	5.6
ITGAX	integrin, alpha X (complement component 3 receptor 4 subunit)	10.8	3.0
GPR155	G protein-coupled receptor 155	10.4	5.3
C1QC	complement component 1, q subcomponent, C chain	9.8	3.0
ARHGAP32	Rho GTPase-activating protein 32	9.8	10.5
HEG1	HEG homolog 1 (zebrafish)	9.5	5.1
HIST1H2BH	similar to Histone H2B 291B	9.4	9.3
CASP2	caspase 2, apoptosis-related cysteine peptidase	9.0	7.3
CCL5	chemokine (C-C motif) ligand 5	8.9	7.8
C18orf45	chromosome 18 open reading frame 45	8.8	8.8
NR4A1	nuclear receptor subfamily 4, group A, member 1	8.6	5.8
CSRP1	Cysteine and Glycine-Rice Protein 1	8.3	3.8
SCAMP5	similar to secretory carrier membrane protein 5	8.2	4.4
GUCY1A3	Guanylate Cyclase 1, Soluble, Alpha 3	8.2	5.3
CYFIP2	similar to cytoplasmic FMR1 interacting protein 2	8.2	5.6
SASH1	SAM and SH3 domain containing 1	8.1	2.5
NKG7	natural killer cell group 7 sequence	8.0	4.8
NKG2D	NKG2D protein	8.0	5.7
C1QB	similar to Complement C1q subcomponent subunit B precursor	8.0	2.3
FMNL2	formin-like 2	7.9	4.7
CARM1	coactivator-associated arginine methyltransferase 1	7.8	3.8
TNF	tumor necrosis factor	7.5	4.7
ITGAD	similar to integrin, alpha D precursor	7.4	3.1
CAMK2G	calcium/calmodulin-dependent protein kinase II gamma	7.4	7.8
ITGAL	integrin, alpha L (antigen CD11A (p180), LFA1; alpha polypeptide)	7.3	2.4

Table 3.6. Top 50 genes expressed ≥ 2.0 -fold by classical and intermediate monocytes in uninfected animals

Gene	Gene Title	Fold change versus nonclassical	
		Classical	Intermediate
VCAN	versican	148.2	86.7
SERPINB2	serpin peptidase inhibitor, clade B (ovalbumin), member 2	109.3	60.3
FN1	fibronectin 1	65.9	46.9
CYP1B1	cytochrome P450, family 1, subfamily B, polypeptide 1	65.7	77.0
ALOX5AP	arachidonate 5-lipoxygenase-activating protein	65.0	25.1
PTGS2	prostaglandin H synth 2	48.4	35.6
SDC2	budding uninhibited by benzimidazoles 3 homolog	47.4	46.1
VEGFA	vascular endothelial growth factor A	46.5	22.8
BASP1	brain abundant, membrane attached signal protein 1	42.4	34.3
RIN2	Ras and Rab interactor 2	37.9	50.7
IL13RA1	Interleukin-13 receptor alpha-1 chain	30.5	25.9
ADAM19	ADAM metallopeptidase domain 19	29.1	19.1
DEPDC1	DEP domain containing 1	26.1	15.9
MS4A6A	membrane-spanning 4-domains, subfamily A, member 6A	24.9	50.0
FCAR	Fc fragment of IgA, receptor for	24.7	12.6
PID1	phosphotyrosine interaction domain containing 1	24.5	18.4
DCP2	DCP2 decapping enzyme	23.9	24.4
KIR3DL	killer immunoglobulin-like receptor KIR3DL	22.4	19.2
ADO	2-aminoethanethiol (cysteamine) dioxygenase	20.2	10.2
CCR1	chemokine (C-C motif) receptor 1	20.1	16.1
ACVR2A	activin A receptor, type IIA	18.8	22.6
SSH2	slingshot 2	18.2	30.4
SLC38A2	solute carrier family 38, member 2	17.9	11.1
F3	coagulation factor III (thromboplastin, tissue factor)	17.9	11.7
FCGR2B	Fc fragment of IgG, low affinity IIb, receptor (CD32)	17.8	19.9
RUNX1	runt-related transcription factor 1	17.5	13.0
GSN	gelsolin	17.1	15.7
PRDM1	PR domain containing 1, with ZNF domain	16.1	19.4
RUNX2	runt-related transcription factor 2	15.6	13.4
ADORA2B	adenosine A2b receptor	15.4	8.0
NEK6	NIMA (never in mitosis gene a)-related kinase 6	13.2	7.1
GAS7	growth-arrest-specific protein 7	13.1	10.8
RB1	retinoblastoma 1	12.3	13.4
CD163	CD163 molecule	12.3	10.9
THBD	thrombomodulin	12.2	8.3
ADRB1	adrenergic, beta-1-, receptor	12.0	11.4
NUFIP1	nuclear fragile X mental retardation protein interacting protein 1	11.7	7.9
EGR2	early growth response 2	11.0	9.2
SERPINB6	serpin peptidase inhibitor, clade B (ovalbumin), member 6	10.7	6.5
LGALS1	lectin, galactoside-binding, soluble, 1	10.7	11.4
KIR3DL17	killer-cell Ig-like receptor KIR3DL17	10.5	9.0
MSR1	macrophage scavenger receptor 1	10.4	14.1
P2RY2	purinergic receptor P2Y, G-protein coupled, 2	10.2	11.9
CSDA	cold shock domain protein A	9.9	8.9
SLC2A5	solute carrier family 2 member 5	9.8	8.1
PLP2	proteolipid protein 2	9.5	5.3
TLR4	toll-like receptor 4	9.4	10.1
HNRPLL	heterogeneous nuclear ribonucleoprotein L-like	9.3	5.3
SEMA4C	Semaphorin 4C	9.2	12.0
GPR183	G protein-coupled receptor 183	9.0	12.6

Table 3.7. Genes expressed ≥ 2.0 -fold by intermediate and nonclassical monocytes in uninfected animals

Gene	Gene Title	Fold change versus classical	
		Intermediate	Nonclassical
FCGR3B	Fc fragment of IgG, low affinity IIIb, receptor	22.6	46.5
PLVAP	plasmalemma vesicle associated protein	7.7	14.2
RNF144B	ring finger protein 144B	4.4	9.8
CCND2	cyclin D2	6.5	9.3
PAQR4	progesterin and adipoQ receptor family member IV	4.6	8.1
PIK3R3	phosphoinositide-3-kinase, regulatory subunit 3 (gamma)	3.0	6.7
LILRA1	leukocyte immunoglobulin-like receptor, subfamily A member 1	4.1	6.6
SUSD3	sushi domain containing 3	3.1	5.5
ARPC1A	actin related protein 2/3 complex subunit 1A	2.7	5.0
LY6E	lymphocyte antigen 6 complex, locus E	2.5	4.8
SPN	sialophorin (CD43)	2.8	4.8
PRR5L	Rho GTPase activating protein 8	2.9	4.7
UCP2	uncoupling protein 2	3.4	4.4
SQLE	squalene epoxidase	3.0	4.4
VMO1	Vitelline membrane outer layer protein 1 homolog	3.3	4.4
PALLD	palladin, cytoskeletal associated protein	2.2	4.1
LRRRC25	leucine rich repeat containing 25	2.3	3.8
HSPD1	60 kDa heat shock protein, mitochondrial precursor	3.5	3.8
LILRB1	leukocyte immunoglobulin-like receptor, subfamily B, member 1 (CD85)	2.0	3.6
CD83	CD83 molecule	2.4	3.3
ALDH2	aldehyde dehydrogenase, mitochondrial-like	2.4	3.3
ASCC3	activating signal cointegrator 1 complex subunit 3	2.1	3.2
PLA1A	phospholipase A1 member A	4.1	3.1
DNM1	dynammin-1-like	2.4	3.0
BPTF	nucleosome-remodeling factor subunit BPTF-like	2.8	2.9
CTSC	cathepsin C	3.4	2.7
CD4	CD4 molecule	2.8	2.6
CTPS	CTP synthase	2.7	2.6
NAGA	N-acetylgalactosaminidase, alpha	2.2	2.1

Table 3.8. GO terms for biological process enriched in the set of genes differently expressed across monocyte subsets

GO Term	Subset ^a	Preinfection			26 dpi			Necropsy		
		# ^b	% ^c	p ^d	#	%	p	#	%	p
defense response GO:0006952	C	38	7.6	****	36	5.8	**	41	7.7	****
	I	40	8.8	****	40	6.4	***	36	8.1	****
	N	25	9.5	****	22	13.4	****	9	8.0	*
inflammatory response GO:0006954	C	24	4.8	***	27	4.3	***	28	5.2	****
	I	24	5.3	****	29	4.6	****	27	6.1	****
	N	13	4.9	**	13	7.9	***	7	6.3	*
regulation of T cell activation GO:0050863	C	NS	NS	NS	NS	NS	NS	NS	NS	NS
	I	9	2.0	*	10	1.6	*	8	1.8	*
	N	13	4.9	****	9	5.5	****	7	6.3	****
cell activation GO:0001775	C	NS	NS	NS	NS	NS	NS	NS	NS	NS
	I	NS	NS	NS	NS	NS	NS	NS	NS	NS
	N	17	6.4	****	8	4.9	*	11	9.8	****
positive regulation of cell proliferation GO:0008284	C	27	5.4	***	26	4.2	**	26	4.9	**
	I	21	4.6	*	28	4.5	**	21	4.7	**
	N	NS	NS	NS	NS	NS	NS	NS	NS	NS
negative regulation of cell proliferation GO:0008285	C	NS	NS	NS	NS	NS	NS	NS	NS	NS
	I	NS	NS	NS	NS	NS	NS	NS	NS	NS
	N	15	5.7	**	12	7.3	**	10	8.9	***
positive regulation of apoptosis GO:0043065	C	24	4.8	**	NS	NS	NS	NS	NS	NS
	I	NS	NS	NS	26	4.1	*	NS	NS	NS
	N	15	5.7	**	NS	NS	NS	8	7.1	*
negative regulation of apoptosis GO:0043066	C	25	5.0	***	22	3.5	*	22	4.1	**
	I	20	4.4	**	21	3.3	*	18	4.0	*
	N	12	4.5	*	9	5.5	*	7	6.3	*
positive regulation of cell differentiation GO:0045597	C	17	3.4	**	16	2.6	*	17	3.2	**
	I	15	3.3	**	16	2.5	*	13	2.9	*
	N	10	3.8	*	NS	NS	NS	5	4.5	*
wound healing GO:0042060	C	21	4.2	****	15	2.4	**	17	3.2	***
	I	18	4.0	****	13	2.1	*	11	2.5	*
	N	NS	NS	NS	NS	NS	NS	NS	NS	NS
angiogenesis GO:0001525	C	11	2.2	*	13	2.1	**	12	2.2	**
	I	NS	NS	NS	12	1.9	*	11	2.5	**
	N	NS	NS	NS	NS	NS	NS	NS	NS	NS

(Table continues on next page)

a. C: classical. I: intermediate. N: nonclassical.

b. #: number of queried genes associated with the GO term

c. % = (# GO associated genes / total genes queried) x 100

d. p: p-value for enrichment of the GO term. p ≤ 0.05, *. p < 0.01, **. p < 0.001, ***. p < 0.0001, ****.

e. NS: No significant enrichment

Table 3.8. continued

GO Term	Subset	Preinfection			26 dpi			Necropsy		
		#	%	p	#	%	p	#	%	p
endocytosis GO:0006897	C	16	3.2	**	20	3.2	***	18	3.4	***
	I	16	3.5	**	21	3.3	***	16	3.6	***
	N	NS	NS	NS	NS	NS	NS	NS	NS	NS
membrane organization GO:0016044	C	29	5.8	****	31	5.0	****	27	5.0	***
	I	27	6.0	****	32	5.1	****	24	5.4	***
	N	NS	NS	NS	NS	NS	NS	NS	NS	NS
vesicle-mediated transport GO:0016192	C	35	7.0	***	39	6.3	***	33	6.2	**
	I	30	6.6	**	40	6.4	***	29	6.5	**
	N	NS	NS	NS	NS	NS	NS	NS	NS	NS
phagocytosis GO:0006909	C	---	---	---	7	1.1	**	6	1.1	*
	I	6	1.3	**	7	1.1	**	6	1.3	**
	N	NS	NS	NS	NS	NS	NS	NS	NS	NS
regulation of protein kinase cascade GO:0010627	C	23	4.6	****	18	2.9	**	19	3.6	**
	I	18	4.0	***	18	2.9	*	13	2.9	*
	N	NS	NS	NS	NS	NS	NS	NS	NS	NS
regulation of MAP kinase activity GO:0043405	C	12	2.4	**	12	1.9	**	---	---	---
	I	9	2.0	*	13	2.1	**	16	3.6	*
	N	NS	NS	NS	NS	NS	NS	NS	NS	NS
regulation of I-kappaB kinase/ NFkB cascade GO:0043122	C	10	2.0	**	---	---	---	10	1.9	**
	I	9	2.0	**	---	---	---	---	---	---
	N	NS	NS	NS	NS	NS	NS	NS	NS	NS
positive regulation of cytokine production GO:0001819	C	12	2.4	****	10	1.6	**	NS	NS	NS
	I	12	2.6	****	11	1.7	**	NS	NS	NS
	N	NS	NS	NS	NS	NS	NS	NS	NS	NS
cell adhesion GO:0007155	C	31	6.2	*	NS	NS	NS	NS	NS	NS
	I	29	6.4	*	NS	NS	NS	NS	NS	NS
	N	20	7.6	*	NS	NS	NS	10	8.9	*
chemotaxis GO:0006935	C	12	2.4	**	12	1.9	*	12	2.2	*
	I	12	2.6	**	13	2.1	*	NS	NS	NS
	N	NS	NS	NS	7	4.3	**	NS	NS	NS
cell migration GO:0016477	C	19	3.8	**	18	2.9	*	18	3.4	**
	I	14	3.1	*	NS	NS	NS	15	3.4	*
	N	NS	NS	NS	NS	NS	NS	NS	NS	NS
actin cytoskeleton organization GO:0030036	C	13	2.6	*	15	2.4	*	15	2.8	*
	I	13	2.9	*	12	1.9	*	14	3.1	**
	N	10	3.8	**	NS	NS	NS	NS	NS	NS
posttranscriptional regulation of gene expression GO:0010608	C	NS	NS	NS	18	2.9	**	15	2.8	**
	I	NS	NS	NS	17	2.7	**	12	2.7	*
	N	NS	NS	NS	NS	NS	NS	NS	NS	NS

Figure 3.1. Gating strategy, microarray validation, and identification of differently expressed genes.

A. Classical, intermediate, and nonclassical monocytes were isolated from total PBMCs from each animal at each infection timepoint. Monocytes were selected based on high forward scatter and intermediate side scatter. HLA-DR⁺ cells were positively selected and CD3⁺ T-cells and CD20⁺ B-cells were excluded. Non-overlapping populations of classical (CD14⁺⁺CD16⁻, red gate), intermediate (CD14⁺⁺CD16⁺, blue gate), and nonclassical (CD14⁺CD16⁺⁺, green gate) monocytes were sorted based on expression of CD14 and CD16. **B.** Paired XY values for gene expression values determined by microarray and qRT-PCR. For qRT-PCR analysis, cDNA was made from the same RNA used in the microarray analysis. Nine samples had sufficient RNA remaining to validate four targets each. GAPDH was used as a housekeeping gene. Gene expression values determined by qRT-PCR significantly correlated with the gene expression values determined by microarray (Spearman $r = 0.56$, $p = 0.0003$). **C.** The number comparisons with ≥ 2.0 -AFC between monocyte subsets prior to infection, at 26 dpi, and at necropsy. The length of the line between monocyte subsets is proportional to the number of differently expressed genes. Intermediate monocytes are most similar to classical monocytes, but increase in similarity to nonclassical monocytes terminally with AIDS.

Figure 3.1

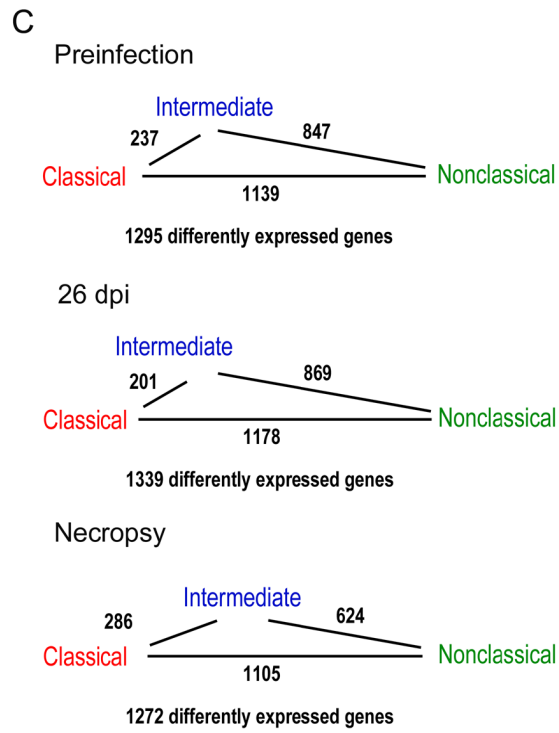
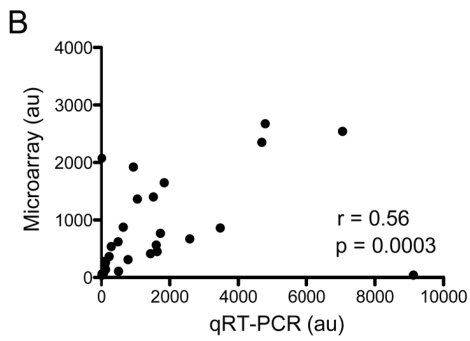
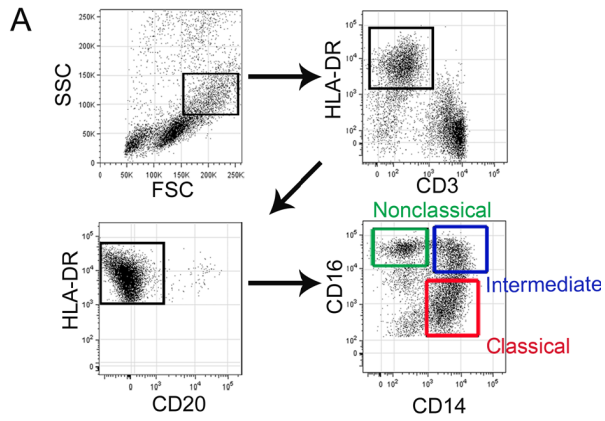


Figure 3.2. Expression profiles of subset-specific genes, prior to SIV infection

Expression variability of subset-specific genes that differentiate classical (“C”, red), intermediate (“I”, blue), and nonclassical (“N”, green) monocytes prior to infection. Each of 813 genes was assigned to one of five gene expression patterns (gray bar graphs). The size of each slice is proportional to the number of genes specific to the indicated subset(s). Classical and intermediate monocytes are most similar and nonclassical monocytes are more dissimilar based on the number of differently expressed genes.

Figure 3.2

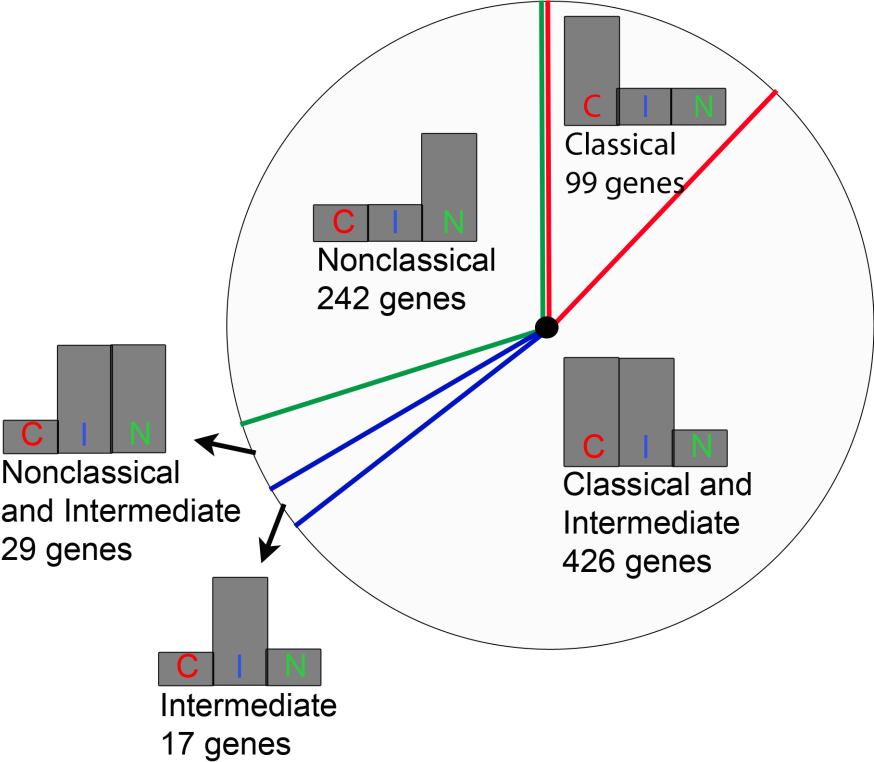


Figure 3.3. Identification of transcripts that differentiate the three monocyte subsets prior to and with SIV infection.

Heat maps of the 172 genes that differentiate the three monocyte subsets prior to and with SIV infection. Rows are the average normalized intensity for the gene indicated. Green indicates lower expression, and red indicates higher expression. Columns are the different monocyte subsets for each of the three infection timepoints. Ten genes were expressed ≥ 2.0 -fold by classical monocytes at all timepoints. Twenty-two genes were expressed ≥ 2.0 -fold by both intermediate and nonclassical monocytes at all timepoints. Twenty-two genes were expressed ≥ 2.0 -fold by nonclassical monocytes at all timepoints. Two genes (C3AR1, MERTK) were expressed ≥ 2.0 -fold by intermediate monocytes (data not shown). One hundred and sixteen genes were expressed ≥ 2.0 -fold by classical and intermediate monocytes at all timepoints; for simplicity, only the top 70 genes are shown.

Figure 3.3.

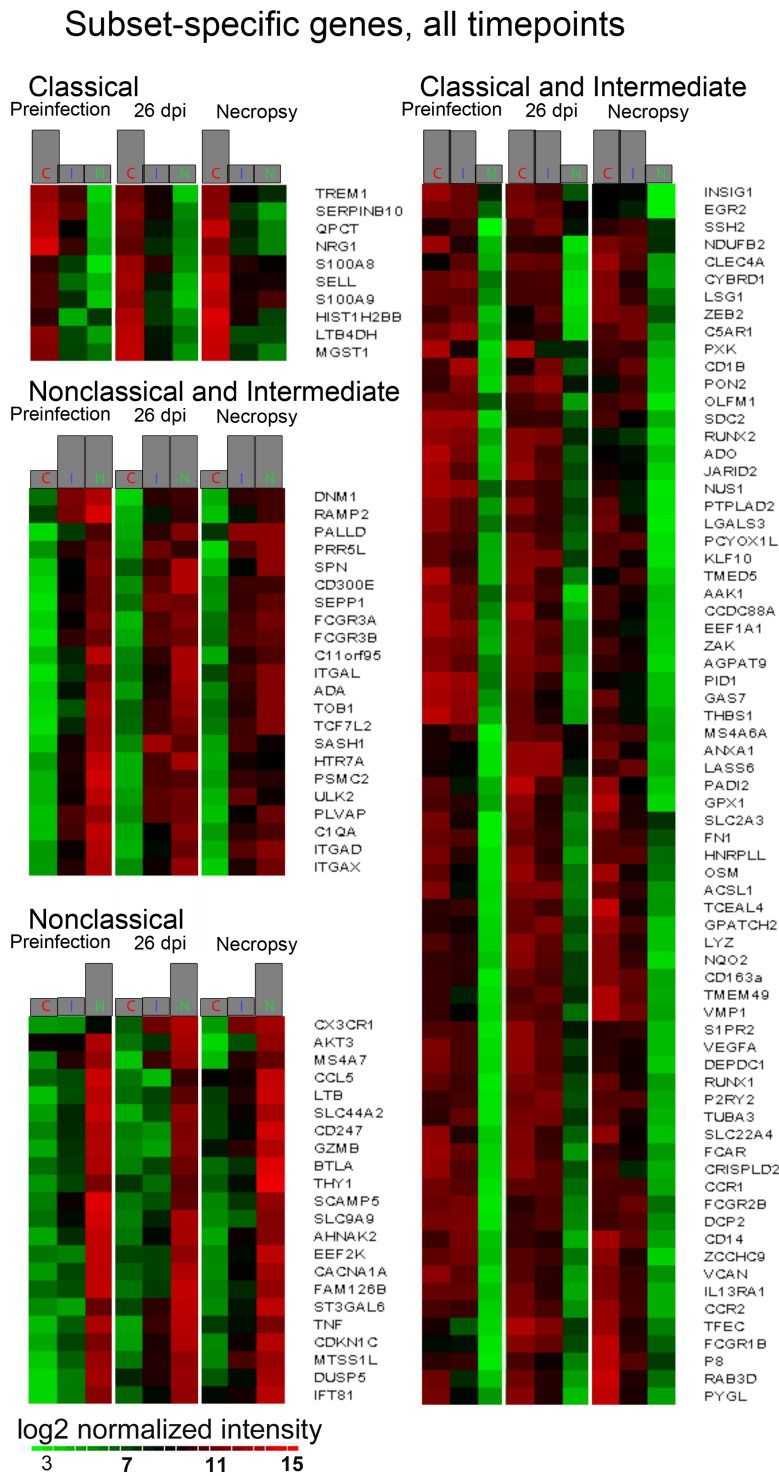


Figure 3.4. *In silico* analysis of gene-associated biological processes reveals the functional nature of monocyte subsets.

Representative GO terms for biological processes associated with genes expressed ≥ 2.0 -fold by classical monocytes or both classical and intermediate monocytes (left panels) and nonclassical or both intermediate and nonclassical monocytes (right panels) prior to infection are shown. Gene expression values are the log₂ transformed fold change in classical, intermediate or nonclassical monocytes normalized to expression in intermediate monocytes. Representative genes are shown for each cluster. Complete data for functional enrichment categories at each infection timepoint are in Table 3.8. Classical monocytes show enrichment for genes associated with defense response (38 genes), positive regulation of cell proliferation (27 genes), regulation of protein kinase cascade (23 genes), endocytosis (16 genes), and wound healing (21 genes). Nonclassical monocytes show enrichment for genes associated with defense response (25 genes), negative regulation of cell proliferation (15 genes), regulation of T-cell activation (13 genes), and cellular activation (17 genes).

Figure 3.4.

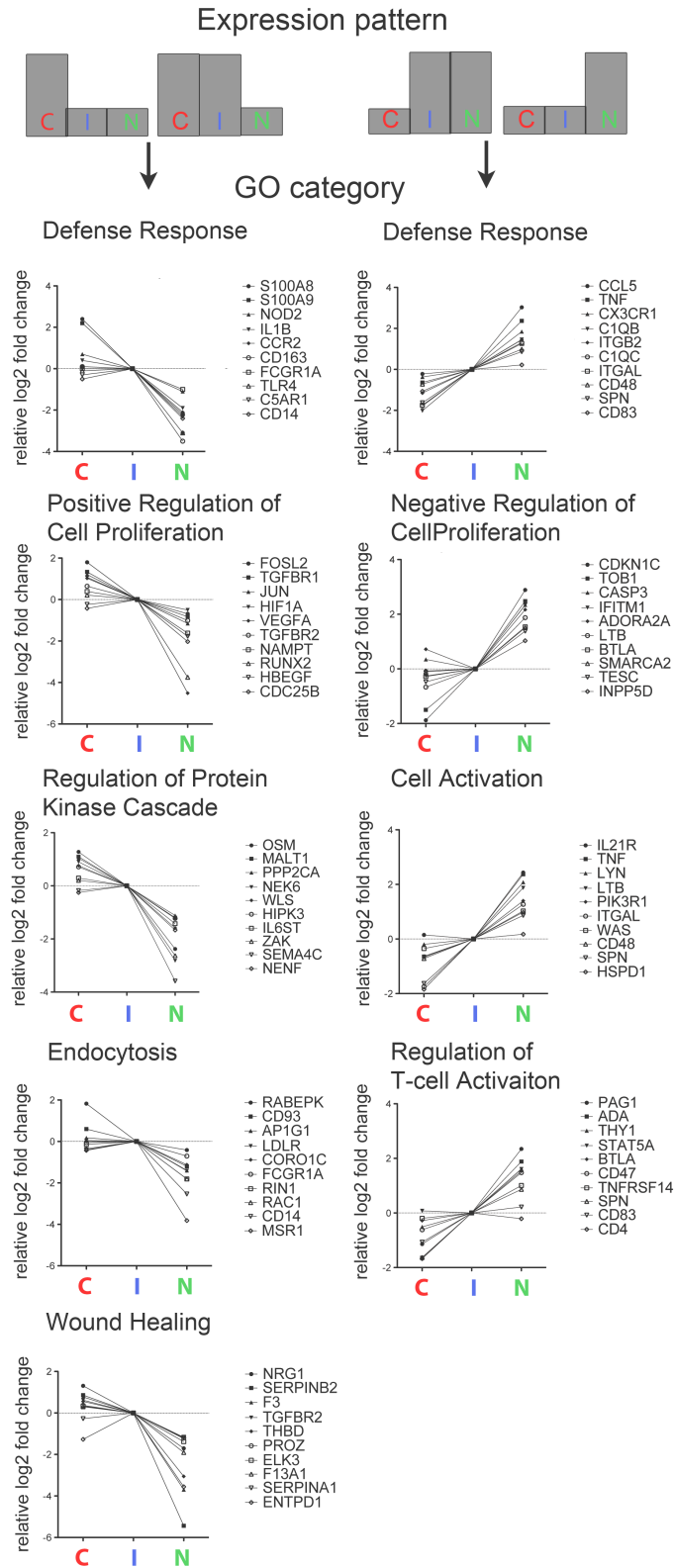
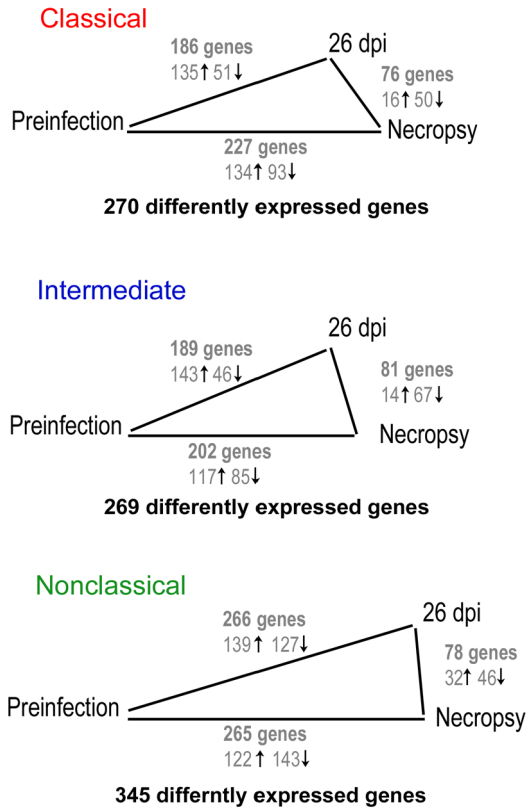


Figure 3.5. Changes in monocyte gene expression with SIV infection are present by 26 dpi and include induction of interferon stimulated and innate immune genes.

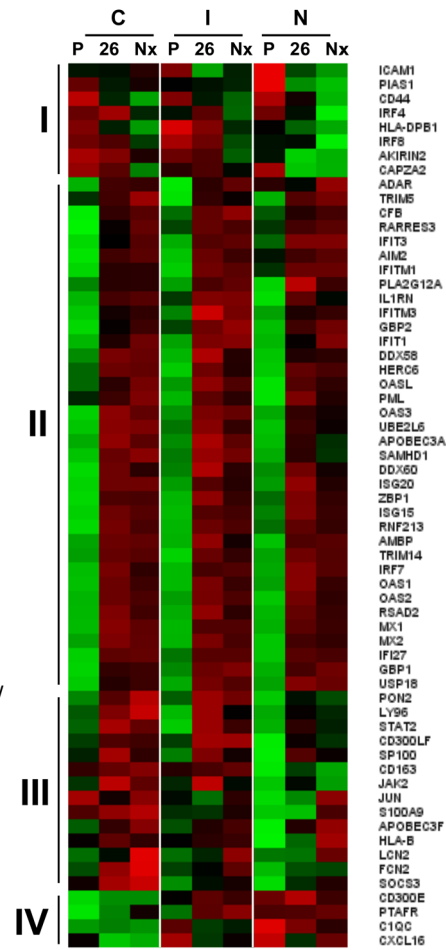
A. The number comparisons with ≥ 2.0 -AFC between infection timepoints in each monocyte subset. The length of the line between infection timepoints is proportional to the number of differently expressed genes. The majority of changes in gene expression occur between preinfection and 26 dpi in all subsets. More genes are differently expressed by nonclassical monocytes with SIV infection compared to classical and intermediate monocytes. **B-D.** Heat maps of immune-associated genes that are differently expressed with SIV infection. Rows are the average normalized intensity for the gene indicated. Green indicates lower expression, and red indicates higher expression. Columns are the different infection timepoints (P: preinfection, 26: 26 dpi, Nx: Necropsy) for each of the three monocyte subsets (C: classical, I: intermediate, N: nonclassical). Genes were selected based on GO annotation for innate immune response (**B**), response to interferon (**C**), and adaptive immune response (**D**). **B.** 62 genes associated with innate immune response are differently expressed with SIV infection. Hierarchical clustering reveals 4 distinct patterns of gene expression (I - IV). The majority of innate immune genes are induced in all three subsets at 26 dpi and necropsy. **C.** 42 interferon stimulated genes are differently expressed with SIV infection. The majority of ISG are upregulated in all three monocyte subsets with SIV infection. **D.** 24 genes associated with adaptive immune response are differently expressed with SIV infection. The majority of these are upregulated in all three monocyte subsets or both intermediate and nonclassical monocytes.

Figure 3.5

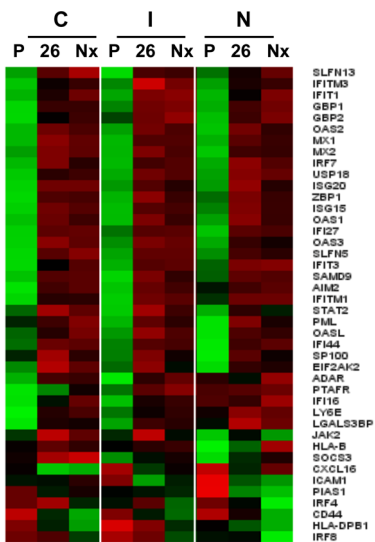
A



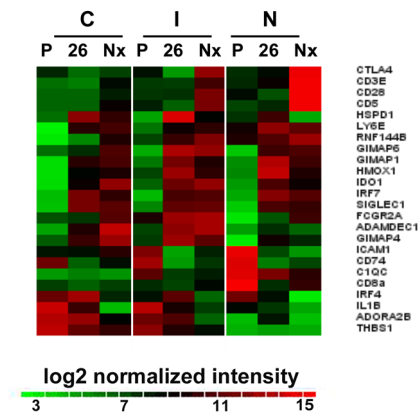
B Innate immunity



C Interferon stimulated genes



D Adaptive immunity



Chapter 4. SIVE lesions are comprised of CD163+ macrophages present in the CNS during early SIV infection and SIV+ macrophages recruited terminally with AIDS

Chapter Overview

CNS inflammation during early SIV infection is characterized by recruitment of MAC387+ macrophages throughout the CNS. Overall, more BrdU macrophages were present in the meninges and choroid plexus compared to the perivascular space and lesions. BrdU+ cells in the CNS were primarily MAC387+ macrophages; but CD163+BrdU+ macrophages were present in the meninges and choroid plexus terminally with AIDS. Terminally with AIDS, macrophages accumulated in the perivascular space and SIVE lesions, but not in the meninges and choroid plexus. The ratio of CD163+ macrophages to MAC387+ macrophages in the CNS was greater in animals with SIVE than animals without SIVE. The majority ($81.6 \pm 1.8\%$) of macrophages in SIVE lesions were present in the CNS early, by 20 days post infection (dpi), before lesions were present. The percentage of productively infected macrophages was 2.6-fold greater in macrophages that entered the CNS late, after 49 dpi, compared to early macrophages ($p < .05$). The rate of CD163+ macrophage recruitment to the CNS was inversely correlated with time to death ($p < .03$) and was greater with SIVE. In animals with SIVE, soluble CD163 in plasma correlated with CD163+ macrophage recruitment to the CNS ($p = .02$). We conclude that the majority of perivascular macrophages that comprise SIVE lesions and MNGCs were present in the CNS early and SIV-infected macrophages traffic to the CNS terminally with AIDS.

Early CNS inflammation with SIV infection is characterized by recruitment of MAC387+ macrophages to the perivascular space, meninges, and choroid plexus.

We and others have previously described two populations of macrophages ($M\phi$) recruited to the CNS^{88,181}. One is phenotypically defined as CD163+CD68+MAC387- perivascular macrophages, and the second is MAC387+CD163-CD68- “inflammatory” macrophages. Using single color IHC, we counted the number of CD163+ and MAC387+ macrophages in the CNS of uninfected animals (Uninfected, n = 3), SIV-infected animals sacrificed at 22 dpi (SIV 22dpi, n = 3), and SIV infected animals that progressed to AIDS with SIVE (SIVE, n = 5) and without SIVE (SIVnoE, n = 4) (Figure 4.1). MAC387+ macrophages were absent from CNS tissues of uninfected animals but were numerous at 22 dpi (perivascular space: $2 \pm 1 M\phi/mm^2$ uninfected, $13 \pm 3 M\phi/mm^2$ SIV 22dpi, p = .0007; meninges: $14 \pm 6 M\phi/mm^2$ uninfected, $770 \pm 100 M\phi/mm^2$ SIV 22dpi, p = .002; choroid plexus: $17 \pm 3 M\phi/mm^2$ uninfected, $180 \pm 100 M\phi/mm^2$ SIV 22dpi) (Figure 4.1A-D, open circles). The number of CD163+ macrophages was not significantly increased in infected animals sacrificed at 22 dpi compared to uninfected animals (Figure 4.1A-D). No SIVE lesions were present in the CNS of animals sacrificed at 22 dpi. These data indicate that with SIV infection early CNS inflammation is characterized by recruitment of MAC387+ macrophages and the absence of SIVE lesions.

There is a greater ratio of CD163+ to MAC387+ macrophages in the perivascular space, meninges and choroid plexus of animals sacrificed with AIDS and SIVE.

CNS pathology with SIV infection may be influenced not only by the absolute number of macrophages in the CNS, but also the relative proportion of CD163+ perivascular macrophages to MAC387+ inflammatory macrophages¹⁸¹. Because of this we determined the ratio of CD163+ to MAC387+ macrophages in the perivascular space, meninges, and choroid plexus of SIV infected animals (ratio = absolute cell count CD163+ M ϕ / absolute count MAC387+ M ϕ per region). Because SIVE lesions were not present in SIVnoE animals or animals sacrificed at 22 dpi, inter-group comparisons were not made with regard to SIVE lesions. A higher ratio of CD163+ to MAC387+ macrophages (representing increased numbers of CD163+ macrophages and decreased numbers of MAC387+ macrophages) was found in SIVE animals compared to SIVnoE animals or SIV-infected animals sacrificed at 22 dpi (Figure 1A, C, D). Extending our prior observation that increased severity of SIVE lesions was reflected in a greater ratio of CD163+ to MAC387+ macrophages in SIVE lesions,¹⁸¹ we now find that the ratio of CD163+ to MAC387+ macrophages was also higher in the perivascular space, meninges, and choroid plexus. This suggests that accumulation of CD163+ macrophages and decreased numbers of MAC387+ macrophages are associated with the development of AIDS and SIVE. Overall, both MAC387+ and CD163+ macrophages accumulated primarily in the perivascular space and SIVE lesions and not in the meninges or choroid plexus.

The phenotype of BrdU+ macrophages recruited to the CNS varies by CNS compartment.

To investigate differences in macrophage traffic from the bone marrow to the CNS in acute infection versus AIDS, monocyte progenitors in the bone marrow were labeled by BrdU administered at 6 dpi and 20 dpi (“Early”, n = 7) or 49 dpi and 48h prior to necropsy (“Late”, n = 5) (Table 4.1). Analysis of CNS tissue was stratified by timing of BrdU administration and CNS pathology, and BrdU+ cells were counted in the perivascular space, SIVE lesions (when present), meninges, and choroid plexus (Table 4.2, Figure 4.2). MAC387+BrdU+ and CD163+BrdU+ macrophages together accounted for essentially all of the BrdU+ cells in the CNS (Figure 4.2). We did not find CD3+BrdU+ T-lymphocytes as previously reported (data not shown)⁴².

Low numbers of BrdU+ macrophages were found in the perivascular space (range: 0- 6 BrdU+ macrophages/mm²) where both MAC387+BrdU+ and CD163+BrdU+ macrophages were present (Table 4.2, Figure 4.2A, B). In SIVE lesions, the majority of BrdU+ macrophages were MAC387+BrdU+ with rare CD163+BrdU+ macrophages as previously reported^{42,181} (Table 4.2, Figure 4.2C, D). In the meninges, the majority of BrdU+ macrophages were MAC387+BrdU+ in animals sacrificed at 22 dpi, but equal numbers of MAC387+BrdU+ and CD163+BrdU+ macrophages were present in the meninges of animals sacrificed with AIDS, with and without SIVE (Table 4.2, Figure 4.2E, F). In the choroid plexus, CD163+BrdU+ macrophages outnumbered MAC387+BrdU+ macrophages regardless of timing of BrdU administration or CNS pathology (Table 4.2, Figure 4.2G, H). The observation that CD163+ macrophages

present in the meninges at 22 dpi and in SIVE lesions terminally were not BrdU+ suggests these CD163+ macrophages were already present in the CNS prior to BrdU administration or, alternatively, they may not be recruited from the bone marrow. The differences we find in the relative proportion of MAC387+BrdU+ and CD163+BrdU+ macrophages in SIVE lesions, meninges, and choroid plexus may reflect different traffic patterns or mechanisms of recruitment between these CNS compartments or between macrophage subsets.

Recruitment of BrdU+ macrophages to the CNS is greatest terminally with AIDS and SIVE

A greater number of BrdU+ macrophages were present in the CNS of SIVE animals compared to SIVnoE animals, and in animals given BrdU late compared to animals given BrdU early (Table 4.2, Figure 4.2). Recruitment of MAC387+BrdU+ macrophages to the CNS was greatest terminally in animals with AIDS and SIVE in the perivascular space ($p < 0.05$), SIVE lesions ($p < 0.01$), and meninges ($p < 0.05$), but not choroid plexus (Table 4.2, Figure 4.2). The number of CD163+BrdU+ macrophages recruited to the CNS was greater terminally in animals with AIDS and SIVE in the meninges ($p < 0.05$) and choroid plexus, but not the perivascular space or SIVE lesions (Table 4.2, Figure 4.2). The presence of CD163+BrdU+ macrophages in the meninges terminally suggests that the lack of CD163+BrdU+ macrophages in SIVE lesions is likely not due to differences in labeling affinity between macrophage subsets. Overall, these data indicate that recruitment of CNS macrophages from the bone marrow is greatest during end stage disease in animals with SIVE, and recruitment of MAC387+BrdU+

macrophages is more widespread within the CNS compared to CD163+BrdU+ macrophages.

Dextran dyes preferentially label CD163+ macrophages *in vivo* and CD163+ monocytes *in vitro*.

Because BrdU only labels monocytes and macrophages that traffic to the CNS, we used dextran dyes injected into the CSF to assess macrophage turnover within the CNS of infected animals. Macrophages within the perivascular space, meninges, and choroid plexus were labeled by serial injection of fluorescently-conjugated dextran dyes into the cerebrospinal fluid of 12 rhesus macaques (Table 4.1, Figure 4.3). Across all CNS regions, post-mortem examination showed that dextran-labeled cells were CD163+ and MAC387+ macrophages. CD163+ macrophages accounted for $94.2 \pm 1.1\%$ of all dextran-labeled cells, and $98.7 \pm 0.4\%$ of CD163+ macrophages were dextran-labeled. MAC387+ macrophages accounted for $7.0 \pm 1.0\%$ of all dextran-labeled cells and $16.5\% \pm 2.4\%$ of MAC387+ macrophages were dextran labeled (Figure 4.4). No other CNS cell types, including endothelial cells, astrocytes, and parenchymal microglia were dextran-labeled.

Because of the preferential uptake of dextran dyes by CD163+ macrophages compared to MAC387+ macrophages, both of which are monocyte derived, we assessed dextran uptake in *ex vivo* monocytes from uninfected animals (n= 6) (Figure 4.5). Following a 15 minute incubation of whole blood with dextran dyes *in vitro*, all monocyte subsets were dextran-labeled. Dextran uptake was greater in CD14⁺⁺CD16⁺ intermediate monocytes

compared to CD14⁺⁺CD16⁻ classical monocytes ($p = .03$) or CD14⁺CD16⁺⁺ nonclassical monocytes ($p = .002$) (Figure 4.5). These data could indicate that differences in labeling affinity between monocyte and macrophage subsets reflect differences in lineage, maturation, or activation

The percentage of productively infected macrophages in animals with AIDS and SIVE is 2.6-fold greater for macrophages that enter the CNS late compared to macrophages present in the CNS at 20 dpi.

SIVE lesions were evaluated to determine at which time macrophages that comprise SIVE lesions entered the CNS and to determine which cells are productively infected ($n = 4$ animals, 21 SIVE lesions total) (Figure 4.6). Using the dextran labeling scheme (Table 4.1, Figure 4.3A), macrophages labeled with Dextran:FITC (administered at 20 dpi) were present in the CNS prior to or on day 20 pi and are termed “early macrophages”, and macrophages that were not Dextran:FITC labeled were recruited to the CNS after 20 dpi and are termed “late macrophages”. Surprisingly, we found $70.7 \pm 3\%$ of cells in SIVE lesions were Dextran:FITC labeled, early macrophages and $29.3 \pm 3\%$ were late macrophages (Figure 4.6A, C). This was not expected because we do not observe SIVE lesions in animals sacrificed at 22 dpi. Interestingly, CD163⁺ multinucleated giant cells (MNGC's) are productively infected and are Dextran:FITC labeled indicating they are likely derived from macrophages that were present in the CNS early prior to lesion formation (Figure 4.6A, B arrow). These data suggest that CD163⁺ macrophages present in the CNS early contribute to SIVE lesion formation terminally with AIDS and comprise the majority of macrophages in SIVE lesions.

In SIVE lesions, the majority of productively infected (SIVp28+) cells were dextran-labeled (CD163+) macrophages, which is consistent with previous observations that CD163+ macrophages are a primary target cell for productive infection in the CNS (Figure 4.6A, B).^{88,181} In these cells, CD163+ expression was confirmed in adjacent serial sections (Figure 4.6B). Using 4-color immunofluorescence, we found early and late macrophages were productively infected (Figure 4.6A, C). Within each population, $11.0 \pm 1\%$ of early macrophages were SIVp28+ and $28.7 \pm 8\%$ of late macrophages were SIVp28+ ($p < 0.05$, early vs. late) (Figure 4.6C). Scattered SIVp28+ cells that were not dextran labeled were also present and are likely representative of parenchymal microglia or infected macrophages that were not present in the perivascular space at the time of dextran labeling. These data indicate that both early and late macrophages are productively infected and that the frequency of productive infection is 2.6-fold greater in macrophages that entered the CNS late compared to early macrophages.

Early CD163+ macrophages comprise the majority of CNS macrophages terminally with AIDS

Using a combination of dextran dye injections, we characterized the distribution of dextran-labeled CNS macrophages to determine the timing of CD163+ macrophage recruitment to CNS compartments in animals sacrificed with AIDS (Table 4.3). For this, we determined CD163+ macrophage recruitment from 20 dpi to necropsy (% late macrophages) in all animals with AIDS ($n = 9$). A subset of animals ($n = 4$) that received all three dyes, the recruitment period was divided into 20 dpi to 49 dpi and 49 dpi to

necropsy, which allowed us to evaluate macrophage recruitment after viremia and terminally with AIDS. For all animals with AIDS, the percentage of late macrophages was greater in the choroid plexus ($73.0 \pm 6.2\%$, range 61.9 - 92.4%) than the meninges ($27.3 \pm 4.0\%$, range 13.0 - 55.9%, $p = .001$) or perivascular space ($29.0 \pm 3.9\%$, range 10.7 - 47.2%, $p = .001$) (Table 4.3). Interestingly, in SIVE animals the percentage of macrophages that arrive late was lower in SIVE lesions ($18.4 \pm 1.8\%$, range 14.1 – 21.7%) than in the perivascular space ($30.1 \pm 4.3\%$, range 13.8 – 37.9%) (Table 4.3). Surprisingly, the percentage of late macrophages was not significantly different between SIVnoE and SIVE animals in the perivascular space ($27.6 \pm 7.6\%$ SIVnoE, $30.1 \pm 4.3\%$ SIVE), meninges ($25.8 \pm 2.5\%$ SIVnoE, $28.5 \pm 7.3\%$ SIVE) and choroid plexus ($65.5 \pm 1.7\%$ SIVnoE, $77.9 \pm 8.8\%$ SIVE) (Table 4.3). We only found difference between SIVnoE and SIVE animals in the number of late macrophages in SIVE lesions, underscoring the importance of these cells in pathogenesis.

The rate of CD163+ macrophage recruitment to the CNS is increased with SIV infection and correlates with rapid death.

The time to death of all animals in this study sacrificed with AIDS ranged from 55 to 141 dpi and was shorter in animals with SIVE (91 ± 14 days) compared to animals without SIVE (111 ± 19 days). To account for differences in the time to death from 20 dpi, we compared rates of CD163+ macrophage recruitment by normalizing the percentage of dextran-labeled cells that entered the CNS in a given time period by the number of days in that period. For all animals sacrificed with AIDS ($n = 9$), the CD163+ macrophage recruitment rate was determined for the time period from 20 dpi to necropsy. We found

that a shorter time to death correlated with an increased rate of CD163+ macrophage recruitment in the perivascular space ($r = -0.8$, $p = 0.03$), SIVE lesions ($r = -1.0$, $p = 0.08$), meninges ($r = -0.8$, $p = 0.02$), and choroid plexus ($r = -0.9$, $p = 0.03$) for all animals (Figure 4.7).

For all animals with AIDS, SIV infection increased the rate of CD163+ macrophage recruitment from 20 dpi to necropsy in the perivascular space (range: 4.9 – 36.3 fold, mean: 21.0 ± 3 , $p < .0001$), the meninges (range: 2.2 – 8.7 fold, mean: 4.6 ± 0.8 , $p < .001$), and the choroid plexus (range: 8.4 – 27.9 fold, mean: 14.3 ± 3.5 , $p < .05$) compared to uninfected controls (Figure 4.8A-C)¹⁷⁹. The CD163+ macrophage recruitment rate in animals with SIVE was 16% greater in the perivascular space and 26% greater in the meninges compared to animals with AIDS and SIVnoE, although the differences did not reach statistical significance (Figure 4.8A, B). These data indicate that, overall, SIV infection greatly increases the rate of CD163+ macrophage recruitment to the CNS and that increased macrophage recruitment to the CNS is associated with rapid death.

For the subset of animals that received all three dyes ($n = 4$), the rate of CD163+ macrophage recruitment from 20 dpi to 49 dpi and from 49 dpi to necropsy were compared (Figure 4.8D-F). We found that in SIVE lesions, $21.4 \pm .01\%$ of CD163+ macrophages entered the CNS after 20 dpi (Table 4.3). For these cells, the rate of CD163+ macrophage recruitment in SIVE lesions was greater from 49dpi to necropsy than from 20 dpi to 49dpi (range: 2.4 – 2.8 fold, mean 2.6 ± 0.2 , $p = .0003$) (Figure 4.8D).

In contrast, the rate of CD163+ macrophage recruitment in the perivascular space was greater between 20dpi to 49dpi than 49dpi to necropsy in all animals (range: 2.32 – 7.1 fold, mean: 4.7 ± 1.2 , $p < .001$) (Figure 4.8E). The recruitment rate in the perivascular space was 68% greater in animals with SIVE than animals with SIVnoE during the post acute period 20 dpi to 49dpi ($p = .002$) but was not significantly different with regard to SIVE terminally with AIDS (Figure 4.8E). In the meninges the CD163+ macrophage recruitment rate was 91% greater in animals with SIVE compared to animals with SIVnoE terminally with AIDS ($p < 0.05$) (Figure 4.8F). These data may suggest that the rate of CD163+ macrophage recruitment in the perivascular space is greatest post acute infection and CD163+ macrophage recruitment in the meninges and SIVE lesions is greatest terminally with AIDS.

The expansion of activated CD14++CD16+ monocytes is associated with greater CD163+ macrophage recruitment and SIVE.

It has previously been demonstrated that increased monocyte activation is associated with the development of HAND and SIVE lesions^{39,42,68,252}. Soluble CD163 (sCD163) is shed by activated CD14++CD16+ monocytes, and plasma levels of sCD163 serve as a marker of monocyte activation^{248,249}. Higher sCD163 in plasma correlated with a greater percentage of late CD163+ macrophages recruited in the perivascular space and SIVE lesions in animals with AIDS and SIVE (perivascular space: $r = 1.0$, $p = .02$; SIVE lesions: $r = 1.0$, $p = .08$) (Figure 4.9A, B). This did not occur in animals with AIDS and SIVnoE. There was no correlation between plasma sCD163 and the percentage of late macrophages in the meninges and choroid plexus (Figure 4.9C, D). This suggests that

monocyte activation in the periphery is associated with accumulation of CD163+ macrophages in the perivascular space and SIVE lesions in animals with SIVE.

Because CD14++CD16+ monocytes are putative precursors of CD163+ macrophages in the CNS, we investigated the relationship between the rate of CD163+ macrophage recruitment, the number of CD14++CD16+ blood monocytes, and the development of SIVE (Figure 4.10). We found the average CD14++CD16+ monocyte count was greater in animals with SIVE compared to animals with SIVnoE (SIVnoE: 36 ± 4 cells/ μ L, SIVE: 104 ± 16 cells/ μ L, $p = 0.02$) (Figure 4.10). In animals with SIVE, an increased rate of CD163+ macrophage recruitment in the perivascular space and meninges was associated with a reduced number of CD14+CD16+ monocytes in the blood, though this trend was not statistically significant (perivascular space: $r = -0.9$; meninges: $r = -0.8$) (Figure 4.10). Here we demonstrate that SIVE is associated with the expansion of CD14++CD16+ monocytes, increased monocyte activation, and accumulation of CNS macrophages. These data may suggest that monocyte dysregulation leads to increased numbers of activated monocytes and that this population is reduced in the blood as monocytes traffic to the CNS, which results in macrophages accumulation in the CNS with SIVE.

Conclusions

These studies characterize macrophage accumulation and productive SIV infection in the CNS with the development of SIVE. Interestingly, we found that the majority of CD163⁺ macrophages in SIVE lesions were already present in the CNS by 20 dpi. Late CD163⁺ macrophages recruited after 20 dpi and MAC387⁺ macrophages recruited terminally with AIDS were also present in SIVE lesions. Early and late CD163⁺ macrophages were productively infected and the percentage of productively infected macrophages was 2.6-fold greater in late CD163⁺ macrophages compared to early macrophages. This suggests that SIV may be reintroduced into the CNS by traffic of infected monocytes/macrophages during end stage disease. Together these data indicate that SIVE lesions are formed by redistribution of resident perivascular macrophages, traffic of productively infected CD163⁺ macrophages from the periphery, and recruitment inflammatory MAC387⁺ macrophages from the bone marrow terminally with AIDS.

We found differences in CD163⁺ and MAC387⁺ macrophage accumulation between CNS compartments. Early infection was characterized by the recruitment of MAC387⁺ macrophages throughout the CNS during primary/acute infection. Terminally with AIDS, both CD163⁺ and MAC387⁺ macrophages accumulated in perivascular cuffs and SIVE lesions. We found that the ratio of CD163⁺ to MAC387⁺ macrophages in the perivascular space, meninges, and choroid plexus was greater in animals with AIDS and SIVE than animals with AIDS and SIVnoE or SIV without AIDS. It is possible that MAC387⁺ macrophages represent an M1 polarized subpopulation that promotes an

antimicrobial microenvironment that limits viral replication in the CNS and that a switch to an M2 polarized microenvironment is associated with the development of SIVE.

Recruitment of bone marrow derived (BrdU+) cells to the CNS, the majority of which were MAC387+, was greatest in the meninges and choroid plexus compared to the perivascular space and SIVE lesions. Additionally, the meninges and choroid plexus did not show significant macrophage accumulation with AIDS and SIVE suggesting a higher rate of turnover in these compartments. Overall recruitment of monocytes/macrophages from the bone marrow was greatest terminally with AIDS and SIVE. Although CD163+BrdU+ macrophages accounted for more than half of all BrdU+ cells in the meninges and choroid plexus terminally with AIDS, few CD163+BrdU+ macrophages were present in the perivascular space or SIVE lesions. This may indicate that CD163+ macrophages that accumulate in SIVE lesions are derived from within the CNS or are recruited from outside the bone marrow. These data likely indicate that different mechanisms of macrophage recruitment exist between CNS compartments and macrophage subsets.

In animals with SIVE, we observed increased monocyte activation and expansion of the CD14+CD16+ subset that correlated with increased accumulation of CD163+ macrophages in the perivascular space and in SIVE lesions. This may indicate that increased numbers activated monocytes in the periphery leads to greater accumulation of macrophages in the CNS. In all animals, SIV infection increased the rate of macrophage recruitment to the CNS and rapid recruitment was associated with shorter

time to death. Together, these data suggest that with SIV infection increased monocyte activation and expansion leads to more rapid traffic of monocytes/macrophages to the CNS, which contributes to the development of SIVE.

These studies indicate that the development of SIVE is a dynamic process affected by systemic immune activation, macrophage heterogeneity, and productive infection of the CNS. SIV infection leads to CNS inflammation during primary/acute infection and increased recruitment of monocytes/macrophages throughout disease. Increased numbers of activated monocytes and increased traffic of monocytes/macrophages from the bone marrow in animals with SIVE suggests that CNS disease is associated with monocyte dysregulation and the inability to limit systemic immune activation. An increased frequency of productive infection in CD613+ macrophages recruited to the CNS terminally with AIDS may indicate that traffic of activated/infected monocytes/macrophages to the CNS during end stage disease contributes to SIVE. Importantly we have demonstrated that resident perivascular macrophages play a major role in SIVE lesion formation in end stage disease.

Table 4.1: Experimental design for dextran labeling studies.

Treatment^a	SIV, 22dpi Early BrdU 1 dye n = 3	AIDS Early BrdU 2 dyes n = 2	AIDS Early BrdU 3 dyes n = 2	AIDS Late BrdU 2 dyes n = 3	AIDS Late BrdU 3 dyes n = 2
BrdU	6 & 20 dpi	6 & 20 dpi	6 & 20 dpi	49 dpi & Nec.	49 dpi & Nec.
Dextran:FITC	20 dpi	20 dpi	20 dpi	20 dpi	20 dpi
Dextran:AF647	---	Nec. ^b	49 dpi	Nec. ^b	49 dpi
Dextran:Biotin	---	---	Nec. ^b	---	Nec. ^b
Sacrificed	22dpi	AIDS	AIDS	AIDS	AIDS

a. All animals were infected with SIVmac251 (1ng SIVp27, *iv*) on day 0. Anti-CD8 antibody was administered at 6 dpi, 8 dpi, and 12 dpi.

b. "Nec." indicates administration of BrdU or dextran 48 hours prior to necropsy.

Table 4.2: Macrophage traffic from the bone marrow to the CNS is greatest terminally with AIDS.

Group ^a	Subset	Perivascular Space ^b	SIVE lesions ^c	Meninges ^b	Choroid Plexus ^b
SIV, 22dpi BrdU Early n = 3	CD163+	2 ± 0.4	---	45 ± 8	110 ± 30 ^d
	MAC387+	2 ± 0.8	---	260 ± 40	35 ± 30 ^d
SIVE, AIDS BrdU Early n = 3	CD163+	1 ± 0.2	2 ± 0.4	120 ± 30	160
	MAC387+	2 ± 0.3	6 ± 2	120 ± 40	45
SIV, AIDS BrdU Late n = 3	CD163+	2 ± 0.2	---	150 ± 30	290
	MAC387+	1 ± 0.3	---	250 ± 100	100 ± 90 ^d
SIVE, AIDS BrdU Late n = 2	CD163+	1 ± 0.3	1 ± 0.2	310 ± 40	270 ± 50 ^d
	MAC387+	4 ± 0.5	21 ± 4	340 ± 90	70 ± 20 ^d

a. Early: BrdU administered at 6 dpi and 20 dpi. Late: BrdU administered at 49 dpi and 48 h prior to necropsy.

b. Counts are the mean ± SEM of the number of CD163+BrdU+ or MAC387+BrdU+ macrophages per mm².

c. Counts are the mean ± SEM of the number of CD163+BrdU+ or MAC387+BrdU+ macrophages per SIVE lesion.

d. Choroid plexus tissue was available from 2 animals in this group

Table 4.3: Distribution of dextran-labeled CD163+ macrophages in CNS tissues.

CNS Region	CNS Pathology	Present 20 dpi ^a	Entered 20-Nec. ^a	Entered 20-49 dpi ^b	Entered 49 dpi-Nec. ^b
Perivascular Space	SIVE	69.9 ± 4.3 %	30.1 ± 4.3 %	27.6 ± 2.8 %	7.3 ± 0.5 %
	SIVnoE	72.4 ± 7.6 %	27.6 ± 7.6 %	16.1 %	12.7 %
SIVE lesion	SIVE	81.6 ± 1.8 %	18.4 ± 1.8 %	4.3 ± 0.1 %	17.1 ± 0.1 %
	SIVnoE	---	---	---	---
Meninges	SIVE	71.5 ± 7.3 %	28.5 ± 7.3 %	14.2 ± 3.6 %	21.3 ± 6.8 %
	SIVnoE	74.2 ± 2.5 %	25.8 ± 2.5 %	12.4	20.3 %
Choroid Plexus	SIVE	22.1 ± 8.8 ^c %	77.9 ± 8.8 ^c %	ND ^d	ND ^d
	SIVnoE	34.5 ± 1.7 ^c %	65.5 ± 1.7 ^c %	ND ^d	ND ^d

Dextran labeled macrophages in the CNS were counted by sampling 3000-4000 cells from frontal, temporal parietal, and occipital cortices, 1000 cells from meninges, and 2 sections of choroid plexus per animal. When present, 10 or more SIVE lesions were counted per animal. Values are the mean ± SEM percentage of all dextran labeled macrophages for n animals.

a. SIVE (n = 5), SIV (n = 4)

b. For animals that received the three dye regimen, the period 20 dpi-Necropsy can be subdivided into 20 dpi- 49 dpi and 49 dpi- Necropsy. SIVE (n = 3), SIV (n = 1)

c. p < 0.02, choroid plexus vs. perivascular space, meninges, or SIVE lesions.

d. ND: Not done.

Figure 4.1. CD163+ and MAC387+ macrophages accumulate in the perivascular space and SIVE lesions in SIV infected animals. A-D. Single-label IHC for CD163 (closed squares) or MAC387 (open circles) in uninfected animals (n = 3), SIV-infected animals sacrificed at 22 dpi (SIV 22 dpi, n = 3), and SIV-infected animals that progressed to AIDS with encephalitis (SIVE, n = 5) or without (SIVnoE, n = 4). Each data point represents one tissue section or one SIVE lesion. **A-D.** MAC387+ macrophages are not present in the normal, uninfected CNS but are recruited to the CNS with SIV infection. CD163+ macrophages outnumber MAC387+ macrophages in uninfected and SIV-infected animals. **A & B.** In animals with AIDS, CD163+ and MAC387+ macrophages accumulate primarily in the perivascular space (**A**) and in SIVE lesions (**B**). **B.** SIVE lesions are only observed terminally in animals that progressed to AIDS. **C & D.** In the meninges (**C**) and choroid plexus (**D**), MAC387+ macrophages are more numerous at 22dpi than terminally with AIDS. **A-D.** Animals with AIDS and SIVE have higher ratios of CD163+ to MAC387+ macrophages than animals with AIDS and no SIVE or animals sacrificed at 22dpi. The numbers above each graph are the average ratio of CD163+ to MAC387+ macrophages for SIV infected animals. NA: Not Applicable. * P < .05, ** P < .01, *** P < .001, **** P < .0001.

Figure 4.1

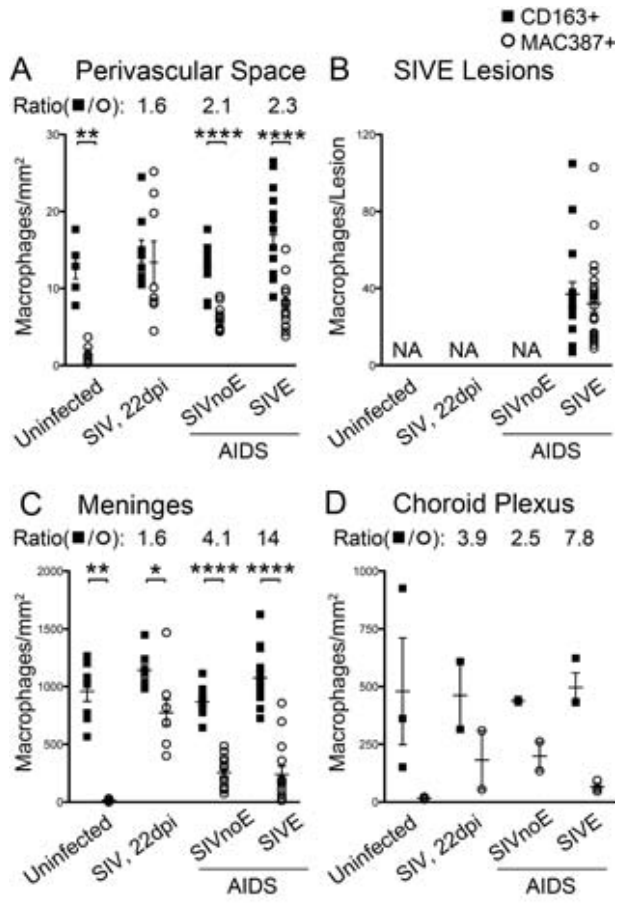
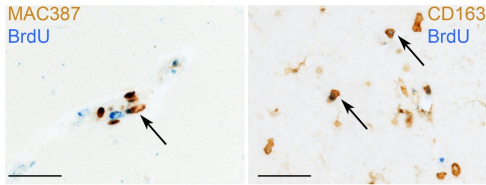


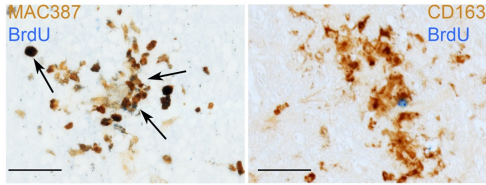
Figure 4.2. Recruitment of MAC387+ and CD163+ macrophages from the bone marrow differs in timing and magnitude by CNS region. Recruitment of CNS macrophages from the bone marrow was determined by BrdU labeling of monocyte progenitors during early (6 dpi & 20 dpi) and late (49 dpi & 48h pre necropsy) SIV infection. Double-label IHC for BrdU (blue) and MAC387 or CD163 (brown) was used to determine the number of BrdU+ macrophages in SIV-infected animals stratified by timing of BrdU administration and CNS pathology: Early BrdU, 22 dpi (n = 3); Early BrdU, SIVE (n = 3); Late BrdU, SIVnoE (n = 3); Late BrdU, SIVE (n = 2). Each data point represents one tissue section or one SIVE lesion. **A.** BrdU+ macrophages in the perivascular space are MAC387+BrdU+ and CD163+BrdU+ in CNS tissue from all animals. Arrows indicate MAC387+BrdU+ or CD163+BrdU+ macrophages. Scale bars are 50µm. **B.** Few BrdU+ macrophages are present in the perivascular space, overall. More MAC387+BrdU+ macrophages are present in animals sacrificed with AIDS and SIVE that were given BrdU late. **C.** BrdU+ macrophages in SIVE lesions are MAC387+BrdU+ with rare CD163+BrdU+ macrophages. **D.** More MAC387+BrdU+ macrophages are present in SIVE lesions in animals sacrificed with AIDS and SIVE that were given BrdU late. **E.** BrdU+ macrophages in the meninges are MAC387+BrdU+ and CD163+BrdU+. **F.** In animals sacrificed at 22dpi, the majority of BrdU+ macrophages in the meninges are MAC387+BrdU+ with few CD163+BrdU+ macrophages present. In animals sacrificed with AIDS, BrdU+ meningeal macrophages are MAC387+BrdU+ and CD163+BrdU+. More MAC387+BrdU+ and CD163+BrdU+ macrophages are present in animals given BrdU late compared to animals given BrdU early and animals with SIVE compared to animals with SIVnoE. **G.** BrdU+ macrophages in the choroid plexus are CD163+BrdU+ with scattered MAC387+BrdU+ macrophages present. **H.** CD163+BrdU+ are more numerous than MAC387+BrdU+ macrophages regardless of timing of BrdU administration or CNS pathology. More CD163+BrdU+ macrophages are present in animals that were given BrdU late compared to animals that were given BrdU early. NA: Not applicable. * P < .05, ** P < .01, *** P < .001, **** P < .0001.

Figure 4.2

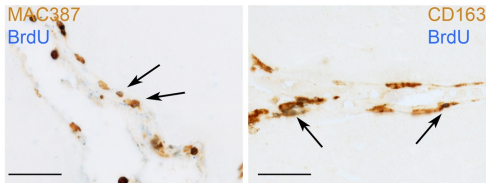
A Perivascular Space



C SIVE Lesions



E Meninges



G Choroid Plexus

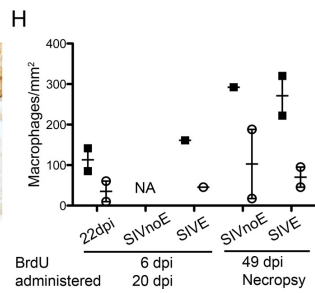
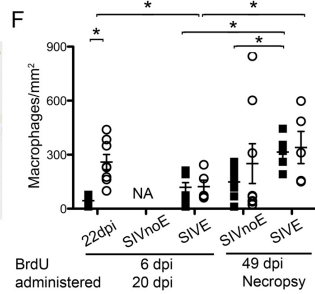
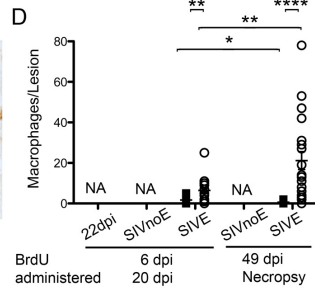
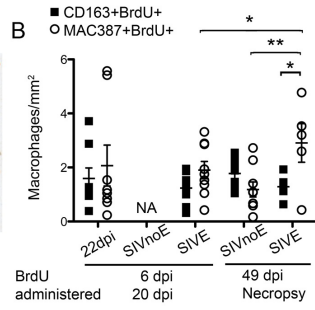
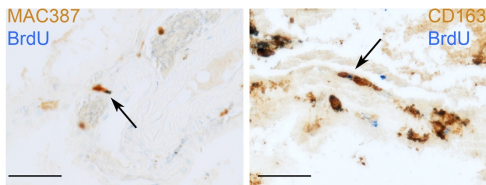


Figure 4.3. Experimental design for dextran labeling of CNS macrophages.

A. Injection of fluorescent-conjugated dextran dyes into the cisterna magna labels macrophages in the perivascular space, meninges, and choroid plexus at the time of administration. Serial injection of dextran conjugated to different fluorophores allows for determination of time of CNS entry: fluorescein - 20 dpi, Alexa Fluor 647- 49 dpi, biotin - 48h pre-necropsy. Triple-labeled macrophages (fluorescein+AlexaFluor647+biotin+) were present at 20 dpi, double-labeled macrophages (AlexaFluor647+biotin+) entered the CNS 20 dpi- 49 dpi, and single-labeled macrophages (biotin+) entered the CNS after 49 dpi. **B.** Three-color immunofluorescence of a blood vessel and associated perivascular macrophages in the cerebral cortex of an animal sacrificed with AIDS and SIVE. Triple- (long arrow), double- (short arrow), and single- (arrowhead) labeled macrophages are present. Note that the majority of macrophages were present in the CNS at 20 dpi. Insets are single channel images. Scale bar is 50 μ m.

Figure 4.3

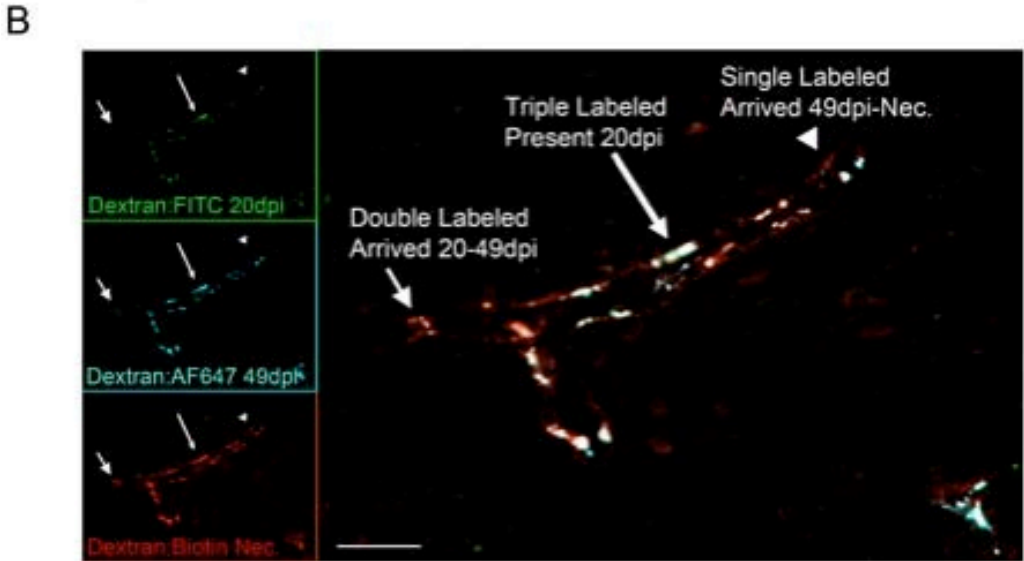
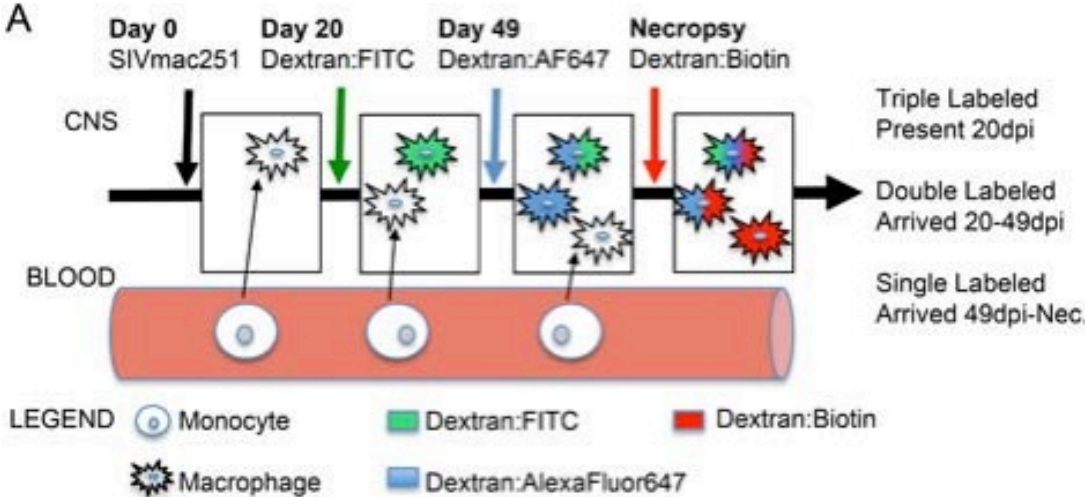
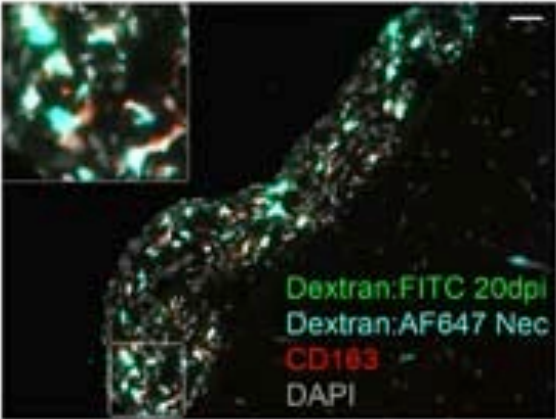


Figure 4.4. Dextran dyes robustly label CD163+ and not MAC387+ CNS

macrophages. Immunofluorescent staining for CD163 (**A**) or MAC387 (**B**) in cortical meninges from an animal that was given two dextran dyes: fluorescein - 20 dpi, Alexa Fluor 647 - 48h pre-necropsy. Images are representative of all CNS regions examined from 12 animals. Insets are enlargements of the area indicated by a white rectangle. Scale bar is 50 μ m. **A.** The majority of dextran-labeled cells are CD163+ macrophages. Almost all CD163+ macrophages are dextran-labeled. **B.** Some dextran-labeled cells are MAC387+ macrophages. The majority of MAC387+ macrophages are not dextran-labeled.

Figure 4.4

A



B

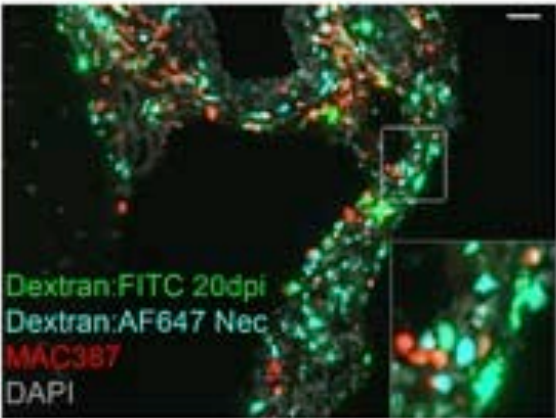


Figure 4.5. Dextran uptake varies between monocyte subsets *ex vivo*.

Dextran uptake in normal monocytes was determined by FACS after *in vitro* labeling of whole blood with fluorescein-conjugated dextran (Dextran:FITC). **A.** A representative histogram (n =6 animals) of Dextran:FITC uptake by classical (CD14⁺⁺CD16⁻), intermediate (CD14⁺⁺CD16⁺), and nonclassical (CD14⁺CD16⁺⁺) monocytes. **B.** Dextran:FITC is taken up by all monocyte subsets. Dextran uptake is greatest in CD14⁺⁺CD16⁺ intermediate monocytes, a putative CD163⁺ macrophage precursor *P < .05, ** P < .01.

Figure 4.5

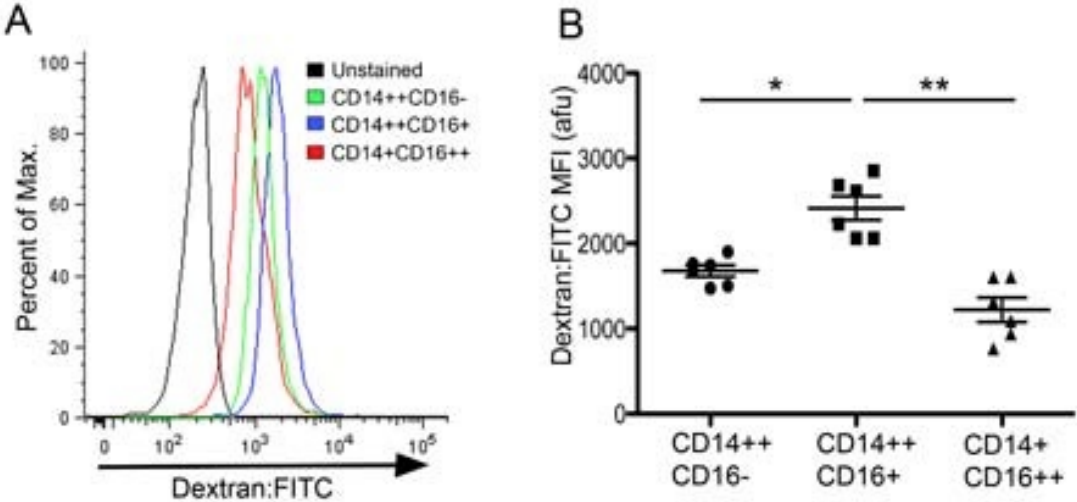
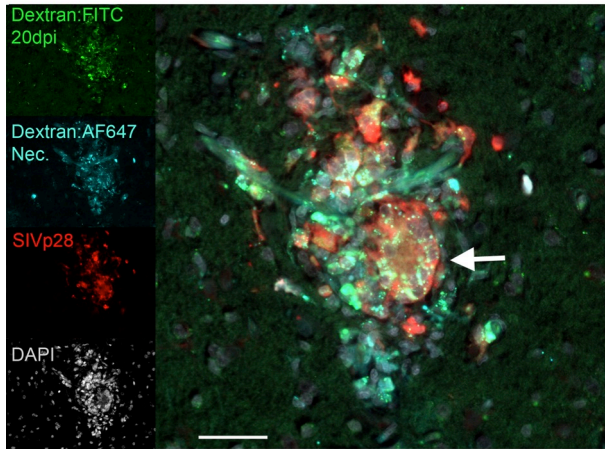


Figure 4.6. Macrophages that enter the CNS late in animals with AIDS and SIVE are the primary cell type that is productively infected.

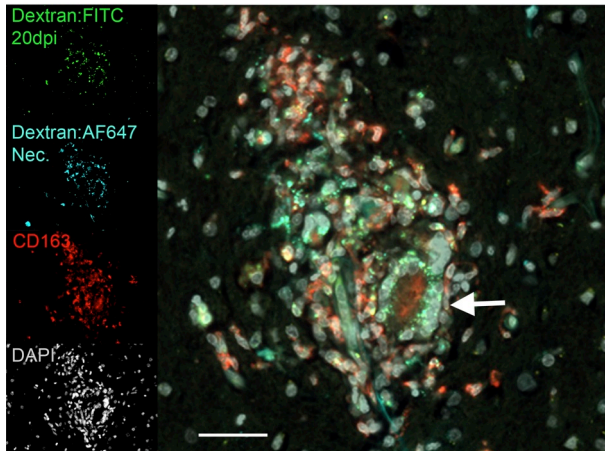
A & B. Immunofluorescent staining for SIVp28 (**A**, red) or CD163 (**B**, red) in serial sections (10 μm) of an SIVE lesion from an animal that received Dextran:FITC (green, 20 dpi), Dextran:AF647 (cyan, 138 dpi), and was sacrificed at 140 dpi with AIDS and SIVE. DAPI was used to stain nuclei (gray). The images presented here are representative of more than 20 lesions from four SIVE animals sampled from multiple cortical regions. The majority of productively infected cells (SIVp28+) were dextran-labeled CD163+ macrophages. SIVp28+, productively infected macrophages that are not dextran labeled are present. These cells may be parenchymal microglia or macrophages that were not present in the perivascular space at the time of dextran administration. A SIVp28+CD163+ multinucleated giant cell (MNGC, white arrows) is Dextran:FITC+ indicating that the macrophages that compose the MNGC were present in the CNS by 20 dpi. Boxes inset on the left are single channel control images. The scale bar is 25 μm . **C.** Four color IF was used as above to determine the frequency of productive infection in “Early” (Dextran:FITC+, present at 20 dpi) and “Late” (Dextran:FITC-, entered after 20 dpi) macrophages in SIVE lesions for each SIVE animal. The majority of macrophages in SIVE lesions were uninfected macrophages present in the CNS prior to 20 dpi. SIVp28+ early macrophages and SIVp28+ late macrophages (black bars) were present in approximately equal numbers. In SIVE lesions $11.0 \pm 1\%$ of early macrophages and $28.7 \pm 8\%$ of late macrophages were SIVp28+.

Figure 4.6

A



B



C

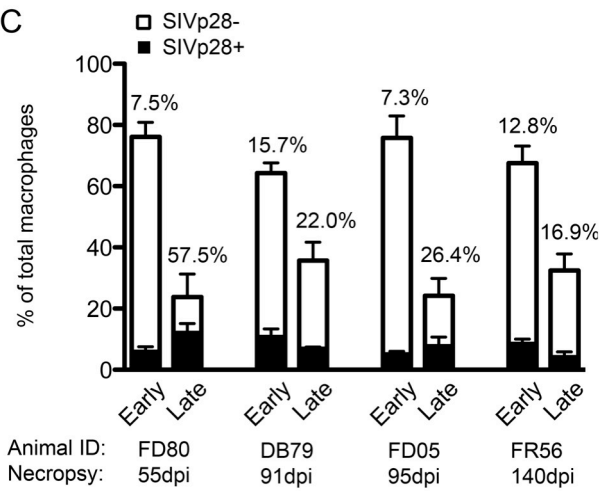
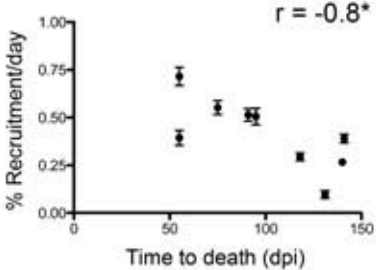


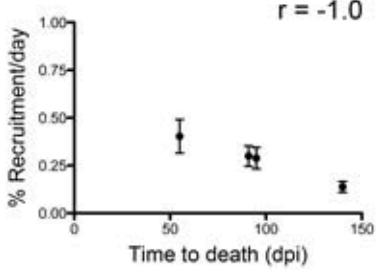
Figure 4.7. The recruitment rate of CD163+ macrophages to the CNS is inversely proportional to time to death. Paired XY values for time to death and CD163+ macrophage recruitment rate are plotted for animals sacrificed with AIDS (n = 9). Time to death is inversely correlated with the rate of CD163+ macrophage recruitment to the perivascular space (**A**), SIVE lesions (**B**), meninges (**C**), and choroid plexus (**D**) in SIVE and SIVnoE animals. A Spearman rank test is used for correlation statistics. * P < .05.

Figure 4.7

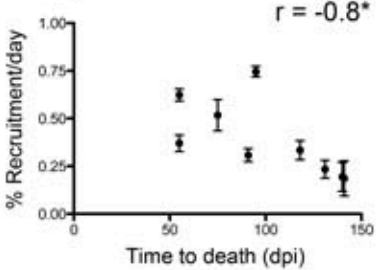
A Perivascular Space



B SIVE Lesions



C Meninges



D Choroid Plexus

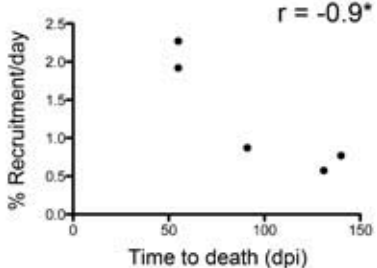
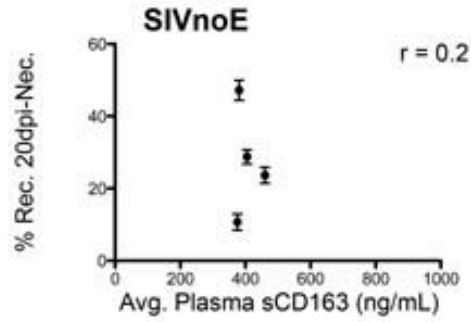
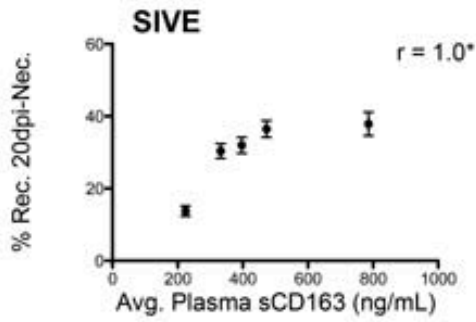


Figure 4.8. The rate of CD163+ macrophage recruitment to the CNS is increased with SIV infection and is greater in animals with SIVE. The rate of CD163+ macrophage recruitment was derived by normalizing the percentage of dextran-labeled cells that entered the CNS in a given period (Table 4.3) by the number of days in that period. Each data point represents one lesion or one tissue section (11-14 cortical sections, 3-4 sections of meninges, and 1 choroid plexus section per animal). **A-C.** The recruitment rate was determined 20 dpi- necropsy for all animals that progressed to AIDS (n = 9). Basal turnover of perivascular, meningeal, and choroid plexus macrophages was determined in uninfected animals reconstituted with EGFP-expressing CD34+ stem cells (n = 3). Compared to uninfected animals, the recruitment rate of CD163+ macrophages 20 dpi- necropsy in animals sacrificed with AIDS is increased 20-fold in the perivascular space (**A**), 5-fold in the meninges (**B**), and 15-fold in the choroid plexus (**C**). The CD163+ macrophage recruitment rate is greater in animals with SIVE (n = 5) than animals with SIVnoE (n = 4) although this did not reach statistical significance (**A & B**). **D-F.** In a subset of animals that progressed to AIDS and received all three dyes (n = 4), the recruitment rate was determined 20 dpi- 49 dpi and 49 dpi- necropsy to compare differences in recruitment post acute infection and terminally with AIDS, respectively. **D.** In SIVE lesions, the rate of CD163+ macrophage recruitment is greater terminally, 49 dpi- necropsy, compared to 20 dpi- 49 dpi. **E.** In the perivascular space, the CD163+ macrophage recruitment rate is greater 20 dpi- 49 dpi compared to 49 dpi-necropsy in both SIVE and SIVnoE animals. The CD163+ macrophage recruitment rate is 68% greater in animals with SIVE than animals with SIVnoE post acute infection, 20 dpi- 49 dpi, but was not significantly different terminally with AIDS, 49 dpi-necropsy. **F.** In the meninges the CD163+ macrophage recruitment rate is 91% greater in SIVE animals than SIVnoE animals terminally with AIDS. * P < .05, ** P < .01, *** P < .001, **** P < .0001.

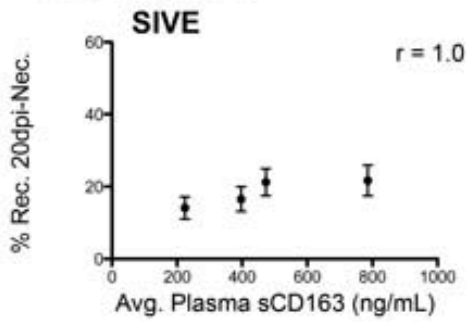
Figure 4.9. Increased CD163+ macrophage recruitment in the perivascular space and SIVE lesions correlates with higher concentration of sCD163 in plasma in SIVE animals. Paired XY values for plasma concentration of sCD163, an activation marker shed by CD14++CD16+ monocytes, and percentage of dextran-labeled CD163+ macrophages that entered the CNS after 20 dpi are plotted. Values for sCD163 are the average of weekly measurements from 20 dpi- necropsy. **A & B.** Higher plasma levels of sCD163 are associated with increased CD163+ macrophage recruitment to the perivascular space (**A**) and SIVE lesions (**B**) in SIVE but not SIVnoE animals. **C & D.** Plasma levels of sCD163 are not correlated with CD163+ macrophage recruitment to the meninges (**C**) or choroid plexus (**D**) in SIVE and SIVnoE animals. * P < .05.

Figure 4.9

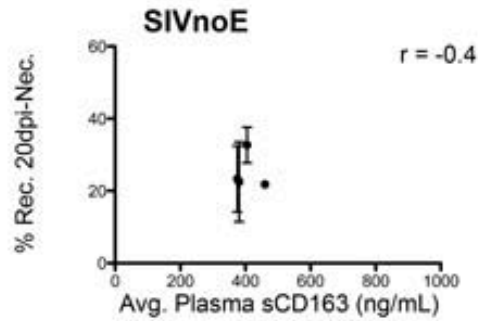
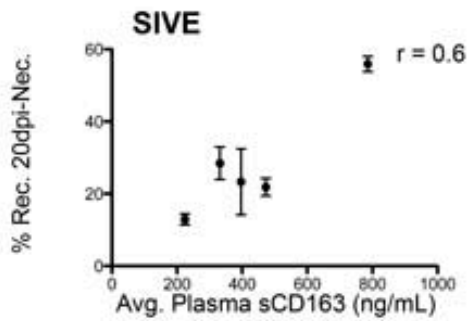
A Perivascular Space



B SIVE Lesions



C Meninges



D Choroid Plexus

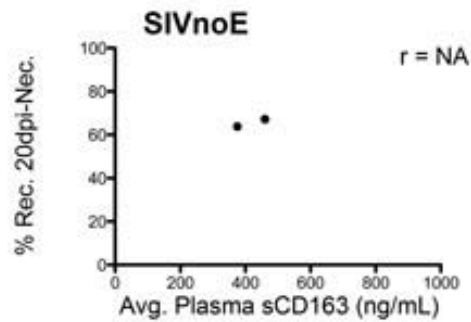
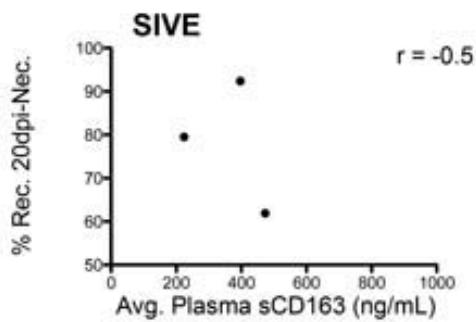
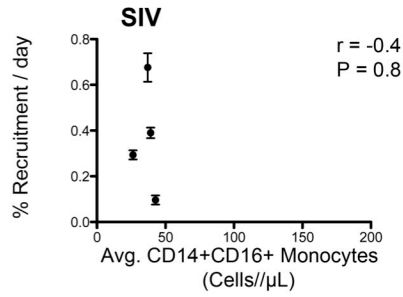
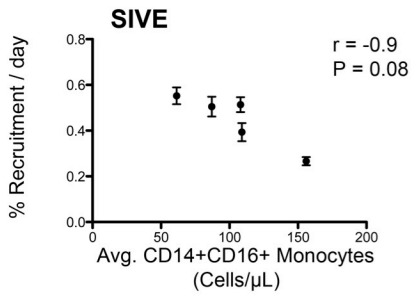


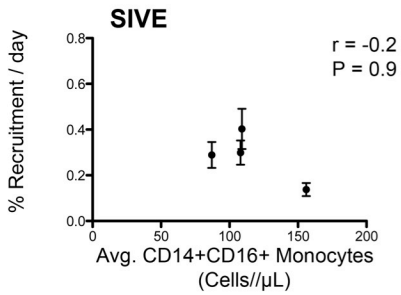
Figure 4.10. CD163+ macrophage recruitment to the perivascular space and meninges is associated with lower numbers of CD14++CD16+ monocytes in the blood. Paired XY values for average number of CD14++CD16+ monocytes and CD163+ macrophage recruitment rate are plotted. Activated CD14++CD16+ monocytes are more numerous in SIVE animals than SIVnoE animals (104 ± 16 cells/ μ L vs. 36 ± 4 cells/ μ L, $p = 0.02$). **A, C.** Higher rates of CD163+ macrophage recruitment to the perivascular space (**A**) and meninges (**C**) are associated with lower numbers of CD14++CD16+ monocytes in the blood in SIVE but not SIVnoE animals. **B, D.** There was no correlation between CD14++CD16+ monocyte number and macrophage recruitment rate in SIVE lesions (**B**) or choroid plexus (**D**). A Spearman rank test is used for correlation statistics.

Figure 4.10

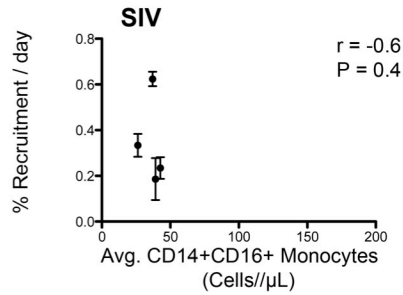
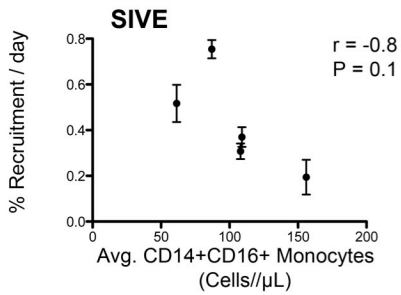
A Perivascular Space



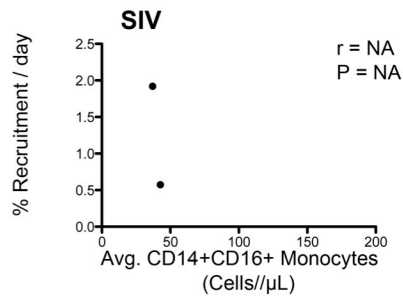
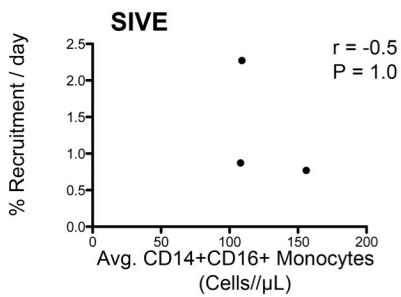
B Lesions



C Meninges



D Choroid Plexus



Chapter 5: PCNA is expressed by CD163+ CNS macrophages in SIV-infected macaques and is associated with decreased macrophage apoptosis with SIV infection *in vitro*.

Chapter Overview

A subset of CNS macrophages express PCNA in the context of SIV or HIV infection. PCNA expression occurs absent standard markers of cell proliferation (Ki-67, BrdU, Topoisomerase II) and correlates with both SIV and HIV infection in the same cell. The biological function of PCNA in SIV or HIV infected macrophages in the CNS is not known. In these studies, we characterized the pattern of PCNA expression in monocytes and macrophages in SIV-infected rhesus macaques and performed siRNA knockdown in primary monocyte-derived macrophages *in vitro* to investigate the role of PCNA in SIV infection. We found that PCNA is expressed by CD163+ macrophages, but not MAC387+ macrophages in SIVE lesions. PCNA was not detected in CD14+ monocytes from uninfected or chronically SIV-infected animals. We also found that few PCNA+ macrophages in the CNS are BrdU-labeled, which suggests that PCNA expression is independent of recent proliferation in the bone marrow. *In vitro* siRNA-mediated knockdown of PCNA in primary monocyte-derived macrophages prior to SIV infection was associated with an increase in SIVp27 production. We also observed that PCNA knockdown is associated with increased apoptosis following SIV infection compared to nonsilencing controls. These data suggest that PCNA expression is restricted to CD163+ macrophages in the CNS, which may be productively infected, and

is independent of proliferation. Additionally, PCNA mediated inhibition of apoptosis may be a mechanism by which SIV-infected macrophages are long-lived in the CNS.

PCNA is expressed by CD163+ macrophages and is rarely present in MAC387+ or BrdU+ macrophages in SIVE lesions.

Previous studies have shown that PCNA is expressed by CNS macrophages in SIV infected macaques and that a high percentage of PCNA+ macrophages are productively infected (SIVp28+ and SIV RNA+)^{216,217}. We characterized PCNA expression in two subpopulations of CNS macrophages: 1) CD163+ perivascular macrophages, which are the primary cell type infected in the CNS,^{88,185} and 2) MAC387+ inflammatory macrophages, which are not productively infected in the CNS (Table 5.1, Figure 5.1)¹⁸¹. In SIVE lesions, $70.7 \pm 2.8\%$ of PCNA+ cells were PCNA+CD163+ macrophages and $4.8 \pm 1.2\%$ of PCNA+ cells were PCNA+MAC387+ macrophages (Table 5.1, Figure 5.1 A, B). Because PCNA has been associated with cell proliferation, we investigated whether PCNA+ macrophages were labeled with BrdU, a marker of recent proliferation in the bone marrow. We found $14.4 \pm 5.8\%$ of PCNA+ cells were BrdU+, which suggests that the majority of PCNA+ cells were not proliferating (Table 5.1, Figure 5.1C). Thus in the CNS, PCNA is expressed primarily in CD163+ perivascular macrophages, but not in inflammatory MAC387+ macrophages. These data suggest that PCNA expression is not due to recent cell division in the periphery and is restricted to CD163+ macrophages that may be productively infected.

PCNA is not expressed by circulating monocytes in normal and chronically SIV-infected animals.

We next investigated whether PCNA is expressed by monocytes, which are the precursors of CNS macrophages. CD14⁺ monocytes were isolated from both uninfected (n = 4) and chronically SIV-infected (n = 4, 120 dpi) animals (Figure 5.2). PCNA mRNA was not detected in CD14⁺ monocytes from uninfected or SIV infected animals by qRT-PCR (Figure 5.2A). As a control, GAPDH mRNA was detected in all samples. Additionally, PCNA protein was not detected in CD14⁺ monocytes from uninfected or SIV infected animals (Figure 5.2B). As a control PCNA was detected in an equivalent amount of lysate from THP-1 cells, a myelomonocytic cell line. These data further support the hypothesis that expression of PCNA in CNS macrophages is not carried over from expression in the periphery.

SIV infection induces PCNA expression in MDM *in vitro*

Because PCNA expression in CNS macrophages is associated with productive infection in the same cell, we sought to investigate whether PCNA expression was induced by SIV infection *in vitro*. Monocytes from uninfected animals were cultured *in vitro* with fetal bovine serum and macrophage colony stimulating factor (M-CSF) to generate monocyte-derived macrophages (MDM). After 5 days in culture, $22.1 \pm 7\%$ of MDM were PCNA⁺ by immunofluorescence (Figure 5.3). The PCNA promoter is serum responsive, and PCNA expression by MDM *in vitro* may be due to mitogenic factors in the culture medium^{253,254}. PCNA expression may also be associated with the maturation of MDM *in vitro*. To assess whether PCNA was induced by SIV infection, MDM were

infected with SIV316* and PCNA expression was assessed by qRT-PCR at 0 dpi, 1 dpi and 3 dpi. PCNA mRNA was increased 1.6-fold at 1 dpi and 2-fold at 3 dpi relative to uninfected controls (Figure 5.4). These data indicate that PCNA is induced in MDM in response to SIV infection.

PCNA knockdown in primary MDM increases SIVp27 production and increases the percentage of apoptotic macrophages.

To determine whether PCNA has a specific effect on viral replication, we treated MDM with PCNA-specific siRNA (siRNA-5 or siRNA-6) or a nonsilencing control (siRNA-NS) prior to SIV infection. The commercially available PCNA-specific siRNAs were designed from the human PCNA reference sequence. The sequence of siRNA-5 was a perfect match to the *M. mulatta* PCNA reference sequence, and the sequence of siRNA-6 contained a single base pair mismatch relative to the *M. mulatta* PCNA reference sequence. siRNA treatment of MDM decreased PCNA mRNA by $52 \pm 4\%$ for siRNA-5 and $30 \pm 5\%$ for siRNA-6 relative to a nonsilencing siRNA, measured at 3 dpi (Figure 5.5A). The decrease in PCNA protein was commensurate to the reduction in PCNA mRNA (Figure 5.5B). SIVp27 production, measured at 3 dpi, was 2.0 ± 0.3 fold greater ($p = 0.03$) in samples treated with PCNA-specific siRNA relative to nonsilencing controls (Figure 5.5C). Because lower levels of PCNA were associated with increased SIVp27 production, PCNA may have an antiviral effect in primary MDM.

Conducting the siRNA knockdown experiments, we noted that PCNA knockdown frequently lead to the death of primary MDM cultures and that numerous small cells that

appeared apoptotic were present in samples treated with PCNA-specific RNA compared to controls. To confirm this observation, we performed TUNEL staining on SIV-infected, siRNA-treated primary MDM. As noted previously, siRNA-5 decreased PCNA expression more efficiently than siRNA-6. Lower PCNA expression was associated with an increase in the percentage of apoptotic (TUNEL+) macrophages with SIV infection ($25.2 \pm 3.6\%$ siRNA-5, $p = 0.004$ vs. control; $15.3 \pm 2.5\%$ siRNA-6, $p = 0.008$ vs. control; $5.2 \pm 2.5\%$ siRNA-NS) (Figure 5.5D). These data suggest that PCNA expression prevents apoptosis in SIV-infected macrophages.

Conclusions

These studies investigate the role of PCNA expression in CNS macrophages in the context of SIV infection. PCNA expression has classically been associated with DNA replication in cycling cells; however, human and monkey monocytes and macrophages are thought to be terminally differentiated cells that do not divide outside of the bone marrow^{57,74,75}. Consistent with this, we found that PCNA is not expressed by circulating monocytes and few PCNA+ macrophages in the CNS were BrdU labeled following an intravenous BrdU pulse. These observations support the hypothesis that PCNA expression in CNS macrophages is not associated with recent proliferation in the bone marrow.

In SIVE lesions, PCNA was expressed in CD163+ perivascular macrophages, which are a primary target of SIV infection, and was not expressed in MAC387+ inflammatory macrophages, which are rarely productively infected^{88,181,185}. We also found that SIV infection increased PCNA expression in macrophage cultures *in vitro*. These data suggest that PCNA is expressed in CD163+ macrophages with SIV infection.

PCNA knockdown was associated with increased SIVp27 production *in vitro*, which may indicate a direct role for PCNA in inhibiting viral replication. Moreover, we show that PCNA knockdown was associated with increased macrophage apoptosis with SIV infection. Thus PCNA expression may limit viral replication and inhibit apoptosis in SIV infected macrophages.

Taken together, these data suggest that PCNA is expressed by CD163+ macrophages in the CNS in response to SIV infection independent of cell proliferation. PCNA-mediated inhibition of apoptosis may be a mechanism by which CNS macrophages are more long-lived and thus contribute to the formation and maintenance of a viral reservoir in the CNS.

Table 5.1: Phenotype of PCNA+ macrophages in SIVE lesions.

Population	Percentage^a
PCNA+CD163+ vs. total PCNA+	70.7 ± 2.8%; n ^b = 42
PCNA+MAC387+ vs. total PCNA+	4.8 ± 1.2%; n ^b = 25
PCNA+BrdU+ vs. total PCNA+	14.4 ± 5.8%; n ^b = 38
PCNA+CD163+ vs. total CD163+	65.4 ± 7.5%; n ^b = 42
PCNA+MAC387+ vs. total MAC387+	16.7 ± 8.4%; n ^b = 25
PCNA+BrdU+ vs. total BrdU+	59.0 ± 21%; n ^b = 38

- a. Data are the Mean ± SEM, for 4 SIVE animals. Three or more CNS regions were examined per animal for each stain.
- b. n is the total number of lesions evaluated for each stain.

Figure 5.1. PCNA is expressed by CD163+ CNS macrophages but is rarely present in MAC387+ or BrdU+ macrophages. Double label IHC for PCNA (brown) and CD163 (blue, **A**), MAC387 (blue, **B**), or BrdU (red, **C**). Images are representative of multiple cortical regions ($n \geq 3$ regions) examined from each of four animals with SIVE. Scale bar is 50 μ m. **A.** The majority of PCNA+ cells (brown) in SIVE lesions are CD163+ macrophages (blue). PCNA+CD163- and CD163+PCNA- cells are present. The arrow indicates a multinucleated giant cell that is CD163+ and has several PCNA+ nuclei. **B.** Few PCNA+ cells (brown) in SIVE lesions are inflammatory MAC387+ macrophages (blue). Many PCNA+MAC387- and MAC387+PCNA- cells are present. **C.** Few PCNA+ cells (brown) are BrdU+ macrophages (red) recently recruited from the bone marrow. Many PCNA+BrdU- cells are present. Few BrdU+PCNA- cells are present.

FIGURE 5.1

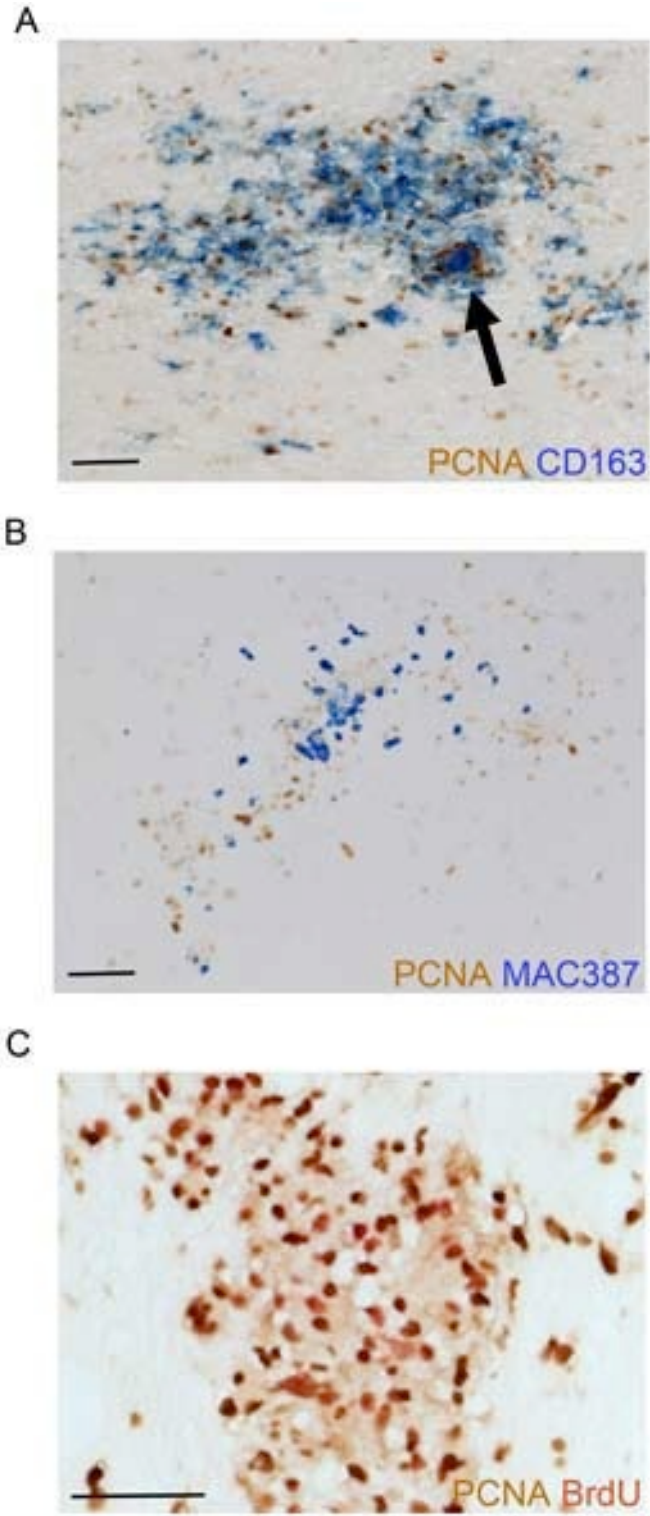
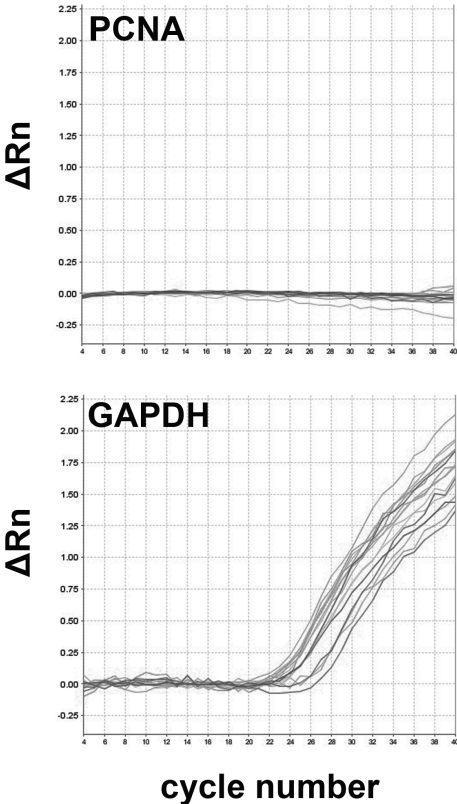


Figure 5.2. PCNA is not expressed by CD14+ monocytes in uninfected or chronically SIV-infected animals. RNA and protein were isolated from CD14+ monocytes from uninfected (n = 4) and chronically SIV-infected (n = 4, 120 dpi) animals. **A.** qRT-PCR for PCNA transcripts was performed on cDNA (3 ng) made from total CD14+ monocyte RNA. PCNA mRNA was not detected in CD14+ monocytes from uninfected or SIV-infected animals. GAPDH served as an internal control. **B.** Western blot for PCNA was performed on soluble protein (20 µg) from whole cells lysates. PCNA protein was not detected in CD14+ monocytes from uninfected or SIV-infected animals. PCNA was detected in 20 µg lysate from cycling THP-1 cells. Actin was used as the loading control.

FIGURE 5.2

A



B

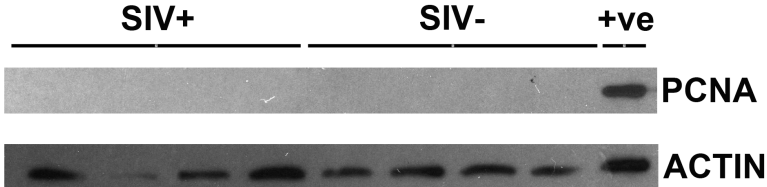


FIGURE 5.3. Monocyte-derived macrophages express PCNA *in vitro*.

Immunofluorescence for PCNA (red) in primary monocyte-derived macrophages (MDM) after 5 days of culture in RPMI1640 with 10% FBS and 10ng/mL M-CSF. DAPI (blue) was used as a nuclear counterstain. Arrows indicate PCNA+ macrophages. Insets are single channel images. Scale bar is 50um. After 5 days in culture, $22.1 \pm 7\%$ of MDM were PCNA+ (n = 3 animals).

FIGURE 5.3

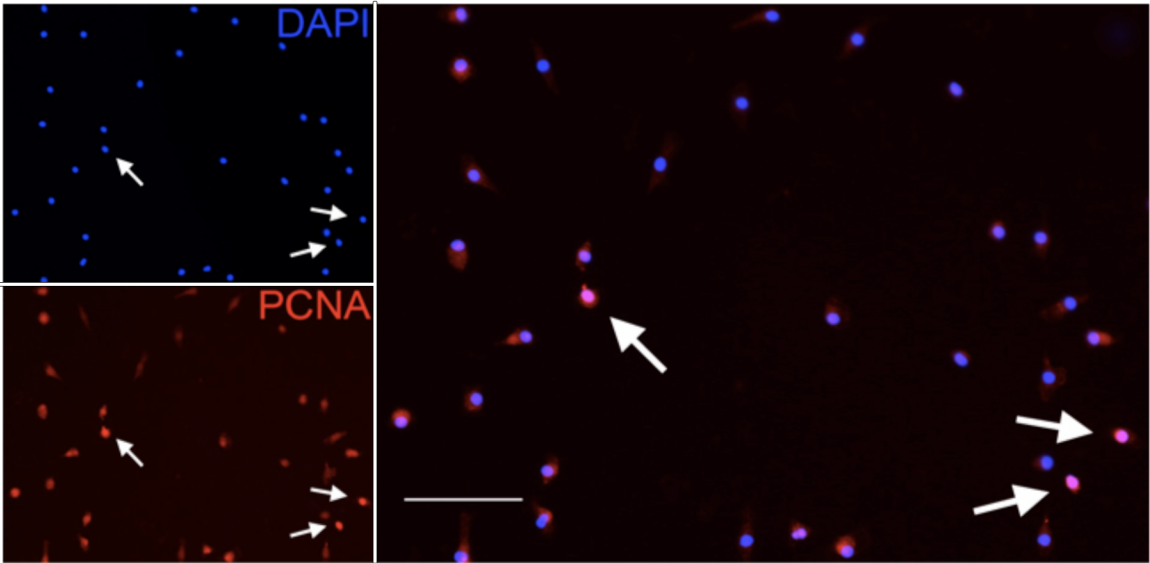


Figure 5.4. SIV infection increases PCNA expression in primary MDM.

PCNA expression in uninfected and SIV-infected MDM as determined by qRTPCR.

Total RNA was harvested from uninfected MDM, and MDM infected with SIV316* at 1 dpi and 3 dpi (n = 4 animals). PCNA expression was normalized to GAPDH and fold-change was calculated using the $\Delta\Delta CT$ method. For each animal, the fold-change in SIV-infected MDM was calculated relative to the uninfected timepoint. Each symbol represents one animal. Dashed line and error bars are the mean \pm SEM of all animals. SIV infection increased PCNA mRNA 1.6 ± 0.4 -fold at 1 dpi and 2.0 ± 0.3 -fold at 3 dpi relative to the uninfected timepoint.

Figure 5.4

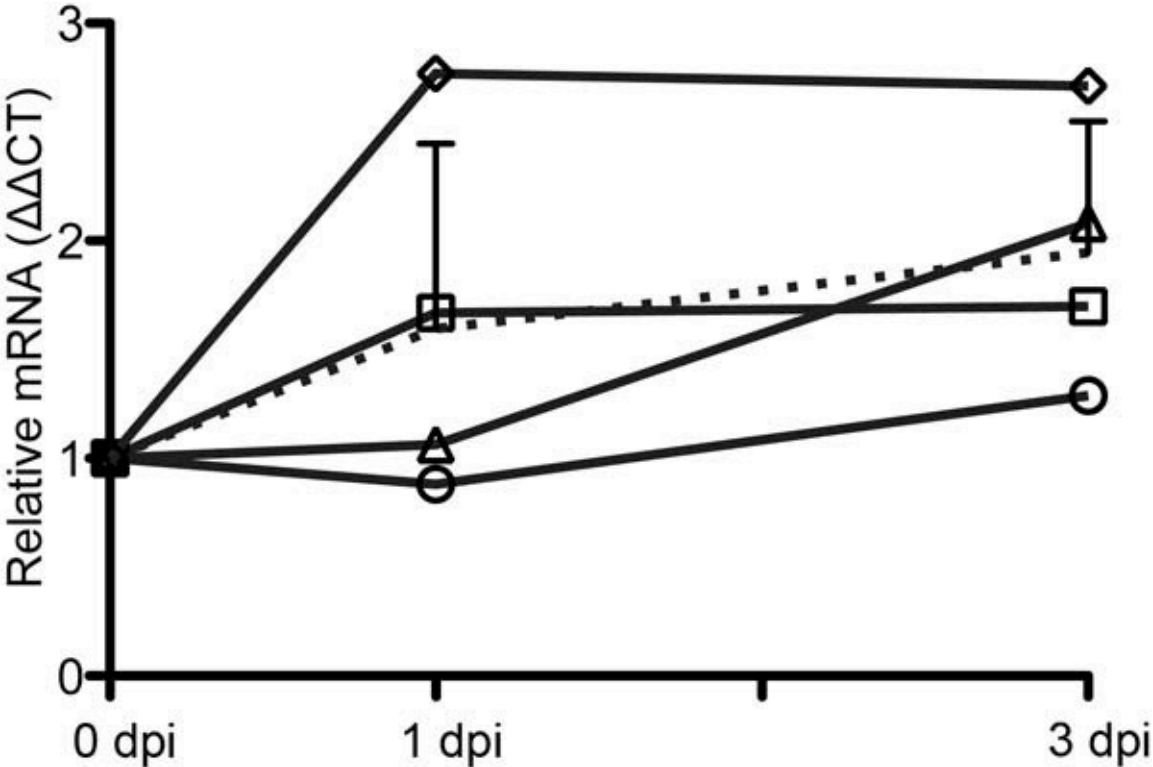
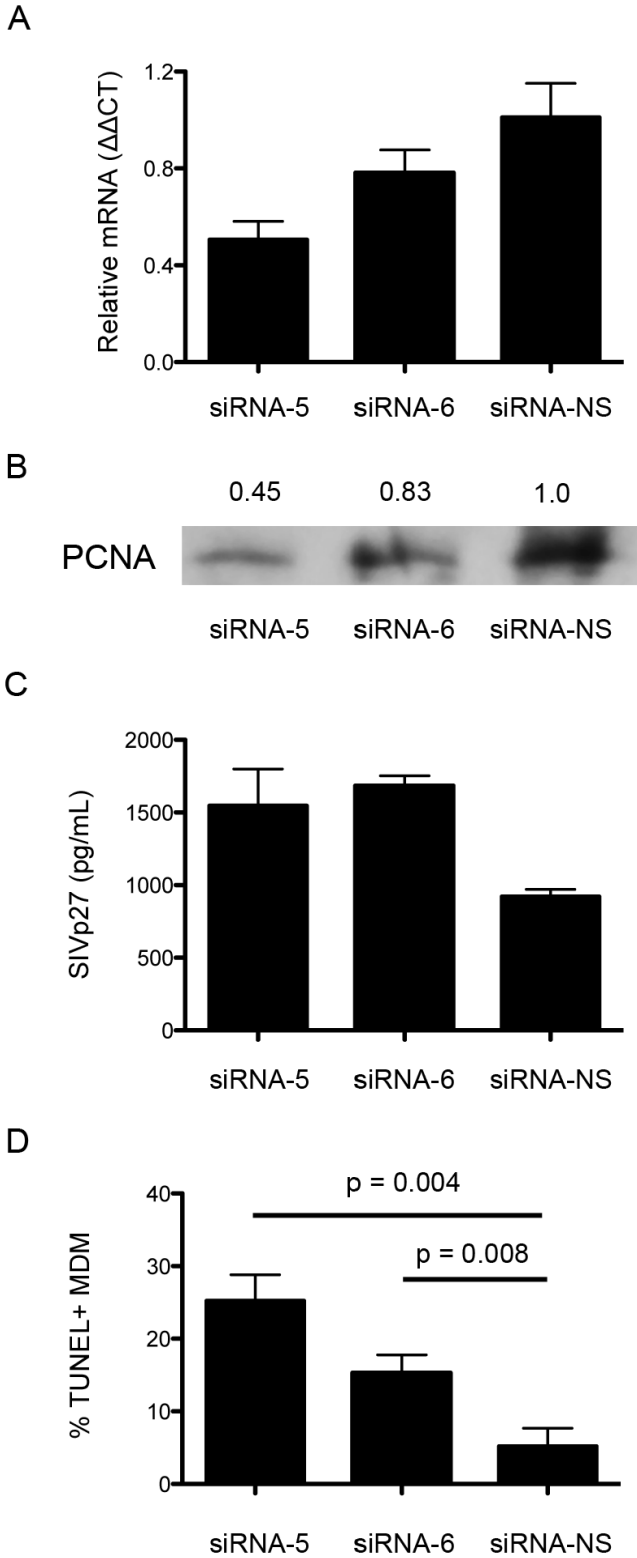


Figure 5.5. PCNA knockdown in primary MDM increases SIVp27 production and increases the frequency of macrophage apoptosis.

Data presented here are representative of three experiments in triplicate. CD14⁺ monocytes were cultured with M-CSF for 5 days, transfected with siRNA, and then infected with SIV316*. At 3 dpi, protein, RNA, and culture supernatants were harvested and TUNEL staining was performed. **A.** Treatment of MDM with PCNA-specific siRNA decreased PCNA mRNA by 49% for siRNA-5 and 22% for siRNA-6, relative to a nonsilencing control (siRNA-NS). PCNA expression was normalized to GAPDH and fold-change was calculated using the $\Delta\Delta CT$ method. **B.** Treatment of MDM with PCNA-specific siRNA decreased PCNA protein by 55% for siRNA5 and 17% for siRNA6, relative to a nonsilencing control as determined by western blot. The numbers above each lane indicate relative band density as determined using ImageJ densitometry tools. **C.** Treatment of MDM with PCNA-specific siRNA increased viral replication to 1547 ± 250 pg/mL for siRNA-5 and 1684 ± 280 pg/mL for siRNA-6, compared to 921 ± 120 pg/mL for the nonsilencing control, as determined by ELISA for SIVp27. **D.** In samples treated with nonsilencing siRNA, $5.2 \pm 2.5\%$ of MDM were TUNEL⁺. PCNA knockdown increased the frequency of apoptotic macrophages to $15.3 \pm 2.5\%$ for siRNA-6 ($p = 0.008$ vs. nonsilencing) and $25.2 \pm 3.6\%$ for siRNA-5 ($p = 0.004$ vs. nonsilencing).

FIGURE 5.5



DISCUSSION:

Discussion Overview

This thesis provides new data regarding: 1) differences in gene expression between monocyte subsets and changes in gene expression with SIV infection (manuscript submitted to Blood), 2) recruitment and turnover of CNS macrophages, the timing of viral neuroinvasion, and the development of SIVE (manuscript submitted to Am J Pathol), and 3) PCNA expression and function with regard to macrophage retention in the CNS (manuscript in preparation). Here we will discuss the specific implications of each set of studies with regard to the current understanding of monocyte/macrophage biology in SIV infection and the development of SIVE and HIVE.

I. Differences in gene expression between monocyte subsets and changes in gene expression with SIV infection (Chapter 3)

With HIV infection, the progression to AIDS and the development of HIVE are associated with expansion of blood monocytes and increased monocyte activation. We performed a microarray analysis to characterize changes in gene expression that occur at acute infection and terminally with AIDS in classical (CD14⁺⁺CD16⁻), intermediate (CD14⁺⁺CD16⁺), and nonclassical (CD14⁺CD16⁺⁺) monocytes. We find that the majority of changes in gene expression occur early in infection and persist through end stage disease. With SIV infection we observe expansion of the CD16⁺ monocyte subsets and increased similarity between intermediate and nonclassical monocytes terminally with AIDS. Although the set of genes expressed by each subset changes

over time, we define a panel of 172 genes that differentiate the three monocyte subsets in uninfected and SIV infected animals. Overall, we find that classical monocytes have an immature myeloid phenotype and express genes associated with cell proliferation and detection of immune ligands; whereas nonclassical monocytes have a macrophage-like phenotype and express genes associated with inhibition of cell cycle and immune effector functions. Despite apparent functional differences between monocyte subsets, innate immune genes, including interferon-stimulated genes, are upregulated in all three subsets with SIV infection. We conclude that SIV infection is associated with changes in gene expression indicative of monocyte dysregulation early in SIV infection, induction of a shared innate immune response dominated by induction of interferon-stimulated genes, and increased maturation of intermediate monocytes terminally with AIDS.

Identification of unique markers of classical, intermediate, and nonclassical monocytes in macaques with and without SIV infection

We found that only 172 of 813 genes differently expressed between monocyte subsets prior to infection were also differently expressed in SIV-infected animals. In this study we show that in uninfected and SIV-infected macaques classical monocytes express CD62L/SELL, S100A8, and S100A9, while nonclassical monocytes express CX3CR1. These markers are also differently expressed between classical and nonclassical monocytes in humans and mice^{58,61}. The chemokine and Fc receptors FcγRIa, CCR1, and CCR2, which are expressed on classical monocytes and not intermediate monocytes in humans and mice, were expressed on both classical and intermediate monocytes in rhesus macaques^{61,64}. Few markers uniquely differentiate the intermediate

subset as they share markers with classical and nonclassical monocytes. We identified two genes in macaques specific to intermediate monocytes whose proteins are known to be expressed on the cell surface: MERTK and C3AR1. In humans, the receptor tyrosine kinase MERTK is a marker of intermediate monocytes, and C3AR1 was reported to be more highly expressed in CD16+ monocytes^{56,61}. MERTK is involved in leukocyte migration, clearance of apoptotic cells, inhibition of lymphocyte activation, and has been linked to susceptibility to multiple sclerosis²⁵⁵. The subset-specific genes identified herein may provide useful markers of the individual monocyte subsets in uninfected and SIV- infected animals.

Transcripts expressed by classical and nonclassical monocytes suggest differences in the biological function of monocyte subsets

Genes expressed by classical monocytes were associated with defense response, proliferation, and wound healing. Expression of CCR1, CCR2, and CD62L suggests that classical monocytes can be mobilized in response to CCR1 and CCR2 ligands (CCL2/MCP-1, CCL7/MCP-3, CCL5/RANTES), home to lymphoid organs or sites of inflammation (via CD62L/SELL), and mediate inflammation or wound healing. Classical monocytes also express transcripts for S100A8 and S100A9 whose proteins comprise the antigen (calprotectin, S100A8/S100A9) recognized by the antibody MAC387^{250,256}. MAC387 has been used to identify a population of inflammatory macrophages that is recruited to the CNS in response to acute inflammation^{181,250,256}. Notably, MAC387+ macrophages present in SIVE lesions were found to have recently emigrated from the bone marrow, as indicated by BrdU labeling of proliferating monocyte precursors^{42,181}.

Expression of genes associated with cell proliferation in classical monocytes also may suggest their recent proliferation in the bone marrow. Thus, the classical monocyte pool may represent precursors of inflammatory MAC387+ macrophages found in tissues. Though we did not perform functional studies in macaques, the biological functions suggested by genes enriched in the classical monocyte subset appear to recapitulate the known biology of mouse classical (Ly6C+) monocytes, which are mobilized from the bone marrow in a CCR2 dependent manner, are recruited to sites of inflammation, and differentiate into classically activated (M1 polarized) macrophages in inflamed tissue⁶⁶.

Nonclassical monocytes express transcripts associated with defense response, cell cycle inhibition, cellular activation, and macrophage phenotype. The withdrawal from the cell cycle and similarities to tissue macrophages may suggest that nonclassical monocytes are at a later stage of maturation than classical monocytes⁷⁵. Genes expressed by nonclassical monocytes, or both intermediate and nonclassical monocytes, suggest the ability to mediate a range of immune effector functions including cell mediated cytotoxicity and T-cell activation. Notably, intermediate and nonclassical monocytes were more transcriptionally similar terminally with AIDS compared to early infection or preinfection timepoints. This may indicate increased activation or maturation of the intermediate subset with fulminant disease and reflect a phenotypic plasticity in response to the pathogenic microenvironment. Expression of CX3CR1 on nonclassical monocytes suggests that they are able to migrate in response to fractalkine, which is upregulated in the CNS with AIDS and HIVE²⁰⁴. Additionally, expression of integrins on nonclassical monocytes likely indicates the ability to bind

activated endothelial cells and migrate into tissues. Recruited nonclassical monocytes could contribute to neurodegeneration by elaborating proinflammatory mediators and recruiting additional leukocytes through production of TNF α and CCL5. The expansion of both nonclassical and intermediate monocytes may negatively contribute to AIDS progression and SIVE through increased traffic of activated and infected monocytes into the CNS and elaboration of chemoattractant and proinflammatory cytokines.

Changes in monocyte gene expression begin early in SIV infection and indicate a role for nonclassical monocytes in AIDS pathogenesis

Comparing early and end-stage disease, we observed that the majority of changes in gene expression were present by 26 dpi and were then sustained throughout infection. We have previously shown that increased monocyte egress from the bone marrow is detectable within weeks of primary infection, and the magnitude of the expansion of blood monocytes is predictive of how rapidly the animals progress to AIDS and the severity of macrophage mediated AIDS related pathogenesis⁴². This suggests that monocyte dysregulation with SIV infection is present early after infection and prior to AIDS onset. Although, intermediate monocytes have been the primary focus of previous research, we observed that the nonclassical subset had the greatest number of genes that were differently expressed with SIV infection. Moreover, expansion of these cells correlates with AIDS related pathologies including CNS and cardiac disease^{42,93}. This suggests that nonclassical monocytes merit additional focus going forward. Because nonclassical monocytes are innate effector cells, likely precursors to tissue macrophages, and regulators of adaptive immunity, changes to nonclassical monocyte

biology may have varied effects. It is likely that these cells expand in response to macrophage turnover in the lymph nodes with AIDS and as a general innate immune response to tissue damage^{42,52}. Further studies to elucidate the mechanisms and consequences of monocyte dysregulation in early SIV infection are needed.

SIV infection is associated with the induction of interferon-stimulated genes in all monocyte subsets

We found that interferon-stimulated genes (ISG) were upregulated in all three monocyte subsets by 26 dpi and terminally with AIDS indicating a sustained interferon response that likely indicates ongoing immune activation that may contribute to exhaustion of the immune system with chronic SIV infection. IFN α , which is produced primarily by plasmacytoid dendritic cells in response to TLR signaling, has been implicated as a major mediator of chronic immune activation in HIV and SIV infection²⁵⁷⁻²⁶¹. Whereas the direct effect of HIV or SIV on monocytes is likely limited by the low frequency of infected monocytes, the effects of IFN- α signaling on monocytes may be more widespread. Gene array studies of CD14+ monocytes from HIV-infected patients and whole blood from SIV-infected rhesus macaques have demonstrated a robust and sustained induction of ISG^{208,258-260}. In humans, greater monocyte ISG induction is associated with higher viral load and increased neuronal damage, suggesting a link between type-I interferon responses and HIVE^{208,258}. Importantly, comparisons between pathogenic infection of humans and rhesus macaques, and nonpathogenic infection of sooty mangabees or African green monkeys have demonstrated that increased IFN- α production and failure to downregulate ISG induction after acute viremia are associated

with pathogenic infection²⁵⁹⁻²⁶¹. We also observed upregulation of genes associated with detection of cytosolic nucleic acids and host restriction factors (APOBEC3A, TRIM5, SAMHD1), which may contribute to limited infection of monocytes *in vivo*. Despite heterogeneity of monocyte subsets, the pattern of induction of ISG and genes associated with innate immunity was similar between the three monocyte subsets, indicating a conserved immune response to SIV infection.

Caveats of the rapid macaque model of SIV infection

We found that intermediate monocytes and classical monocytes share more expressed genes in macaques, whereas intermediate monocytes and nonclassical monocytes share more expressed genes in humans⁶¹. This suggests that the biology of monocyte subsets may vary between humans and nonhuman primates. Additionally, the genes identified in these studies may be affected by the depletion of CD8+ lymphocytes. Studies of SIV infection without CD8+ depletion and in HIV-infected humans are necessary to validate the findings herein. We found high inter-animal variability in gene expression, which indicates that the genes identified as differently expressed in a given study will be greatly affected by the subject pool. Studies that evaluate the effect of antiretroviral therapy on gene expression in monocyte subsets and associated changes in disease progression are also needed.

II. Recruitment and turnover of CNS macrophages, timing of viral neuroinvasion, and the development of SIVE (Chapter 4)

The development of SIVE is influenced by SIV infection and macrophage accumulation in the CNS. In these studies we characterized recruitment of CD163+ perivascular macrophages and inflammatory MAC387+ macrophages to the CNS with SIV infection. We find that early CNS inflammation is characterized by recruitment of MAC387+ macrophages through the CNS. The meninges and choroid plexus show greater recruitment of BrdU+ macrophages from the blood with a high rate of turnover. In contrast, CD163+ and MAC387+ macrophages accumulate in the perivascular space and SIVE lesion with the development of AIDS and SIVE. We observed that throughout the CNS, higher ratios of CD163+ to MAC387+ macrophages are associated with AIDS and SIVE. These studies indicate that the basal rate of macrophage recruitment is increased with SIV infection and the higher rates are associated with shorter time to death. Additionally, increased macrophage activation in the periphery is associated with the development of SIVE in these animals. Importantly, we find that SIVE lesions are composed primarily of CD163+ macrophages present in the CNS early, at 20 dpi, in addition to productively infected macrophages recruited to the CNS terminally with AIDS.

SIVE lesions are formed by redistribution of resident CD163+ macrophages and recruitment of hematogenous macrophages

A major and surprising observation of this study was that 81.6% of CD163+ macrophages in SIVE lesions were present in the CNS early in infection prior to the

development of SIVE lesions. After 20 dpi approximately 4.3% of CD163+ macrophages in SIVE lesions entered the CNS from 20 dpi to 49 dpi and 17.1% entered the CNS after 49 dpi. These data fit the hypothesis that SIVE lesions arise more so from the focal redistribution of perivascular macrophages already present in the CNS than from the recruitment of monocytes from the periphery. It has been previously demonstrated that perivascular macrophages and juxtavascular microglia are able to migrate along the CNS vasculature in response to activation²⁶². Low macrophage recruitment in SIVE lesions from 20 dpi to 49 dpi could also be explained by occlusion of CNS blood vessels, which would prevent extravasation until recanalization of the blood vessel^{263,264}.

Formation of CNS lesions by redistribution of resident macrophages and recruitment of hematogenous macrophages has been previously described in multiple sclerosis (MS)²⁶⁵⁻²⁶⁷. In MS aggregation of parenchymal CD68+HLA-DR+ macrophages is thought to represent the earliest stage of lesion formation²⁶⁵. These preactive lesions progress to early active MS lesions that contain CD68+ microglia and hematogenous CD68+ perivascular macrophages and MRP14+ macrophages^{266,267}. These are likely the same three populations of CNS macrophages we describe with HIVE and SIVE^{42,181,266,267}. In contrast to early active lesions, late active or inactive MS lesions consist primarily of CD68+ macrophages and few MRP14+ macrophages are present²⁶⁷. These observations parallel ours in that an increased ratio of CD163+ to MAC387+ macrophages is associated with disease progression. In active lesion formation, the transition from early active MS lesions to late/inactive MS lesions is thought to be mediated by macrophage activation and redistribution of CNS macrophages rather than

accumulation of recruited hematogenous macrophages^{266,267}. A redistribution of macrophages to CNS lesions was also reported in a mouse model of spinal cord injury²⁶⁸. Blood-derived monocytes and macrophages were present diffusely throughout the spinal cord at 1 and 3 days post injury but coalesced into a lesion 7- 14 days post injury prior to resolution of the lesion²⁶⁸. These similarities between HIV and SIVE, MS, and spinal cord suggest recruitment of hematogenous macrophages and redistribution of local macrophages are involved in CNS lesion formation.

Timing of SIV infection of the CNS and the development AIDS and SIVE

Data from this study suggest that there is a 2.6-fold higher percentage of productive infection in macrophages that enter the CNS late, but we also find cells that entered the CNS early that are productively infected. Additionally, MNGCs, many of which are SIVp28+, were also comprised of CD163+ macrophages that were present in the CNS at 20 dpi. This is consistent with two hypotheses: 1) SIV is introduced into the CNS early but is controlled by the immune response until it recrudesces with AIDS, and/or 2) Acute virus is cleared from the CNS and reintroduction of infectious virus by traffic on infected monocytes/macrophages at the onset of AIDS is necessary to reestablish and maintain CNS infection^{12-16,186,189,193,269}. Previous analysis of viral sequences from peripheral and CNS tissue from two of the animals sacrificed at 22 dpi indicate compartmentalization of SIV in the CNS as early as 20 dpi³⁷. Additionally, using molecular clocks, phylogenetic analysis of peripheral and CNS viral sequences from four of the animals sacrificed with AIDS we found multiple instances of late SIV neuroinvasion beginning at approximately 50 dpi in animals sacrificed with AIDS (Marco

Salemi, unpublished data). Together the phylogenetic data discussed above and our observation that late macrophages have a higher frequency of productive infection support a hypothesis of late SIV neuroinvasion by traffic of infected CD163+ macrophages into the perivascular space. It is important to note that these studies utilized CD8+ lymphocyte depletion which compresses the window of disease from 1- 3 years to 2- 4months such that early and end stage events are not as temporally distant as in a natural history.

Resident CD163+ perivascular macrophages are important in the development of AIDS and SIVE

Perivascular macrophages are considered important in the development of HIV and SIV encephalitis and neuronal dysfunction, as they are the primary cell type productively infected^{26,85,185,270}. A significant role for perivascular macrophages in the development of CNS pathology is supported by the observation that rate of turnover of perivascular macrophages increased from <0.2%/week in uninfected macaques to ~3%/week in SIV-infected animals and that 71% of perivascular macrophages were present in the CNS at 20 dpi suggesting there is an accumulation of perivascular macrophages with little or no turnover. Previous studies on the rate of perivascular macrophage turnover in rodents (~8%/week as determined in mouse bone marrow chimeras and ~2%/week as determined by serial dextran labeling in rats) indicate that the total population of perivascular macrophages is replaced over several months although individual macrophages may reside in the CNS for years^{176,171,177,271}. The slow turnover rate of perivascular macrophages in the CNS, some of which may be infected, likely contribute

to the maintenance of a viral reservoir in the CNS with HIV or SIV infection. Previous research has indicated that the number of activated macrophages in the CNS is a better correlate of HIV dementia than viral replication in the CNS¹⁹⁸.

Peripheral monocyte activation predicts CD163+ macrophage recruitment in SIVE animals

Perivascular macrophages are monocyte derived, and activation and expansion of the CD16+ monocyte compartment with AIDS leads to increased trafficking of monocytes to the CNS^{42,48,88,93}. Peripheral correlates of SIVE underscore the important concept that the mechanism(s) that drive neuropathogenesis are not only limited to factors within the CNS compartment. Notably, the range of values for plasma sCD163 and CD14+CD16+ monocyte count is greater between SIVE animals than between SIVnoE animals. This suggests that animals that develop SIVE have lost the ability to regulate monocyte homeostasis. We found that peripheral monocytes in SIVE animals show increased activation relative to SIVnoE animals and concomitantly develop a more severe CNS pathology with increased CD163+ macrophage recruitment and presence of SIVE lesions. This relationship between increased monocyte activation, increased macrophage recruitment to the CNS, and SIVE support the hypothesis that lack of immune regulation in the periphery contributes to the development of SIVE.

Macrophage turnover via cell death or traffic out of the CNS

A major assumption of our dextran labeling model is that once macrophages are present in the CNS they remain. Thus we do not account for cell death or macrophages

that exit the CNS. Apoptosis of perivascular macrophages and microglia is considered to be low to negligible in the normal CNS, and HIV-1 infection has been shown to reduce the frequency of apoptotic CD68+ macrophages *in vivo*^{165,272}. Overall, studies of macrophage death in the normal CNS and in response to activation and infection have not been done. CNS macrophages are able to actively migrate from the brain to the cervical lymph nodes along olfactory nerves that penetrate the cribriform plate, but the factors that drive this process are not known²⁷³⁻²⁷⁵. Recirculation of macrophages from the CNS to the blood is thought to be impaired with HIV or SIV infection, which may be a mechanism of macrophage retention and SIVE lesion formation^{205,276,277}. Osteopontin, a cytokine that is elevated in the CNS with HIV and SIVE, inhibits macrophage apoptosis and promotes macrophage retention in the CNS²⁰⁵. All of these factors contribute to macrophage retention in the CNS and accumulation of macrophages over time.

A higher ratio of CD163+ to MAC387+ macrophages is associated with the development of AIDS and SIVE

We have previously observed that the severity of SIV encephalitis was related to an increased ratio of CD68+ to MAC387+ macrophages in HIV and SIVE lesions¹⁸¹. In this study we extend this observation and found that the CD163:MAC387 ratio is greater in animals with AIDS compared to SIV-infected animals without AIDS, and in animals with SIVE compared to animals with SIVnoE. We have previously suggested that resident perivascular macrophages are M2 polarized and inflammatory MAC387+ macrophages are M1 polarized^{181,209,278}. M1 polarized macrophages are considered to

be proinflammatory, classically activated macrophages that mediate antiviral Th1 type immune responses. Conversely, M2 alternatively activated macrophages mediate Th2 type immune response and have been associated with tissue repair and resolution of inflammation. We observed an increased influx of MAC387+ macrophages at 22 dpi throughout the CNS prior to significant accumulation of CD163+ macrophages. This may suggest that during the early stages of CNS infection a M1 polarized, antiviral immune response predominates and is a response to CNS infection. In animals sacrificed with AIDS, particularly with SIVE, the number of MAC387+ macrophages had decreased relative to 22 dpi and many more CD163+ macrophages were present which may indicate a switch to a M2 microenvironment. This suggests that a shift from M1 to M2 polarization is associated with the progression of neuroAIDS and the development of SIVE.

MAC387+ macrophage do not differentiate into CD163+CD68+ resident macrophages in the CNS

We have previously demonstrated that MAC387 is marker of recently recruited macrophages in the CNS^{42,181}. It is not known whether MAC387+ macrophages are able to differentiate into CD163+CD68+ macrophages or CD68+CD163- microglia. Our BrdU data show that MAC387+ macrophages found at necropsy had entered the CNS prior to 20 dpi. This indicates that with long-term residence in the CNS (35-121 days in this study), these particular cells did not differentiate into a CD163+CD68+ macrophage phenotype.

CD163+BrdU- macrophages in the CNS may represent proliferation of resident macrophages or recruitment from a site other than the bone marrow.

Very few CD163+BrdU+ macrophages were present in the perivascular space and SIVE lesions of animals sacrificed with AIDS and SIVE in spite of the higher number of total CD163+ macrophages in SIVE animals. The lack of CD163+BrdU+ macrophages in SIVE lesions is consistent with the notion that SIVE lesions are made up of local perivascular macrophages recruited from within the CNS, and may also represent macrophage proliferation *in situ*. In mice, tissue macrophages have been shown to proliferate in response to IL-4 produced in Th2 immune responses²⁷⁹. Although, macrophages are not thought to divide in humans and nonhuman primates, the local microenvironment in SIVE or HIVE may support proliferation of CD163+ macrophages. Another possibility is that CD163+ macrophages are recruited to the perivascular space and SIVE lesions from sites other than the bone marrow. In HIV-infected humans and SIV-infected macaques virus isolated from the CNS was shown to have sequences similar to virus isolated from the spleen, which could indicate traffic of splenic monocytes to the CNS^{188,280,281}. A splenic reservoir of monocytes has been identified in mice, which is mobilized in response to myocardial infarction and lung adenocarcinoma^{83,282}.

The presence of CD163+BrdU+ macrophages in the meninges and choroid plexus underscores differences between CNS compartments and a possible route of viral entry into the CNS

Given that we did not find CD163+BrdU+ macrophages in the perivascular space and SIVE lesions, it is interesting that we did find CD163+BrdU+ macrophages in the meninges and choroid plexus in numbers equal to or greater than MAC387+BrdU+ macrophages. This observation suggests that these two compartments are more similar to each other, and possibly the blood, than to the perivascular space and CNS parenchyma. As the vascular compartment of the CNS, the meninges are a direct link between the blood and the brain. Importantly, cell associated HIV has been shown to traffic to the brain through the meninges¹²⁰. Thus, it is possible that virus may be continually reintroduced into the brain in end stage disease due to traffic of infected CD163+ macrophages through the meninges.

Overall, these studies identify differences in recruitment of inflammatory and perivascular macrophage subsets across different CNS compartments. Differences in macrophage recruitment and turnover suggest that the meninges and choroid plexus are routes of monocyte traffic, and that macrophages associated with pathogenesis accumulate in the perivascular space and SIVE lesions. These studies identify late infiltrating CD163+ macrophages as a primary target of SIV infection with AIDS and SIVE. Importantly, our observations indicate that formation of SIVE lesions is a dynamic process involving multiple populations of resident and recruited CNS macrophages that is likely dependent on viral replication in the CNS during end stage disease.

III. PCNA expression and macrophage retention in the CNS (Chapter 5)

PCNA is not expressed by macrophages in the normal CNS, but PCNA+ macrophages, most of which are productively infected, are present in the CNS with HIVE and SIVE. In these studies we characterized PCNA expression in monocyte and macrophage subpopulations with and without SIV infection, and investigated the function of PCNA in these cells. We find that PCNA is expressed by CD163+ macrophages but not MAC387+ macrophages in SIVE lesions. PCNA+ macrophages in the CNS are not BrdU+ macrophages that have recently undergone division in the bone marrow. Additionally, PCNA is not detected in CD14+ blood monocytes in uninfected or chronically SIV infected animals. We find that SIV infection increases PCNA expression in primary monocyte-derived macrophages (MDM) *in vitro*. Furthermore, PCNA knockdown in MDM is associated with increased viral replication and increased macrophage apoptosis. We conclude that PCNA expression in CD163+ macrophages is due to induction in response to SIV infection rather than cell proliferation and is associated with decreased apoptosis in infected macrophages.

PCNA expression by CNS macrophages is not associated with cell proliferation *in vivo*

Historically, PCNA has been used as a marker of cell proliferation in cancer studies. But in humans and monkeys, monocytes and macrophages are considered to be terminally differentiated cells that do not divide after the promonocyte stage in the bone marrow^{57,74,75}. Our data suggest that PCNA expression in CNS macrophages is

independent of proliferation in the periphery as the majority of PCNA+ macrophages in the CNS are not BrdU+ and PCNA is not detected in CD14+ monocytes in the blood. It is possible that PCNA expression exists in monocytes, but is below the limit of detection of our assays. Similarly, PCNA expression may be restricted to a subset of monocytes that give rise to PCNA+ macrophages in tissues⁴⁹. Although proliferation of CNS macrophages is thought to be negligible in healthy animals, alternatively activated, M2 polarized macrophages have been shown to proliferate in mice^{57,74,75}. Whether a corresponding population of proliferating macrophages exists in human and nonhuman primates in Th2 immune responses is not known.

PCNA is induced by SIV infection and is expressed by CD163+ perivascular macrophages and not MAC387+ inflammatory macrophages in the CNS

In the CNS, the majority of productively SIV infected cells express PCNA, and the majority of PCNA+ cells are productively infected (SIVp28+, SIV RNA+)^{216,217}. We find PCNA is expressed by CD163+ macrophages, which are targets of HIV and SIV infection, but not inflammatory MAC387+ macrophages even though these cells are found to be BrdU+ *in situ*. These observations support the hypothesis that PCNA expression in CNS macrophages is associated with SIV infection and not cell proliferation. Further evidence for this hypothesis is the induction PCNA in cultured macrophages following SIV infection. That we did not observe PCNA induction in CD14+ monocytes from chronically SIV infected animals may be explained by the low frequency of infected monocytes in the blood.

Because PCNA expression is associated with productive HIV and SIV infection, it is likely that HIV and SIV induce PCNA via direct mechanisms. Previous studies indicate that DNA damage repair pathways are directly induced by viral replication and viral proteins^{203,229} and PCNA is induced by viral proteins including HTLV-I Tax (transactivator) and adenovirus E1A transforming protein^{283,284}. PCNA+ cells that do not appear to be productively infected, may be latently infected. Additionally, because we observed PCNA expression in monocyte-derived macrophage cultures without SIV infection, PCNA may also be induced indirectly in uninfected bystander cells via soluble viral proteins or production of mitogenic factors^{216,217}.

PCNA expression inhibits viral replication and macrophage apoptosis *in vitro*

The role of PCNA expression in HIV and SIV infection is not known. Our studies suggest that PCNA inhibits viral replication in SIV-infected macrophages. This agrees with previous reports that other DNA damage repair and cell cycle proteins (p21, Rad18, Rad52), which bind to both HIV and PCNA, inhibit HIV infection or replication^{147,230-232}. HIV and SIV infection of macrophages is non-lytic and is characterized by resistance to cytopathic effects of viral replication and lower viral replication compared to infection in CD4+ T-lymphocytes^{86,98}. Thus PCNA expression may be a mechanism of inhibition of viral replication that limits the cytopathic effects of productive HIV or SIV infection in macrophages.

We observed that PCNA knockdown with siRNA was associated with increased apoptosis in SIV-infected culture compared to nonsilencing controls. This may suggest

that PCNA-mediated inhibition of apoptosis provides a mechanism for the observed longevity of HIV and SIV infected macrophages *in vivo* and *in vitro*²³⁵. This hypothesis is supported by our observation that long-term culture of MDM *in vitro* is associated with expression of PCNA. With HIV and SIV infection, the formation and maintenance of a viral reservoir in the CNS is dependent on infection of a long-lived cell type¹³⁵. Our data suggest a scenario where PCNA induction in infected macrophages results in such a reservoir.

These studies suggest that PCNA is induced in CD163+ macrophages by SIV infection, independent of proliferation and that PCNA-mediated inhibition of apoptosis may be associated with limited viral replication in infected macrophages.

IV. Discussion Summary

HIV and SIV infection are associated with changes in monocyte biology that contribute to AIDS pathogenesis. We find altered gene expression in all monocyte subsets as early as 26 dpi, when monocyte expansion is first observed, suggesting that monocyte dysregulation begins early in infection and persists through end stage disease. Overall, the studies in this thesis support the observation that increased monocyte activation and traffic are associated with the development of SIVE. We find SIV infection results in increased numbers of total monocytes, higher rates of monocyte/macrophage recruitment to the CNS, and macrophage accumulation in the CNS. With monocyte expansion from the bone marrow, there is an increase in monocyte activation evidenced by: increased numbers of CD16+ monocytes, transcriptional maturation of the

intermediate monocyte subset (which has not been previously described), and higher levels of sCD163 in plasma. Importantly, sCD163 in plasma predicts traffic of CD163+ macrophages to perivascular cuffs and SIVE lesions, which are the primary sites where macrophages accumulate with SIVE. We also find evidence of chronic monocyte activation as interferon stimulated genes were upregulated in all monocyte subsets with SIV infection.

These studies provide further evidence for the hypothesis that continued recruitment of activated macrophages and reintroduction of virus into the CNS during end stage disease contribute to the development of neuroAIDS and SIVE. We find macrophage recruitment from the bone marrow to the CNS is greatest terminally with AIDS and SIVE. Importantly, in SIVE lesions productive SIV infection is more frequent in CD163+ macrophages recruited terminally with AIDS. We conclude that SIVE lesion formation occurs late in disease and represents a redistribution of resident CD163+ macrophages and recruitment of inflammatory MAC387+ macrophages from the bone marrow, which likely occurs in response to traffic of activated and infected monocyte/macrophage from the periphery.

Our findings underscore the importance of macrophage heterogeneity in SIV infection and neuroAIDS. We extend our previous observation that a higher ratio of CD163+ to MAC387+ macrophages in SIVE lesions is associated with more fulminant disease ¹⁸¹. In this thesis we find that a higher CD163+:MAC387+ ratio is associated with SIVE across CNS compartments. Dextran and BrdU labeling studies indicate that MAC387+

macrophages have a high turnover compared to CD163+ macrophages. Accumulation of CD163+ macrophages with high turnover of MAC387+ macrophages may contribute to a higher CD163+:MAC387+ ratio. The differences in turnover may be explained by selective retention of long-lived CD163+PCNA+ macrophages in the CNS compared to MAC387+ macrophages that do not express PCNA. Additionally, a high CD163+:MAC387+ ratio may reflect accumulation of CD163+PCNA+ macrophages, which are infected and activated and may constitute a viral reservoir, thus contributing to the development of SIVE.

The observed pattern of recruitment of CD163+ and MAC387+ macrophages to the CNS appears similar to the classical model of wound healing in which proinflammatory (M1) macrophages are recruited in response to infection/injury followed by recruitment of reparative (M2) macrophages that attenuate inflammation and promote tissue repair. In the first weeks of SIV infection, there is a rapid influx of MAC387+ macrophages into the CNS, which is likely occurring as part of an antiviral (M1) response to the initial seeding of SIV in the CNS during acute viremia. Subsequently, CD163+ macrophages (M2) are recruited to the CNS and the number of MAC387+ macrophages decreases. Therefore, it is possible that early in the course of infection, the immune system is competent to remove infectious virus from the CNS. However, we do not ultimately observe continued resolution of inflammation, but rather viral replication and recruitment of both CD163+ and MAC387+ macrophages terminally with AIDS. Thus SIVE may reflect the inability of the immune system to properly resolve CNS infection via the standard innate immune response.

It is important to note that although we emphasize end stage events, early events may also contribute to the development of AIDS and SIVE. Notably, we observe that increases in monocyte number, expansion of CD16+ monocytes, changes in monocyte transcription in all subsets, and CNS inflammation all begin early in disease. All together, the studies in this thesis underscore the importance of monocyte dysregulation, chronic immune activation, and changes in the biology of subpopulations of monocytes and macrophages in the pathogenesis of SIV infection and the development of SIVE.

REFERENCES:

1. Cherner M, Masliah E, Ellis RJ, et al. Neurocognitive dysfunction predicts postmortem findings of HIV encephalitis. *Neurology*. 2002;59:1563-1567.
2. Sacktor N. The epidemiology of human immunodeficiency virus-associated neurological disease in the era of highly active antiretroviral therapy. *J Neurovirol*. 2002;8 Suppl 2:115-121.
3. Heaton RK, Franklin DR, Ellis RJ, et al. HIV-associated neurocognitive disorders before and during the era of combination antiretroviral therapy: differences in rates, nature, and predictors. *J Neurovirol*. 2011;17:3-16.
4. Gaskill PJ, Watry DD, Burdo TH, Fox HS. Development and characterization of positively selected brain-adapted SIV. *Virol J*. 2005;2:44.
5. Shen R, Richter HE, Clements RH, et al. Macrophages in vaginal but not intestinal mucosa are monocyte-like and permissive to human immunodeficiency virus type 1 infection. *J Virol*. 2009;83:3258-3267.
6. Cohen MS, Shaw GM, McMichael AJ, Haynes BF. Acute HIV-1 Infection. *N Engl J Med*. 2011;364:1943-1954.
7. Spira AI, Marx PA, Patterson BK, et al. Cellular targets of infection and route of viral dissemination after an intravaginal inoculation of simian immunodeficiency virus into rhesus macaques. *J Exp Med*. 1996;183:215-225.
8. Pope M, Haase AT. Transmission, acute HIV-1 infection and the quest for strategies to prevent infection. *Nature Medicine*. 2003;9:847-852.
9. Sacktor N, Nakasujja N, Skolasky RL, et al. HIV subtype D is associated with dementia, compared with subtype A, in immunosuppressed individuals at risk of cognitive impairment in Kampala, Uganda. *Clin Infect Dis*. 2009;49:780-786.
10. Shaw GM, Hunter E. HIV transmission. *Cold Spring Harb Perspect Med*. 2012;2.
11. Haase AT. Early events in sexual transmission of HIV and SIV and opportunities for interventions. *Annu Rev Med*. 2011;62:127-139.
12. Lane JH, Sasseville VG, Smith MO, et al. Neuroinvasion by simian immunodeficiency virus coincides with increased numbers of perivascular macrophages/microglia and intrathecal immune activation. *J Neurovirol*. 1996;2:423-432.
13. Davis LE, Hjelle BL, Miller VE, et al. Early viral brain invasion in iatrogenic human immunodeficiency virus infection. *Neurology*. 1992;42:1736-1739.
14. Chakrabarti L, Hurtrel M, Maire MA, et al. Early viral replication in the brain of SIV-infected rhesus monkeys. *Am J Pathol*. 1991;139:1273-1280.
15. Clay CC, Rodrigues DS, Ho YS, et al. Neuroinvasion of fluorescein-positive monocytes in acute simian immunodeficiency virus infection. *J Virol*. 2007;81:12040-12048.
16. Witwer KW, Gama L, Li M, et al. Coordinated regulation of SIV replication and immune responses in the CNS. *PLoS One*. 2009;4:e8129.
17. McDermott AB, Koup RA. CD8(+) T cells in preventing HIV infection and disease. *AIDS*. 2012;26:1281-1292.
18. Schmitz JE, Kuroda MJ, Santra S, et al. Control of viremia in simian immunodeficiency virus infection by CD8+ lymphocytes. *Science*. 1999;283:857-860.
19. Stacey AR, Norris PJ, Qin L, et al. Induction of a striking systemic cytokine cascade prior to peak viremia in acute human immunodeficiency virus type 1 infection, in

- contrast to more modest and delayed responses in acute hepatitis B and C virus infections. *J Virol.* 2009;83:3719-3733.
20. Ganusov VV, Goonetilleke N, Liu MK, et al. Fitness costs and diversity of the cytotoxic T lymphocyte (CTL) response determine the rate of CTL escape during acute and chronic phases of HIV infection. *J Virol.* 2011;85:10518-10528.
 21. Tomaras GD, Yates NL, Liu P, et al. Initial B-cell responses to transmitted human immunodeficiency virus type 1: virion-binding immunoglobulin M (IgM) and IgG antibodies followed by plasma anti-gp41 antibodies with ineffective control of initial viremia. *J Virol.* 2008;82:12449-12463.
 22. Wei X, Decker JM, Wang S, et al. Antibody neutralization and escape by HIV-1. *Nature.* 2003;422:307-312.
 23. Simon V, Ho DD. HIV-1 dynamics in vivo: implications for therapy. *Nat Rev Microbiol.* 2003;1:181-190.
 24. CDC. 1993 revised classification system for HIV infection and expanded surveillance case definition for AIDS among adolescents and adults. *JAMA.* 1993;269:729-730.
 25. Swanstrom R, Coffin J. HIV-1 pathogenesis: the virus. *Cold Spring Harb Perspect Med.* 2012;2:a007443.
 26. Gannon P, Khan MZ, Kolson DL. Current understanding of HIV-associated neurocognitive disorders pathogenesis. *Curr Opin Neurol.* 2011;24:275-283.
 27. Daniel MD, Letvin NL, King NW, et al. Isolation of T-cell tropic HTLV-III-like retrovirus from macaques. *Science.* 1985;228:1201-1204.
 28. Kanki PJ, McLane MF, King NW, Jr., et al. Serologic identification and characterization of a macaque T-lymphotropic retrovirus closely related to HTLV-III. *Science.* 1985;228:1199-1201.
 29. Letvin NL, Daniel MD, Sehgal PK, et al. Induction of AIDS-like disease in macaque monkeys with T-cell tropic retrovirus STLV-III. *Science.* 1985;230:71-73.
 30. Apetrei C, Kaur A, Lerche NW, et al. Molecular epidemiology of simian immunodeficiency virus SIVsm in U.S. primate centers unravels the origin of SIVmac and SIVstm. *J Virol.* 2005;79:8991-9005.
 31. Peeters M, Courgnaud, V. Overview of primate lentiviruses and their evolution in non-human primates in Africa. In *HIV Sequence Compendium; HIV sequence compendium. Theoretical Biology and Biophysics Group, Los Alamos National Laboratory: Los Alamos, NM, USA, 2002; pp. 2-23.; 2002.*
 32. Liovat AS, Jacquelin B, Ploquin MJ, Barre-Sinoussi F, Muller-Trutwin MC. African non human primates infected by SIV - why don't they get sick? Lessons from studies on the early phase of non-pathogenic SIV infection. *Curr HIV Res.* 2009;7:39-50.
 33. Luciw PA, Shaw KE, Unger RE, et al. Genetic and biological comparisons of pathogenic and nonpathogenic molecular clones of simian immunodeficiency virus (SIVmac). *AIDS Res Hum Retroviruses.* 1992;8:395-402.
 34. Lackner AA, Vogel P, Ramos RA, Kluge JD, Marthas M. Early events in tissues during infection with pathogenic (SIVmac239) and nonpathogenic (SIVmac1A11) molecular clones of simian immunodeficiency virus. *Am J Pathol.* 1994;145:428-439.
 35. Smith MO, Heyes MP, Lackner AA. Early intrathecal events in rhesus macaques (*Macaca mulatta*) infected with pathogenic or nonpathogenic molecular clones of simian immunodeficiency virus. *Lab Invest.* 1995;72:547-558.

36. Strickland SL, Gray RR, Lamers SL, et al. Significant genetic heterogeneity of the SIVmac251 viral swarm derived from different sources. *AIDS Res Hum Retroviruses*. 2011;27:1327-1332.
37. Strickland SL, Gray RR, Lamers SL, et al. Efficient transmission and persistence of low-frequency SIVmac251 variants in CD8-depleted rhesus macaques with different neuropathology. *J Gen Virol*. 2012;93:925-938.
38. Williams R, Bokhari S, Silverstein P, Pinson D, Kumar A, Buch S. Nonhuman primate models of NeuroAIDS. *J Neurovirol*. 2008;14:292-300.
39. Williams K, Burdo TH. Monocyte mobilization, activation markers, and unique macrophage populations in the brain: observations from SIV infected monkeys are informative with regard to pathogenic mechanisms of HIV infection in humans. *J Neuroimmune Pharmacol*. 2012;7:363-371.
40. Schmitz JE, Simon MA, Kuroda MJ, et al. A nonhuman primate model for the selective elimination of CD8+ lymphocytes using a mouse-human chimeric monoclonal antibody. *Am J Pathol*. 1999;154:1923-1932.
41. Sanchez-Ramon S, Bellon JM, Resino S, et al. Low blood CD8+ T-lymphocytes and high circulating monocytes are predictors of HIV-1-associated progressive encephalopathy in children. *Pediatrics*. 2003;111:E168-175.
42. Burdo TH, Soulas C, Orzechowski K, et al. Increased monocyte turnover from bone marrow correlates with severity of SIV encephalitis and CD163 levels in plasma. *PLoS Pathog*. 2010;6:e1000842.
43. Campbell JH, Burdo TH, Autissier P, et al. Minocycline inhibition of monocyte activation correlates with neuronal protection in SIV neuroAIDS. *PLoS One*. 2011;6:e18688.
44. Sacha JB, Chung C, Reed J, et al. Pol-specific CD8+ T cells recognize simian immunodeficiency virus-infected cells prior to Nef-mediated major histocompatibility complex class I downregulation. *J Virol*. 2007;81:11703-11712.
45. Veazey RS, Acierno PM, McEvers KJ, et al. Increased loss of CCR5+ CD45RA- CD4+ T cells in CD8+ lymphocyte-depleted Simian immunodeficiency virus-infected rhesus monkeys. *J Virol*. 2008;82:5618-5630.
46. Klatt NR, Shudo E, Ortiz AM, et al. CD8+ lymphocytes control viral replication in SIVmac239-infected rhesus macaques without decreasing the lifespan of productively infected cells. *PLoS Pathog*. 2010;6:e1000747.
47. Thieblemont N, Weiss L, Sadeghi HM, Estcourt C, Haeffner-Cavaillon N. CD14^{low}CD16^{high}: a cytokine-producing monocyte subset which expands during human immunodeficiency virus infection. *Eur J Immunol*. 1995;25:3418-3424.
48. Pulliam L, Sun B, Rempel H. Invasive chronic inflammatory monocyte phenotype in subjects with high HIV-1 viral load. *J Neuroimmunol*. 2004;157:93-98.
49. Kim WK, Sun Y, Do H, et al. Monocyte heterogeneity underlying phenotypic changes in monocytes according to SIV disease stage. *J Leukoc Biol*. 2010;87:557-567.
50. Ansari AW, Meyer-Olson D, Schmidt RE. Selective expansion of pro-inflammatory chemokine CCL2-loaded CD14+CD16+ monocytes subset in HIV-infected therapy naive individuals. *J Clin Immunol*. 2013;33:302-306.
51. Kim WK, Corey S, Alvarez X, Williams K. Monocyte/macrophage traffic in HIV and SIV encephalitis. *J Leukoc Biol*. 2003;74:650-656.

52. Hasegawa A, Liu H, Ling B, et al. The level of monocyte turnover predicts disease progression in the macaque model of AIDS. *Blood*. 2009;114:2917-2925.
53. Ziegler-Heitbrock HW, Fingerle G, Strobel M, et al. The novel subset of CD14+/CD16+ blood monocytes exhibits features of tissue macrophages. *Eur J Immunol*. 1993;23:2053-2058.
54. Wong KL, Yeap WH, Tai JJ, Ong SM, Dang TM, Wong SC. The three human monocyte subsets: implications for health and disease. *Immunol Res*. 2012;53:41-57.
55. Ellery PJ, Tippett E, Chiu YL, et al. The CD16+ monocyte subset is more permissive to infection and preferentially harbors HIV-1 in vivo. *J Immunol*. 2007;178:6581-6589.
56. Ancuta P, Liu KY, Misra V, et al. Transcriptional profiling reveals developmental relationship and distinct biological functions of CD16+ and CD16- monocyte subsets. *BMC Genomics*. 2009;10:403.
57. Gordon S, Taylor PR. Monocyte and macrophage heterogeneity. *Nat Rev Immunol*. 2005;5:953-964.
58. Geissmann F, Jung S, Littman DR. Blood monocytes consist of two principal subsets with distinct migratory properties. *Immunity*. 2003;19:71-82.
59. Shi C, Pamer EG. Monocyte recruitment during infection and inflammation. *Nat Rev Immunol*. 2011;11:762-774.
60. Passlick B, Flieger D, Ziegler-Heitbrock HW. Identification and characterization of a novel monocyte subpopulation in human peripheral blood. *Blood*. 1989;74:2527-2534.
61. Wong KL, Tai JJ, Wong WC, et al. Gene expression profiling reveals the defining features of the classical, intermediate, and nonclassical human monocyte subsets. *Blood*. 2011;118:e16-31.
62. Ziegler-Heitbrock L, Ancuta P, Crowe S, et al. Nomenclature of monocytes and dendritic cells in blood. *Blood*. 2010;116:e74-80.
63. Sunderkotter C, Nikolic T, Dillon MJ, et al. Subpopulations of mouse blood monocytes differ in maturation stage and inflammatory response. *J Immunol*. 2004;172:4410-4417.
64. Ingersoll MA, Spanbroek R, Lottaz C, et al. Comparison of gene expression profiles between human and mouse monocyte subsets. *Blood*. 2010;115:e10-19.
65. Cros J, Cagnard N, Woollard K, et al. Human CD14dim monocytes patrol and sense nucleic acids and viruses via TLR7 and TLR8 receptors. *Immunity*. 2010;33:375-386.
66. Robbins CS, Swirski FK. The multiple roles of monocyte subsets in steady state and inflammation. *Cell Mol Life Sci*. 2010;67:2685-2693.
67. Weiner LM, Li W, Holmes M, et al. Phase I trial of recombinant macrophage colony-stimulating factor and recombinant gamma-interferon: toxicity, monocytosis, and clinical effects. *Cancer Res*. 1994;54:4084-4090.
68. Crowe S, Zhu T, Muller WA. The contribution of monocyte infection and trafficking to viral persistence, and maintenance of the viral reservoir in HIV infection. *J Leukoc Biol*. 2003;74:635-641.
69. Whitelaw DM. Observations on human monocyte kinetics after pulse labeling. *Cell Tissue Kinet*. 1972;5:311-317.
70. Ziegler-Heitbrock L. The CD14+ CD16+ blood monocytes: their role in infection and inflammation. *J Leukoc Biol*. 2007;81:584-592.

71. Ragin AB, Wu Y, Storey P, et al. Bone marrow diffusion measures correlate with dementia severity in HIV patients. *AJNR Am J Neuroradiol.* 2006;27:589-592.
72. Herbomel P, Thisse B, Thisse C. Ontogeny and behaviour of early macrophages in the zebrafish embryo. *Development.* 1999;126:3735-3745.
73. Lichanska AM, Hume DA. Origins and functions of phagocytes in the embryo. *Exp Hematol.* 2000;28:601-611.
74. van Furth R, Raeburn JA, van Zwet TL. Characteristics of human mononuclear phagocytes. *Blood.* 1979;54:485-500.
75. Auffray C, Sieweke MH, Geissmann F. Blood monocytes: development, heterogeneity, and relationship with dendritic cells. *Annu Rev Immunol.* 2009;27:669-692.
76. Serbina NV, Pamer EG. Monocyte emigration from bone marrow during bacterial infection requires signals mediated by chemokine receptor CCR2. *Nat Immunol.* 2006;7:311-317.
77. Tsou CL, Peters W, Si Y, et al. Critical roles for CCR2 and MCP-3 in monocyte mobilization from bone marrow and recruitment to inflammatory sites. *J Clin Invest.* 2007;117:902-909.
78. Combadiere C, Potteaux S, Rodero M, et al. Combined inhibition of CCL2, CX3CR1, and CCR5 abrogates Ly6C(hi) and Ly6C(lo) monocytosis and almost abolishes atherosclerosis in hypercholesterolemic mice. *Circulation.* 2008;117:1649-1657.
79. Sanford DE, Belt BA, Panni RZ, et al. Inflammatory monocyte mobilization decreases patient survival in pancreatic cancer: a role for targeting the CCL2/CCR2 axis. *Clin Cancer Res.* 2013;19:3404-3415.
80. Westmoreland SV, Halpern E, Lackner AA. Simian immunodeficiency virus encephalitis in rhesus macaques is associated with rapid disease progression. *J Neurovirol.* 1998;4:260-268.
81. Sui Y, Potula R, Pinson D, et al. Microarray analysis of cytokine and chemokine genes in the brains of macaques with SHIV-encephalitis. *J Med Primatol.* 2003;32:229-239.
82. Leuschner F, Rauch PJ, Ueno T, et al. Rapid monocyte kinetics in acute myocardial infarction are sustained by extramedullary monocytopoiesis. *J Exp Med.* 2012;209:123-137.
83. Swirski FK, Nahrendorf M, Etzrodt M, et al. Identification of splenic reservoir monocytes and their deployment to inflammatory sites. *Science.* 2009;325:612-616.
84. Robbins CS, Chudnovskiy A, Rauch PJ, et al. Extramedullary hematopoiesis generates Ly-6C(high) monocytes that infiltrate atherosclerotic lesions. *Circulation.* 2012;125:364-374.
85. Williams KC, Hickey WF. Central nervous system damage, monocytes and macrophages, and neurological disorders in AIDS. *Annu Rev Neurosci.* 2002;25:537-562.
86. Carter CA, Ehrlich LS. Cell biology of HIV-1 infection of macrophages. *Annual Review of Microbiology.* 2008;62:425-443.
87. Gonzalez-Scarano F, Martin-Garcia J. The neuropathogenesis of AIDS. *Nat Rev Immunol.* 2005;5:69-81.
88. Kim WK, Alvarez X, Fisher J, et al. CD163 identifies perivascular macrophages in normal and viral encephalitic brains and potential precursors to perivascular macrophages in blood. *Am J Pathol.* 2006;168:822-834.

89. Perno CF, Svicher V, Schols D, Pollicita M, Balzarini J, Aquaro S. Therapeutic strategies towards HIV-1 infection in macrophages. *Antiviral Res.* 2006;71:293-300.
90. Spudich S, Gonzalez-Scarano F. HIV-1-related central nervous system disease: current issues in pathogenesis, diagnosis, and treatment. *Cold Spring Harb Perspect Med.* 2012;2:a007120.
91. Williams K, Westmoreland S, Greco J, et al. Magnetic resonance spectroscopy reveals that activated monocytes contribute to neuronal injury in SIV neuroAIDS. *J Clin Invest.* 2005;115:2534-2545.
92. Martin GE, Gouillou M, Hearps AC, et al. Age-associated changes in monocyte and innate immune activation markers occur more rapidly in HIV infected women. *PLoS One.* 2013;8:e55279.
93. Pulliam L, Gascon R, Stubblebine M, McGuire D, McGrath MS. Unique monocyte subset in patients with AIDS dementia. *Lancet.* 1997;349:692-695.
94. Scarlata S, Carter C. Role of HIV-1 Gag domains in viral assembly. *Biochim Biophys Acta.* 2003;1614:62-72.
95. Frankel AD, Young JA. HIV-1: fifteen proteins and an RNA. *Annu Rev Biochem.* 1998;67:1-25.
96. Mashiba M, Collins KL. Molecular mechanisms of HIV immune evasion of the innate immune response in myeloid cells. *Viruses.* 2013;5:1-14.
97. Kilaeski EM, Shah S, Nonnemacher MR, Wigdahl B. Regulation of HIV-1 transcription in cells of the monocyte-macrophage lineage. *Retrovirology.* 2009;6:118.
98. Verani A, Gras G, Pancino G. Macrophages and HIV-1: dangerous liaisons. *Mol Immunol.* 2005;42:195-212.
99. Smith DH, Byrn RA, Marsters SA, Gregory T, Groopman JE, Capon DJ. Blocking of HIV-1 infectivity by a soluble, secreted form of the CD4 antigen. *Science.* 1987;238:1704-1707.
100. Landau NR, Warton M, Littman DR. The envelope glycoprotein of the human immunodeficiency virus binds to the immunoglobulin-like domain of CD4. *Nature.* 1988;334:159-162.
101. Deng H, Liu R, Ellmeier W, et al. Identification of a major co-receptor for primary isolates of HIV-1. *Nature.* 1996;381:661-666.
102. Goodenow MM, Collman RG. HIV-1 coreceptor preference is distinct from target cell tropism: a dual-parameter nomenclature to define viral phenotypes. *J Leukoc Biol.* 2006;80:965-972.
103. Simmons G, Reeves JD, McKnight A, et al. CXCR4 as a functional coreceptor for human immunodeficiency virus type 1 infection of primary macrophages. *J Virol.* 1998;72:8453-8457.
104. Yi Y, Rana S, Turner JD, Gaddis N, Collman RG. CXCR-4 is expressed by primary macrophages and supports CCR5-independent infection by dual-tropic but not T-tropic isolates of human immunodeficiency virus type 1. *J Virol.* 1998;72:772-777.
105. Tuttle DL, Anders CB, Aquino-De Jesus MJ, et al. Increased replication of non-syncytium-inducing HIV type 1 isolates in monocyte-derived macrophages is linked to advanced disease in infected children. *AIDS Res Hum Retroviruses.* 2002;18:353-362.

106. Peters PJ, Sullivan WM, Duenas-Decamp MJ, et al. Non-macrophage-tropic human immunodeficiency virus type 1 R5 envelopes predominate in blood, lymph nodes, and semen: implications for transmission and pathogenesis. *J Virol.* 2006;80:6324-6332.
107. Gray L, Sterjovski J, Churchill M, et al. Uncoupling coreceptor usage of human immunodeficiency virus type 1 (HIV-1) from macrophage tropism reveals biological properties of CCR5-restricted HIV-1 isolates from patients with acquired immunodeficiency syndrome. *Virology.* 2005;337:384-398.
108. Alkhatib G, Liao F, Berger EA, Farber JM, Peden KW. A new SIV co-receptor, STRL33. *Nature.* 1997;388:238.
109. Edinger AL, Amedee A, Miller K, et al. Differential utilization of CCR5 by macrophage and T cell tropic simian immunodeficiency virus strains. *Proc Natl Acad Sci U S A.* 1997;94:4005-4010.
110. Weissman D, Rabin RL, Arthos J, et al. Macrophage-tropic HIV and SIV envelope proteins induce a signal through the CCR5 chemokine receptor. *Nature.* 1997;389:981-985.
111. Choe H. Chemokine receptors in HIV-1 and SIV infection. *Arch Pharm Res.* 1998;21:634-639.
112. Schuitemaker H, Koot M, Kootstra NA, et al. Biological phenotype of human immunodeficiency virus type 1 clones at different stages of infection: progression of disease is associated with a shift from monocytotropic to T-cell-tropic virus population. *J Virol.* 1992;66:1354-1360.
113. Weinberger AD, Perelson AS. Persistence and emergence of X4 virus in HIV infection. *Math Biosci Eng.* 2011;8:605-626.
114. Mild M, Gray RR, Kvist A, et al. High inpatient HIV-1 evolutionary rate is associated with CCR5-to-CXCR4 coreceptor switch. *Infect Genet Evol.* 2013;19:369-377.
115. Desrosiers RC, Hansen-Moosa A, Mori K, et al. Macrophage-tropic variants of SIV are associated with specific AIDS-related lesions but are not essential for the development of AIDS. *Am J Pathol.* 1991;139:29-35.
116. Dunfee RL, Thomas ER, Gorry PR, et al. The HIV Env variant N283 enhances macrophage tropism and is associated with brain infection and dementia. *Proc Natl Acad Sci U S A.* 2006;103:15160-15165.
117. Holman AG, Gabuzda D. A machine learning approach for identifying amino acid signatures in the HIV env gene predictive of dementia. *PLoS One.* 2012;7:e49538.
118. Keele BF, Giorgi EE, Salazar-Gonzalez JF, et al. Identification and characterization of transmitted and early founder virus envelopes in primary HIV-1 infection. *Proc Natl Acad Sci U S A.* 2008;105:7552-7557.
119. Yin L, Liu L, Sun Y, et al. High-resolution deep sequencing reveals biodiversity, population structure, and persistence of HIV-1 quasispecies within host ecosystems. *Retrovirology.* 2012;9:108.
120. Lamers SL, Gray RR, Salemi M, Huysentruyt LC, McGrath MS. HIV-1 phylogenetic analysis shows HIV-1 transits through the meninges to brain and peripheral tissues. *Infect Genet Evol.* 2011;11:31-37.
121. Smyth RP, Davenport MP, Mak J. The origin of genetic diversity in HIV-1. *Virus Res.* 2012;169:415-429.

122. Roberts JD, Bebenek K, Kunkel TA. The accuracy of reverse transcriptase from HIV-1. *Science*. 1988;242:1171-1173.
123. Abram ME, Ferris AL, Shao W, Alvord WG, Hughes SH. Nature, position, and frequency of mutations made in a single cycle of HIV-1 replication. *J Virol*. 2010;84:9864-9878.
124. Paillart JC, Shehu-Xhilaga M, Marquet R, Mak J. Dimerization of retroviral RNA genomes: an inseparable pair. *Nat Rev Microbiol*. 2004;2:461-472.
125. Jung A, Maier R, Vartanian JP, et al. Recombination: Multiply infected spleen cells in HIV patients. *Nature*. 2002;418:144.
126. Yu Q, Chen D, Konig R, Mariani R, Unutmaz D, Landau NR. APOBEC3B and APOBEC3C are potent inhibitors of simian immunodeficiency virus replication. *J Biol Chem*. 2004;279:53379-53386.
127. Holmes RK, Koning FA, Bishop KN, Malim MH. APOBEC3F can inhibit the accumulation of HIV-1 reverse transcription products in the absence of hypermutation. Comparisons with APOBEC3G. *J Biol Chem*. 2007;282:2587-2595.
128. Koning FA, Goujon C, Bauby H, Malim MH. Target cell-mediated editing of HIV-1 cDNA by APOBEC3 proteins in human macrophages. *J Virol*. 2011;85:13448-13452.
129. Song H, Pavlicek JW, Cai F, et al. Impact of immune escape mutations on HIV-1 fitness in the context of the cognate transmitted/founder genome. *Retrovirology*. 2012;9:89.
130. Salazar-Gonzalez JF, Salazar MG, Keele BF, et al. Genetic identity, biological phenotype, and evolutionary pathways of transmitted/founder viruses in acute and early HIV-1 infection. *J Exp Med*. 2009;206:1273-1289.
131. Shan L, Siliciano RF. From reactivation of latent HIV-1 to elimination of the latent reservoir: The presence of multiple barriers to viral eradication. *Bioessays*. 2013;35:544-552.
132. Palmer S, Maldarelli F, Wiegand A, et al. Low-level viremia persists for at least 7 years in patients on suppressive antiretroviral therapy. *Proc Natl Acad Sci U S A*. 2008;105:3879-3884.
133. Davey RT, Jr., Bhat N, Yoder C, et al. HIV-1 and T cell dynamics after interruption of highly active antiretroviral therapy (HAART) in patients with a history of sustained viral suppression. *Proc Natl Acad Sci U S A*. 1999;96:15109-15114.
134. Brown A, Zhang H, Lopez P, Pardo CA, Gartner S. In vitro modeling of the HIV-macrophage reservoir. *J Leukoc Biol*. 2006;80:1127-1135.
135. Igarashi T, Brown CR, Endo Y, et al. Macrophage are the principal reservoir and sustain high virus loads in rhesus macaques after the depletion of CD4+ T cells by a highly pathogenic simian immunodeficiency virus/HIV type 1 chimera (SHIV): Implications for HIV-1 infections of humans. *Proc Natl Acad Sci U S A*. 2001;98:658-663.
136. Carter CC, Onafuwa-Nuga A, McNamara LA, et al. HIV-1 infects multipotent progenitor cells causing cell death and establishing latent cellular reservoirs. *Nat Med*. 2010;16:446-451.
137. Siliciano JD, Kajdas J, Finzi D, et al. Long-term follow-up studies confirm the stability of the latent reservoir for HIV-1 in resting CD4+ T cells. *Nat Med*. 2003;9:727-728.

138. Gendelman HE, Orenstein JM, Martin MA, et al. Efficient isolation and propagation of human immunodeficiency virus on recombinant colony-stimulating factor 1-treated monocytes. *J Exp Med.* 1988;167:1428-1441.
139. Aquaro S, Calio R, Balzarini J, Bellocchi MC, Garaci E, Perno CF. Macrophages and HIV infection: therapeutical approaches toward this strategic virus reservoir. *Antiviral Res.* 2002;55:209-225.
140. Schnell G, Joseph S, Spudich S, Price RW, Swanstrom R. HIV-1 replication in the central nervous system occurs in two distinct cell types. *PLoS Pathog.* 2011;7:e1002286.
141. Harrington PR, Schnell G, Letendre SL, et al. Cross-sectional characterization of HIV-1 env compartmentalization in cerebrospinal fluid over the full disease course. *AIDS.* 2009;23:907-915.
142. Alexaki A, Wigdahl B. HIV-1 infection of bone marrow hematopoietic progenitor cells and their role in trafficking and viral dissemination. *PLoS Pathog.* 2008;4:e1000215.
143. Bergamaschi A, Pancino G. Host hindrance to HIV-1 replication in monocytes and macrophages. *Retrovirology.* 2010;7:31.
144. Kitagawa M, Lackner AA, Martfeld DJ, Gardner MB, Dandekar S. Simian immunodeficiency virus infection of macaque bone marrow macrophages correlates with disease progression in vivo. *Am J Pathol.* 1991;138:921-930.
145. Gill V, Shattock RJ, Freeman AR, et al. Macrophages are the major target cell for HIV infection in long-term marrow culture and demonstrate dual susceptibility to lymphocytotropic and monocytotropic strains of HIV-1. *Br J Haematol.* 1996;93:30-37.
146. Shen H, Cheng T, Preffer FI, et al. Intrinsic human immunodeficiency virus type 1 resistance of hematopoietic stem cells despite coreceptor expression. *J Virol.* 1999;73:728-737.
147. Zhang J, Attar E, Cohen K, Crumpacker C, Scadden D. Silencing p21(Waf1/Cip1/Sdi1) expression increases gene transduction efficiency in primitive human hematopoietic cells. *Gene Ther.* 2005;12:1444-1452.
148. Majka M, Rozmyslowicz T, Ratajczak J, et al. The limited infectability by R5 HIV of CD34(+) cells from thymus, cord, and peripheral blood and bone marrow is explained by their ability to produce beta-chemokines. *Exp Hematol.* 2000;28:1334-1342.
149. Neal TF, Holland HK, Baum CM, et al. CD34+ progenitor cells from asymptomatic patients are not a major reservoir for human immunodeficiency virus-1. *Blood.* 1995;86:1749-1756.
150. Stanley SK, Kessler SW, Justement JS, et al. CD34+ bone marrow cells are infected with HIV in a subset of seropositive individuals. *J Immunol.* 1992;149:689-697.
151. Davis BR, Schwartz DH, Marx JC, et al. Absent or rare human immunodeficiency virus infection of bone marrow stem/progenitor cells in vivo. *J Virol.* 1991;65:1985-1990.
152. Banda NK, Tomczak JA, Shpall EJ, et al. HIV-gp120 induced cell death in hematopoietic progenitor CD34+ cells. *Apoptosis.* 1997;2:61-68.
153. Gibellini D, Vitone F, Buzzi M, et al. HIV-1 negatively affects the survival/maturation of cord blood CD34(+) hematopoietic progenitor cells differentiated towards

- megakaryocytic lineage by HIV-1 gp120/CD4 membrane interaction. *J Cell Physiol.* 2007;210:315-324.
154. Maciejewski JP, Weichold FF, Young NS. HIV-1 suppression of hematopoiesis in vitro mediated by envelope glycoprotein and TNF-alpha. *J Immunol.* 1994;153:4303-4310.
 155. Zauli G, Vitale M, Gibellini D, Capitani S. Inhibition of purified CD34+ hematopoietic progenitor cells by human immunodeficiency virus 1 or gp120 mediated by endogenous transforming growth factor beta 1. *J Exp Med.* 1996;183:99-108.
 156. Liu Y, Tang XP, McArthur JC, Scott J, Gartner S. Analysis of human immunodeficiency virus type 1 gp160 sequences from a patient with HIV dementia: evidence for monocyte trafficking into brain. *J Neurovirol.* 2000;6 Suppl 1:S70-81.
 157. McElrath MJ, Pruett JE, Cohn ZA. Mononuclear phagocytes of blood and bone marrow: comparative roles as viral reservoirs in human immunodeficiency virus type 1 infections. *Proc Natl Acad Sci U S A.* 1989;86:675-679.
 158. Sonza S, Mutimer HP, Oelrichs R, et al. Monocytes harbour replication-competent, non-latent HIV-1 in patients on highly active antiretroviral therapy. *AIDS.* 2001;15:17-22.
 159. Naif HM, Li S, Alali M, et al. CCR5 expression correlates with susceptibility of maturing monocytes to human immunodeficiency virus type 1 infection. *J Virol.* 1998;72:830-836.
 160. Rich EA, Chen IS, Zack JA, Leonard ML, O'Brien WA. Increased susceptibility of differentiated mononuclear phagocytes to productive infection with human immunodeficiency virus-1 (HIV-1). *J Clin Invest.* 1992;89:176-183.
 161. Peng G, Greenwell-Wild T, Nares S, et al. Myeloid differentiation and susceptibility to HIV-1 are linked to APOBEC3 expression. *Blood.* 2007;110:393-400.
 162. Zhu T, Muthui D, Holte S, et al. Evidence for human immunodeficiency virus type 1 replication in vivo in CD14(+) monocytes and its potential role as a source of virus in patients on highly active antiretroviral therapy. *J Virol.* 2002;76:707-716.
 163. Christ F, Thys W, De Rijck J, et al. Transportin-SR2 imports HIV into the nucleus. *Curr Biol.* 2008;18:1192-1202.
 164. Jacque JM, Stevenson M. The inner-nuclear-envelope protein emerlin regulates HIV-1 infectivity. *Nature.* 2006;441:641-645.
 165. Cosenza MA, Zhao ML, Lee SC. HIV-1 expression protects macrophages and microglia from apoptotic death. *Neuropathol Appl Neurobiol.* 2004;30:478-490.
 166. Giri MS, Nebozyhn M, Raymond A, et al. Circulating monocytes in HIV-1-infected viremic subjects exhibit an antiapoptosis gene signature and virus- and host-mediated apoptosis resistance. *J Immunol.* 2009;182:4459-4470.
 167. Lindl KA, Marks DR, Kolson DL, Jordan-Sciutto KL. HIV-associated neurocognitive disorder: pathogenesis and therapeutic opportunities. *J Neuroimmune Pharmacol.* 2010;5:294-309.
 168. Crowe SM, Mills J, Kirihara J, Boothman J, Marshall JA, McGrath MS. Full-length recombinant CD4 and recombinant gp120 inhibit fusion between HIV infected macrophages and uninfected CD4-expressing T-lymphoblastoid cells. *AIDS Res Hum Retroviruses.* 1990;6:1031-1037.

169. Ancuta P, Autissier P, Wurcel A, Zaman T, Stone D, Gabuzda D. CD16+ monocyte-derived macrophages activate resting T cells for HIV infection by producing CCR3 and CCR4 ligands. *J Immunol.* 2006;176:5760-5771.
170. Sharova N, Swingle C, Sharkey M, Stevenson M. Macrophages archive HIV-1 virions for dissemination in trans. *EMBO J.* 2005;24:2481-2489.
171. Chinnery HR, Ruitenber MJ, McMennamin PG. Novel characterization of monocyte-derived cell populations in the meninges and choroid plexus and their rates of replenishment in bone marrow chimeric mice. *J Neuropathol Exp Neurol.* 2010;69:896-909.
172. Ransohoff RM, Kivisakk P, Kidd G. Three or more routes for leukocyte migration into the central nervous system. *Nat Rev Immunol.* 2003;3:569-581.
173. Schilling M, Strecker JK, Ringelstein EB, Kiefer R, Schabitz WR. Turn-over of meningeal and perivascular macrophages in the brain of MCP-1-, CCR-2- or double knockout mice. *Exp Neurol.* 2009;219:583-585.
174. Barron KD. The microglial cell. A historical review. *J Neurol Sci.* 1995;134 Suppl:57-68.
175. Ransohoff RM, Perry VH. Microglial physiology: unique stimuli, specialized responses. *Annu Rev Immunol.* 2009;27:119-145.
176. Bechmann I, Kwidzinski E, Kovac AD, et al. Turnover of rat brain perivascular cells. *Exp Neurol.* 2001;168:242-249.
177. Bechmann I, Priller J, Kovac A, et al. Immune surveillance of mouse brain perivascular spaces by blood-borne macrophages. *Eur J Neurosci.* 2001;14:1651-1658.
178. Hickey WF, Kimura H. Perivascular microglial cells of the CNS are bone marrow-derived and present antigen in vivo. *Science.* 1988;239:290-292.
179. Soulas C, Donahue RE, Dunbar CE, Persons DA, Alvarez X, Williams KC. Genetically modified CD34+ hematopoietic stem cells contribute to turnover of brain perivascular macrophages in long-term repopulated primates. *Am J Pathol.* 2009;174:1808-1817.
180. Unger ER, Sung JH, Manivel JC, Chenggis ML, Blazar BR, Krivit W. Male donor-derived cells in the brains of female sex-mismatched bone marrow transplant recipients: a Y-chromosome specific in situ hybridization study. *J Neuropathol Exp Neurol.* 1993;52:460-470.
181. Soulas C, Conerly C, Kim WK, et al. Recently infiltrating MAC387(+) monocytes/macrophages a third macrophage population involved in SIV and HIV encephalitic lesion formation. *Am J Pathol.* 2011;178:2121-2135.
182. Zhang Z, Zhang ZY, Wu Y, Schluesener HJ. Lesional accumulation of CD163+ macrophages/microglia in rat traumatic brain injury. *Brain Res.* 2012;1461:102-110.
183. Fischer-Smith T, Tedaldi EM, Rappaport J. CD163/CD16 coexpression by circulating monocytes/macrophages in HIV: potential biomarkers for HIV infection and AIDS progression. *AIDS Res Hum Retroviruses.* 2008;24:417-421.
184. Bruck W, Porada P, Poser S, et al. Monocyte/macrophage differentiation in early multiple sclerosis lesions. *Ann Neurol.* 1995;38:788-796.
185. Williams KC, Corey S, Westmoreland SV, et al. Perivascular macrophages are the primary cell type productively infected by simian immunodeficiency virus in the

- brains of macaques: implications for the neuropathogenesis of AIDS. *J Exp Med*. 2001;193:905-915.
186. Thompson KA, Varrone JJ, Jankovic-Karasoulos T, Wesselingh SL, McLean CA. Cell-specific temporal infection of the brain in a simian immunodeficiency virus model of human immunodeficiency virus encephalitis. *J Neurovirol*. 2009;15:300-311.
 187. Kure K, Weidenheim KM, Lyman WD, Dickson DW. Morphology and distribution of HIV-1 gp41-positive microglia in subacute AIDS encephalitis. Pattern of involvement resembling a multisystem degeneration. *Acta Neuropathol*. 1990;80:393-400.
 188. Burkala EJ, He J, West JT, Wood C, Petit CK. Compartmentalization of HIV-1 in the central nervous system: role of the choroid plexus. *AIDS*. 2005;19:675-684.
 189. Gray F, Scaravilli F, Everall I, et al. Neuropathology of early HIV-1 infection. *Brain Pathol*. 1996;6:1-15.
 190. Yadav A, Collman RG. CNS inflammation and macrophage/microglial biology associated with HIV-1 infection. *J Neuroimmune Pharmacol*. 2009;4:430-447.
 191. Zhou L, Ng T, Yuksel A, Wang B, Dwyer DE, Saksena NK. Short communication: absence of HIV infection in the choroid plexus of two patients who died rapidly with HIV-associated dementia. *AIDS Res Hum Retroviruses*. 2008;24:839-843.
 192. Sinclair E, Gray F, Ciardi A, Scaravilli F. Immunohistochemical changes and PCR detection of HIV provirus DNA in brains of asymptomatic HIV-positive patients. *J Neuropathol Exp Neurol*. 1994;53:43-50.
 193. Reinhart TA, Rogan MJ, Huddleston D, Rausch DM, Eiden LE, Haase AT. Simian immunodeficiency virus burden in tissues and cellular compartments during clinical latency and AIDS. *J Infect Dis*. 1997;176:1198-1208.
 194. Kaul M. HIV-1 associated dementia: update on pathological mechanisms and therapeutic approaches. *Curr Opin Neurol*. 2009;22:315-320.
 195. Neuenburg JK, Brodt HR, Herndier BG, et al. HIV-related neuropathology, 1985 to 1999: rising prevalence of HIV encephalopathy in the era of highly active antiretroviral therapy. *J Acquir Immune Defic Syndr*. 2002;31:171-177.
 196. Petit CK, Cho ES, Lemann W, Navia BA, Price RW. Neuropathology of acquired immunodeficiency syndrome (AIDS): an autopsy review. *J Neuropathol Exp Neurol*. 1986;45:635-646.
 197. Kure K, Llena JF, Lyman WD, et al. Human immunodeficiency virus-1 infection of the nervous system: an autopsy study of 268 adult, pediatric, and fetal brains. *Hum Pathol*. 1991;22:700-710.
 198. Glass JD, Fedor H, Wesselingh SL, McArthur JC. Immunocytochemical quantitation of human immunodeficiency virus in the brain: correlations with dementia. *Ann Neurol*. 1995;38:755-762.
 199. Ghorpade A, Holter S, Borgmann K, Persidsky R, Wu L. HIV-1 and IL-1 beta regulate Fas ligand expression in human astrocytes through the NF-kappa B pathway. *J Neuroimmunol*. 2003;141:141-149.
 200. Murta V, Pitossi FJ, Ferrari CC. CNS response to a second pro-inflammatory event depends on whether the primary demyelinating lesion is active or resolved. *Brain Behav Immun*. 2012;26:1102-1115.
 201. Tian C, Erdmann N, Zhao J, Cao Z, Peng H, Zheng J. HIV-infected macrophages mediate neuronal apoptosis through mitochondrial glutaminase. *J Neurochem*. 2008;105:994-1005.

202. Zhou BY, He JJ. Proliferation inhibition of astrocytes, neurons, and non-gial cells by intracellularly expressed human immunodeficiency virus type 1 (HIV-1) Tat protein. *Neurosci Lett*. 2004;359:155-158.
203. Ward J, Davis Z, DeHart J, et al. HIV-1 Vpr triggers natural killer cell-mediated lysis of infected cells through activation of the ATR-mediated DNA damage response. *PLoS Pathog*. 2009;5:e1000613.
204. Tong N, Perry SW, Zhang Q, et al. Neuronal fractalkine expression in HIV-1 encephalitis: roles for macrophage recruitment and neuroprotection in the central nervous system. *J Immunol*. 2000;164:1333-1339.
205. Burdo TH, Wood MR, Fox HS. Osteopontin prevents monocyte recirculation and apoptosis. *J Leukoc Biol*. 2007;81:1504-1511.
206. Wiley CA, Achim C. Human immunodeficiency virus encephalitis is the pathological correlate of dementia in acquired immunodeficiency syndrome. *Ann Neurol*. 1994;36:673-676.
207. Bell JE. The neuropathology of adult HIV infection. *Rev Neurol (Paris)*. 1998;154:816-829.
208. Pulliam L, Rempel H, Sun B, Abadjian L, Calosing C, Meyerhoff DJ. A peripheral monocyte interferon phenotype in HIV infection correlates with a decrease in magnetic resonance spectroscopy metabolite concentrations. *AIDS*. 2011;25:1721-1726.
209. Cassol E, Cassetta L, Alfano M, Poli G. Macrophage polarization and HIV-1 infection. *J Leukoc Biol*. 2010;87:599-608.
210. Lin SL, Castano AP, Nowlin BT, Luper ML, Jr., Duffield JS. Bone marrow Ly6Chigh monocytes are selectively recruited to injured kidney and differentiate into functionally distinct populations. *J Immunol*. 2009;183:6733-6743.
211. Mantovani A, Allavena P, Sica A, Balkwill F. Cancer-related inflammation. *Nature*. 2008;454:436-444.
212. Swirski FK, Weissleder R, Pittet MJ. Heterogeneous in vivo behavior of monocyte subsets in atherosclerosis. *Arterioscler Thromb Vasc Biol*. 2009;29:1424-1432.
213. Martin P, Leibovich SJ. Inflammatory cells during wound repair: the good, the bad and the ugly. *Trends Cell Biol*. 2005;15:599-607.
214. Getts DR, Terry RL, Getts MT, et al. Ly6c+ "inflammatory monocytes" are microglial precursors recruited in a pathogenic manner in West Nile virus encephalitis. *J Exp Med*. 2008;205:2319-2337.
215. Duffield JS. The inflammatory macrophage: a story of Jekyll and Hyde. *Clin Sci (Lond)*. 2003;104:27-38.
216. Fischer-Smith T, Croul S, Adeniyi A, et al. Macrophage/microglial accumulation and proliferating cell nuclear antigen expression in the central nervous system in human immunodeficiency virus encephalopathy. *Am J Pathol*. 2004;164:2089-2099.
217. Williams K, Schwartz A, Corey S, et al. Proliferating cellular nuclear antigen expression as a marker of perivascular macrophages in simian immunodeficiency virus encephalitis. *Am J Pathol*. 2002;161:575-585.
218. Williams K, Bar-Or A, Ulvestad E, Olivier A, Antel JP, Yong VW. Biology of adult human microglia in culture: comparisons with peripheral blood monocytes and astrocytes. *J Neuropathol Exp Neurol*. 1992;51:538-549.

219. Prelich G, Tan CK, Kostura M, et al. Functional identity of proliferating cell nuclear antigen and a DNA polymerase-delta auxiliary protein. *Nature*. 1987;326:517-520.
220. Wood A, Garg P, Burgers PM. A ubiquitin-binding motif in the translesion DNA polymerase Rev1 mediates its essential functional interaction with ubiquitinated proliferating cell nuclear antigen in response to DNA damage. *J Biol Chem*. 2007;282:20256-20263.
221. Shan B, Xu J, Zhuo Y, Morris CA, Morris GF. Induction of p53-dependent activation of the human proliferating cell nuclear antigen gene in chromatin by ionizing radiation. *J Biol Chem*. 2003;278:44009-44017.
222. Moldovan GL, Pfander B, Jentsch S. PCNA, the maestro of the replication fork. *Cell*. 2007;129:665-679.
223. Skalka AM, Katz RA. Retroviral DNA integration and the DNA damage response. *Cell Death Differ*. 2005;12 Suppl 1:971-978.
224. Li L, Olvera JM, Yoder KE, et al. Role of the non-homologous DNA end joining pathway in the early steps of retroviral infection. *EMBO J*. 2001;20:3272-3281.
225. Daniel R. DNA repair in HIV-1 infection: a case for inhibitors of cellular co-factors? *Curr HIV Res*. 2006;4:411-421.
226. Van Maele B, Debyser Z. HIV-1 integration: an interplay between HIV-1 integrase, cellular and viral proteins. *AIDS Rev*. 2005;7:26-43.
227. Smith JA, Daniel R. Up-regulation of HIV-1 transduction in nondividing cells by double-strand DNA break-inducing agents. *Biotechnol Lett*. 2011;33:243-252.
228. Ebina H, Kanemura Y, Suzuki Y, Urata K, Misawa N, Koyanagi Y. Integrase-independent HIV-1 infection is augmented under conditions of DNA damage and produces a viral reservoir. *Virology*. 2012;427:44-50.
229. Sinclair A, Yarranton S, Schelcher C. DNA-damage response pathways triggered by viral replication. *Expert Rev Mol Med*. 2006;8:1-11.
230. Mulder LC, Chakrabarti LA, Muesing MA. Interaction of HIV-1 integrase with DNA repair protein hRad18. *J Biol Chem*. 2002;277:27489-27493.
231. Lau A, Kanaar R, Jackson SP, O'Connor MJ. Suppression of retroviral infection by the RAD52 DNA repair protein. *EMBO J*. 2004;23:3421-3429.
232. Zhang J, Scadden DT, Crumpacker CS. Primitive hematopoietic cells resist HIV-1 infection via p21. *J Clin Invest*. 2007;117:473-481.
233. Tournier S, Leroy D, Goubin F, Ducommun B, Hyams JS. Heterologous expression of the human cyclin-dependent kinase inhibitor p21Cip1 in the fission yeast, *Schizosaccharomyces pombe* reveals a role for PCNA in the chk1+ cell cycle checkpoint pathway. *Mol Biol Cell*. 1996;7:651-662.
234. Li DQ, Pakala SB, Reddy SD, et al. Revelation of p53-independent function of MTA1 in DNA damage response via modulation of the p21 WAF1-proliferating cell nuclear antigen pathway. *J Biol Chem*. 2010;285:10044-10052.
235. Berman MA, Zaldivar F, Jr., Imfeld KL, Kenney JS, Sandborg CI. HIV-1 infection of macrophages promotes long-term survival and sustained release of interleukins 1 alpha and 6. *AIDS Res Hum Retroviruses*. 1994;10:529-539.
236. Sasseville VG, Lackner AA. Neuropathogenesis of simian immunodeficiency virus infection in macaque monkeys. *J Neurovirol*. 1997;3:1-9.

237. Wang X, Das A, Lackner AA, Veazey RS, Pahar B. Intestinal double-positive CD4+CD8+ T cells of neonatal rhesus macaques are proliferating, activated memory cells and primary targets for SIVMAC251 infection. *Blood*. 2008;112:4981-4990.
238. Lifson JD, Rossio JL, Piatak M, Jr., et al. Role of CD8(+) lymphocytes in control of simian immunodeficiency virus infection and resistance to rechallenge after transient early antiretroviral treatment. *J Virol*. 2001;75:10187-10199.
239. Mitsiades N, Mitsiades CS, Poulaki V, et al. Molecular sequelae of proteasome inhibition in human multiple myeloma cells. *Proc Natl Acad Sci U S A*. 2002;99:14374-14379.
240. Jones J, Otu H, Spentzos D, et al. Gene signatures of progression and metastasis in renal cell cancer. *Clin Cancer Res*. 2005;11:5730-5739.
241. Bolstad BM, Irizarry RA, Astrand M, Speed TP. A comparison of normalization methods for high density oligonucleotide array data based on variance and bias. *Bioinformatics*. 2003;19:185-193.
242. Irizarry RA, Hobbs B, Collin F, et al. Exploration, normalization, and summaries of high density oligonucleotide array probe level data. *Biostatistics*. 2003;4:249-264.
243. Li C, Wong WH. Model-based analysis of oligonucleotide arrays: expression index computation and outlier detection. *Proc Natl Acad Sci U S A*. 2001;98:31-36.
244. Huang da W, Sherman BT, Lempicki RA. Systematic and integrative analysis of large gene lists using DAVID bioinformatics resources. *Nat Protoc*. 2009;4:44-57.
245. Huang da W, Sherman BT, Zheng X, et al. Extracting biological meaning from large gene lists with DAVID. *Curr Protoc Bioinformatics*. 2009;Chapter 13:Unit 13 11.
246. Schnell SA, Staines WA, Wessendorf MW. Reduction of lipofuscin-like autofluorescence in fluorescently labeled tissue. *J Histochem Cytochem*. 1999;47:719-730.
247. Mori K, Rosenzweig M, Desrosiers RC. Mechanisms for adaptation of simian immunodeficiency virus to replication in alveolar macrophages. *J Virol*. 2000;74:10852-10859.
248. Burdo TH, Lentz MR, Autissier P, et al. Soluble CD163 made by monocyte/macrophages is a novel marker of HIV activity in early and chronic infection prior to and after anti-retroviral therapy. *J Infect Dis*. 2011;204:154-163.
249. Burdo TH, Lo J, Abbara S, et al. Soluble CD163, a novel marker of activated macrophages, is elevated and associated with noncalcified coronary plaque in HIV-infected patients. *J Infect Dis*. 2011;204:1227-1236.
250. Hessian PA, Fisher L. The heterodimeric complex of MRP-8 (S100A8) and MRP-14 (S100A9). Antibody recognition, epitope definition and the implications for structure. *Eur J Biochem*. 2001;268:353-363.
251. Hosmalin A, Lebon P. Type I interferon production in HIV-infected patients. *J Leukoc Biol*. 2006;80:984-993.
252. Williams K, Alvarez X, Lackner AA. Central nervous system perivascular cells are immunoregulatory cells that connect the CNS with the peripheral immune system. *Glia*. 2001;36:156-164.
253. Liu YC, Chang HW, Lai YC, Ding ST, Ho JL. Serum responsiveness of the rat PCNA promoter involves the proximal ATF and AP-1 sites. *FEBS Lett*. 1998;441:200-204.

254. Chang CD, Ottavio L, Travali S, Lipson KE, Baserga R. Transcriptional and posttranscriptional regulation of the proliferating cell nuclear antigen gene. *Mol Cell Biol.* 1990;10:3289-3296.
255. Ma GZ, Stankovich J, Kilpatrick TJ, Binder MD, Field J. Polymorphisms in the receptor tyrosine kinase MERTK gene are associated with multiple sclerosis susceptibility. *PLoS One.* 2011;6:e16964.
256. Goebeler M, Roth J, Teigelkamp S, Sorg C. The monoclonal antibody MAC387 detects an epitope on the calcium-binding protein MRP14. *J Leukoc Biol.* 1994;55:259-261.
257. Woelk CH, Ottonnes F, Plotkin CR, et al. Interferon gene expression following HIV type 1 infection of monocyte-derived macrophages. *AIDS Res Hum Retroviruses.* 2004;20:1210-1222.
258. Rempel H, Sun B, Calosing C, Pillai SK, Pulliam L. Interferon-alpha drives monocyte gene expression in chronic unsuppressed HIV-1 infection. *AIDS.* 2010;24:1415-1423.
259. Bosinger SE, Li Q, Gordon SN, et al. Global genomic analysis reveals rapid control of a robust innate response in SIV-infected sooty mangabeys. *J Clin Invest.* 2009;119:3556-3572.
260. Jacquelin B, Mayau V, Targat B, et al. Nonpathogenic SIV infection of African green monkeys induces a strong but rapidly controlled type I IFN response. *J Clin Invest.* 2009;119:3544-3555.
261. Mandl JN, Barry AP, Vanderford TH, et al. Divergent TLR7 and TLR9 signaling and type I interferon production distinguish pathogenic and nonpathogenic AIDS virus infections. *Nat Med.* 2008;14:1077-1087.
262. Grossmann R, Stence N, Carr J, Fuller L, Waite M, Dailey ME. Juxtavascular microglia migrate along brain microvessels following activation during early postnatal development. *Glia.* 2002;37:229-240.
263. Chalifoux LV, Simon MA, Pauley DR, MacKey JJ, Wyand MS, Ringler DJ. Arteriopathy in macaques infected with simian immunodeficiency virus. *Lab Invest.* 1992;67:338-349.
264. Yanai T, Lackner AA, Sakai H, Masegi T, Simon MA. Systemic arteriopathy in SIV-infected rhesus macaques (*Macaca mulatta*). *J Med Primatol.* 2006;35:106-112.
265. van Horssen J, Singh S, van der Pol S, et al. Clusters of activated microglia in normal-appearing white matter show signs of innate immune activation. *J Neuroinflammation.* 2012;9:156.
266. Trebst C, Sorensen TL, Kivisakk P, et al. CCR1+/CCR5+ mononuclear phagocytes accumulate in the central nervous system of patients with multiple sclerosis. *Am J Pathol.* 2001;159:1701-1710.
267. Henderson AP, Barnett MH, Parratt JD, Prineas JW. Multiple sclerosis: distribution of inflammatory cells in newly forming lesions. *Ann Neurol.* 2009;66:739-753.
268. Mawhinney LA, Thawer SG, Lu WY, et al. Differential detection and distribution of microglial and hematogenous macrophage populations in the injured spinal cord of lys-EGFP-ki transgenic mice. *J Neuropathol Exp Neurol.* 2012;71:180-197.
269. Bissel SJ, Wang G, Bonneh-Barkay D, et al. Systemic and brain macrophage infections in relation to the development of simian immunodeficiency virus encephalitis. *J Virol.* 2008;82:5031-5042.
270. Persidsky Y, Gendelman HE. Mononuclear phagocyte immunity and the neuropathogenesis of HIV-1 infection. *J Leukoc Biol.* 2003;74:691-701.

271. Kida S, Steart PV, Zhang ET, Weller RO. Perivascular cells act as scavengers in the cerebral perivascular spaces and remain distinct from pericytes, microglia and macrophages. *Acta Neuropathol.* 1993;85:646-652.
272. Kosel S, Egensperger R, Bise K, Arbogast S, Mehraein P, Graeber MB. Long-lasting perivascular accumulation of major histocompatibility complex class II-positive lipophages in the spinal cord of stroke patients: possible relevance for the immune privilege of the brain. *Acta Neuropathol.* 1997;94:532-538.
273. Alvarez A, Conerly C, Lackner A, and Williams KC. Brain perivasacular cells leave the CNS: Implications for AIDS Pathogenesis. Oral presentation at: The 28th Annual Symposium on Nonhuman Primate Models for AIDS; 2010 Oct 19-22; New Orleans, LA.
274. Kaminski M, Bechmann I, Pohland M, Kiwit J, Nitsch R, Glumm J. Migration of monocytes after intracerebral injection at entorhinal cortex lesion site. *J Leukoc Biol.* 2012;92:31-39.
275. Johnston M, Zakharov A, Papaiconomou C, Salmasi G, Armstrong D. Evidence of connections between cerebrospinal fluid and nasal lymphatic vessels in humans, non-human primates and other mammalian species. *Cerebrospinal Fluid Res.* 2004;1:2.
276. Hochmeister S, Zeitelhofer M, Bauer J, et al. After injection into the striatum, in vitro-differentiated microglia- and bone marrow-derived dendritic cells can leave the central nervous system via the blood stream. *Am J Pathol.* 2008;173:1669-1681.
277. Westhorpe CL, Zhou J, Webster NL, et al. Effects of HIV-1 infection in vitro on transendothelial migration by monocytes and monocyte-derived macrophages. *J Leukoc Biol.* 2009;85:1027-1035.
278. Fischer-Smith T, Bell C, Croul S, Lewis M, Rappaport J. Monocyte/macrophage trafficking in acquired immunodeficiency syndrome encephalitis: lessons from human and nonhuman primate studies. *J Neurovirol.* 2008;14:318-326.
279. Jenkins SJ, Ruckerl D, Cook PC, et al. Local macrophage proliferation, rather than recruitment from the blood, is a signature of TH2 inflammation. *Science.* 2011;332:1284-1288.
280. Ryzhova EV, Crino P, Shawver L, Westmoreland SV, Lackner AA, Gonzalez-Scarano F. Simian immunodeficiency virus encephalitis: analysis of envelope sequences from individual brain multinucleated giant cells and tissue samples. *Virology.* 2002;297:57-67.
281. Reddy RT, Achim CL, Sirko DA, et al. Sequence analysis of the V3 loop in brain and spleen of patients with HIV encephalitis. *AIDS Res Hum Retroviruses.* 1996;12:477-482.
282. Cortez-Retamozo V, Etzrodt M, Newton A, et al. Origins of tumor-associated macrophages and neutrophils. *Proc Natl Acad Sci U S A.* 2012;109:2491-2496.
283. Kao SY, Lemoine FJ, Marriott SJ. Suppression of DNA repair by human T cell leukemia virus type 1 Tax is rescued by a functional p53 signaling pathway. *J Biol Chem.* 2000;275:35926-35931.
284. Morris GF, Mathews MB. The adenovirus E1A transforming protein activates the proliferating cell nuclear antigen promoter via an activating transcription factor site. *J Virol.* 1991;65:6397-6406.

APPENDICES.

Publications

Strickland, S.L., Gray, R.R., Lamers, S.L., Burdo, T.H., Huenink, E., Nolan, D.J., **Nowlin, B.**, Alvarez, X., Midkiff, C.C., Goodenow, M.M., Williams, K. & Salemi, M. 2011, "Significant genetic heterogeneity of the SIVmac251 viral swarm derived from different sources", *AIDS Research and Human Retroviruses*, vol. 27, no. 12, pp. 1327-1332.

Strickland, S.L., Gray, R.R., Lamers, S.L., Burdo, T.H., Huenink, E., Nolan, D.J., **Nowlin, B.**, Alvarez, X., Midkiff, C.C., Goodenow, M.M., Williams, K. & Salemi, M. 2012, "Efficient transmission and persistence of low-frequency SIVmac251 variants in CD8-depleted rhesus macaques with different neuropathology", *The Journal of General Virology*, vol. 93, no. Pt 5, pp. 925-938.

Nowlin, B.T., Burdo, T.H., Midkiff, C.C., Salemi, M., Alvarez, X., & Williams, K.C.
"SIVE lesions are comprised of CD163+ macrophages present in the CNS during early SIV infection and SIV+ macrophages recruited terminally with AIDS"
(Manuscript submitted to *Am J Pathol*)

Nowlin, B.T., Wang, J., Autissier, P., Burdo, T.H., & Williams, K.C.
"Monocyte subsets exhibit transcriptional plasticity and a shared response to interferon in SIV-infected rhesus macaques"
(Manuscript submitted to *Blood*)

Conferences and Awards

9th International Symposium on Neurovirology, Miami, FL, June 2-9, 2010.

“Altering SIV infection in monocyte-derived macrophages by siRNA mediated knockdown of PCNA”

28th Annual Symposium on Nonhuman Models for AIDS, New Orleans, LA, Oct. 19-22,

2010. “Modulation of gene expression during SIV pathogenesis in monocyte subpopulations”

18th Conference on Retroviruses and Opportunistic Infections, Boston, MA, Feb. 27-

Mar. 2, 2011. “Increased turnover of perivascular macrophages in the CNS of SIV-infected rhesus macaques is proportional to disease severity and decreased survival time”

19th Conference on Retroviruses and Opportunistic Infections, Seattle, WA, March 5-8,

2012. **Young Investigator Award** “Increased recruitment of CD163+ and MAC387+ macrophages to the CNS of SIV+ rhesus macaques”

8th International Workshop: HIV, Cells of Macrophage/Dendritic Lineage, and Other

Reservoirs: Pathogenic and Therapeutic Implications, Stresa, Italy, May 10-12, 2012

Travel Award “Characterization of the recruitment of CD163+ and MAC387+ macrophages in the CNS of SIV-infected rhesus macaques”.

Best Poster “Microarray analysis of classical, intermediate, and nonclassical monocytes and modulation of gene expression with SIV pathogenesis in rhesus macaques”